Analysis of an Urban Stormwater Bioretention Management Practice in Prince William County, Virginia

by

Suzanne Angelo

Thesis submitted to the faculty of the Virginia Polytechnic Institute and State University in partial fulfillment of the requirements for the degree of

Master of Science

In

Environmental Engineering

Thomas J. Grizzard, Chair

Adil N. Godrej

Harry E. Post

November 21, 2005

Manassas, Virginia

Keywords: Bioretention, BMP, Stormwater Quality

Analysis of an Urban Stormwater Bioretention Management Practice in Prince William County, Virginia

Suzanne Angelo

Abstract

The performance of an urban stormwater bioretention management practice in the Kingsbrooke Subdivision of Prince William County, Virginia was examined over a one-year period.

Bioretention is a relatively new urban stormwater best management practice (BMP) intended to mimic the pollutant-removal characteristics of an upland forest habitat. Typical bioretention areas utilize shallow ponding and highly-infiltrative sandy soils to treat the stormwater runoff from small commercial or residential drainage sites. The Kingsbrooke bioretention area was found to be atypical in several ways, including its relatively large, 14 acre, drainage area and the high clay content of its topsoil.

Hydrologic and chemical data were collected by Virginia Tech staff for a total of 8 months in 2003 and 2004. Analysis of pollutant loading data was complicated by the presence of three unmeasured water flows: overland inflow bypassing the inflow gage, and groundwater flows both entering and exiting the bioretention soils. The BMP did reduce peak runoff rates for some storms, but did not significantly reduce total storm volumes because of the combined effects of the large drainage area to BMP area ratio and the poor infiltration capacity of the soil. Pollutant load calculations determined that the site removed about 28% of total suspended solids, 32% of total phosphorus, and about 15% of total nitrogen. Removals of approximately 16% and 7% were observed for lead and zinc, respectively. Although the Kingsbrooke bioretention area did improve water quality, the pollutant removal efficiencies were lower than those reported in the literature from more conventional bioretention areas.

Table of Contents

Index of Figures

Index of Tables

Acknowledgements

The author would to thank the Prince William County Department of Public Works for providing the funding to instrument and monitor this site. She would also like to thank the staff at the Occoquan Watershed Monitoring Laboratory in Manassas for their help with a majority of the work that was put into this project, including installing and maintaining the flow gages, collecting and analyzing the data, and answering all of the author's many questions.

1 Introduction

Urban nonpoint source pollution is currently of great concern in terms of its impact on downstream water quality. Converting rural land into urban uses generally has a significant impact on both the quantity and quality of stormwater runoff. The total volume and peak flowrate of the runoff increase with the increase in developed impervious surface area. During the development process, sediment loads increase as the land is disturbed by construction activities. After construction, the runoff concentrations of pollutants such as trace metals, oil, and grease may increase from industry, automobiles, and other human activities. Nutrient concentrations also increase as fertilizers are added to the new lawns and other vegetated areas. Because the impervious surfaces in traditional developments are often directly connected to the drainage system, all of these pollutants can flow directly to the receiving stream network without any treatment or mitigation.

A variety of best management practices (BMPs) have been developed to attempt to address the problem of urban nonpoint source pollution. Traditional stormwater detention ponds and wet retention ponds are very successful in reducing peak flow rates and reducing downstream flood dangers, and they have also shown some ability to remove stormwater pollutants. Other structural BMPs include constructed wetlands, vegetated stream buffers, and infiltrating sand filters. The variety of nonstructural BMPs tend to address more closely the source of the pollutants, including switching from leaded to nonleaded gasoline, conducting regular street sweeping, and educating the public on proper lawn fertilizing techniques. The most successful pollution control strategies implement a series of both structural and nonstructural BMPs and consider the land development process from zoning through design, construction, and beyond.

This research was conducted to assess the performance of a specific type of structural BMP that has received much attention in recent years: the bioretention area. Bioretention areas simulate an upland forest habitat, and function as a natural forest's plants, soil, and microbes would to control water quality and quantity. The essential components of a bioretention area are shown in Figure 1.1, including the inflow point with optional grass buffer strip, a ponding area for water storage, the plant material, the planting soil with a high infiltration capacity, a gravel blanket to protect the optional underdrain outlet, and some geotextile fabric along the sides to limit horizontal water flow. The native soil that underlies the bioretention area can also play a critical role in the facility's design and function (Winogradoff and Coffman, 2002).

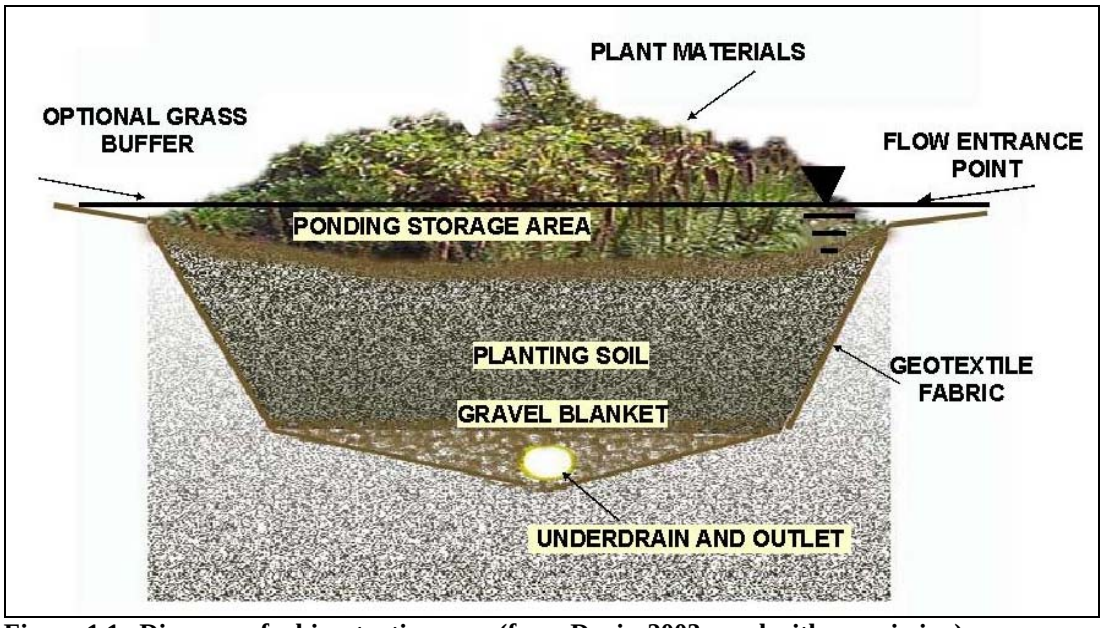

Figure 1.1. Diagram of a bioretention area (from Davis, 2003. used with permission).

Bioretention BMPs are generally intended to be applied at the small-scale, in such places as parking lot medians or landscaped areas on individual residential lots, with the goal of treating runoff close to its source rather than at larger facilities further downstream. This can have hydrologic advantages in that it causes the post-development runoff hydrograph to more closely resemble the pre-development hydrograph. Bioretention and other Low Impact Development (LID) concepts also have the goal of reducing not just the peak discharge, but also the total hydrograph volume. This is accomplished by trapping the runoff near its source through such means as reducing the connected impervious surface area and installing small BMPs (*e.g.* bioretention or rain barrels) on individual lots. The theory is that small quantities of runoff are easier to treat, making pollutant removal more effective if applied further upstream. Many LID techniques, including bioretention, are intended to increase infiltration and evapotranspiration by using pervious soils and plant materials. Small bioretention areas may be incorporated into landscaping areas on residential lots, thus increasing public awareness of environmental concerns. Unfortunately, there are concerns that individual homeowners might not properly maintain such bioretention areas, which could lead to decreased efficiency over time.

Bioretention may have several advantages over more traditional urban stormwater BMPs. The plants in a bioretention area often improve the aesthetics of the BMP over, for example, the standard sand filter, while maintaining some of the same benefits, such as high pollutant removal rates. Compared to a pond or wetland, a bioretention area has the advantage of thermal attenuation: that is, the water temperature of a shallow pond absorbing the sun's rays will increase much more than will the water infiltrating into a bioretention area. Bioretention is also generally less complicated to design and regulate than a conventional wet pond. Contact with the mulch and soils of the bioretention area is intended to cause dramatic reductions in metal concentrations due to adsorption, while water passing through a pond does not interact much with the bottom soils. Increased soil interaction may also help remove excess nutrients by adsorption, bacterial reactions, and plant uptake. For the long-term operation of a bioretention area, vegetation should be regularly harvested and removed from the site, thereby reducing the nutrients and metals inventory that the plants have taken up and preventing them from being re-released when the plants decay.

Bioretention designs may include roof gardens, tree pits, depressed parking medians, and "weep gardens," built into a hill slope. Virtually any design that incorporates plants and water filtration through sandy, organic soils may be called bioretention, even if it does not entirely follow the commonly accepted guidelines published by Prince George's County (Winogradoff and Coffman, 2002). Even the sites that follow those guidelines show an enormous variation in possible designs to fit the variation in sites where this technology can be applied. This large variation in designs has caused difficulties in quantifying the pollutant removal efficiencies that may be expected from bioretention. Schematics of a few possible bioretention designs are shown in Figures 1.2 through 1.4, which follow.

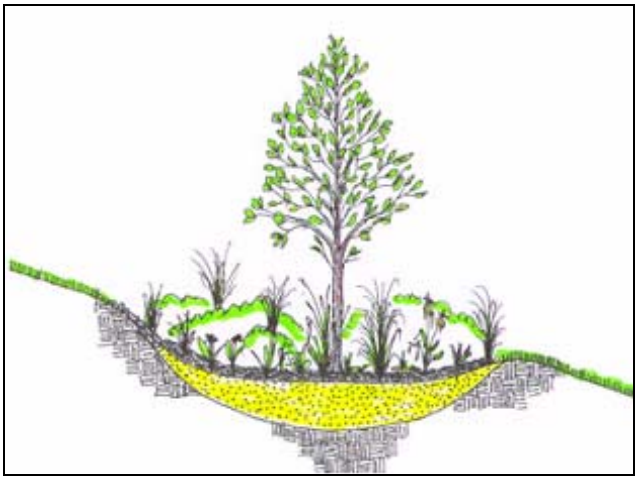

Figure 1.2. A scalloped bioretention area suitable for use on a residential lot (from Winogradoff and Coffman, 2002).

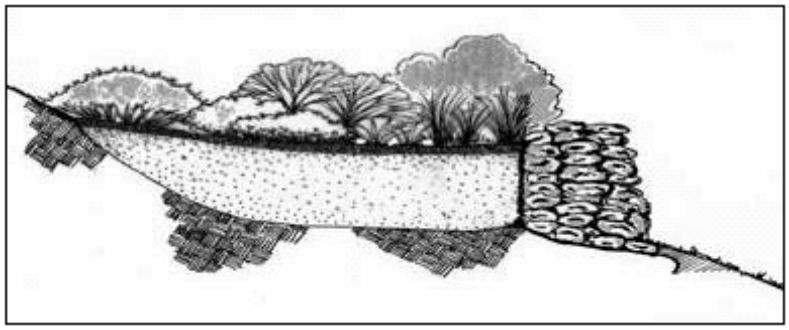

Figure 1.3. A weep garden suitable for sloped areas (from Winogradoff and Coffman, 2002).

Figure 1.4. A typical bioretention area built into a parking median (from Davis, 2003, used with permission).

An interesting new development in the bioretention field has been the production of standardized concrete bioretention boxes, called Filterra® by their producer Americast (Americast, 2004). Filterra® is just as simple as any other bioretention design, consisting of no more than a concrete box filled with a high-infiltration-capacity soil, mulch, underdrain, and a bush. The use of standardized commercial products such as this one may help bioretention research by removing much of the variability currently associated with bioretention designs, but at the same time such proprietary products may increase the cost of adding bioretention BMPs to a site. Figure 1.5 shows a schematic diagram of a Filterra® system.

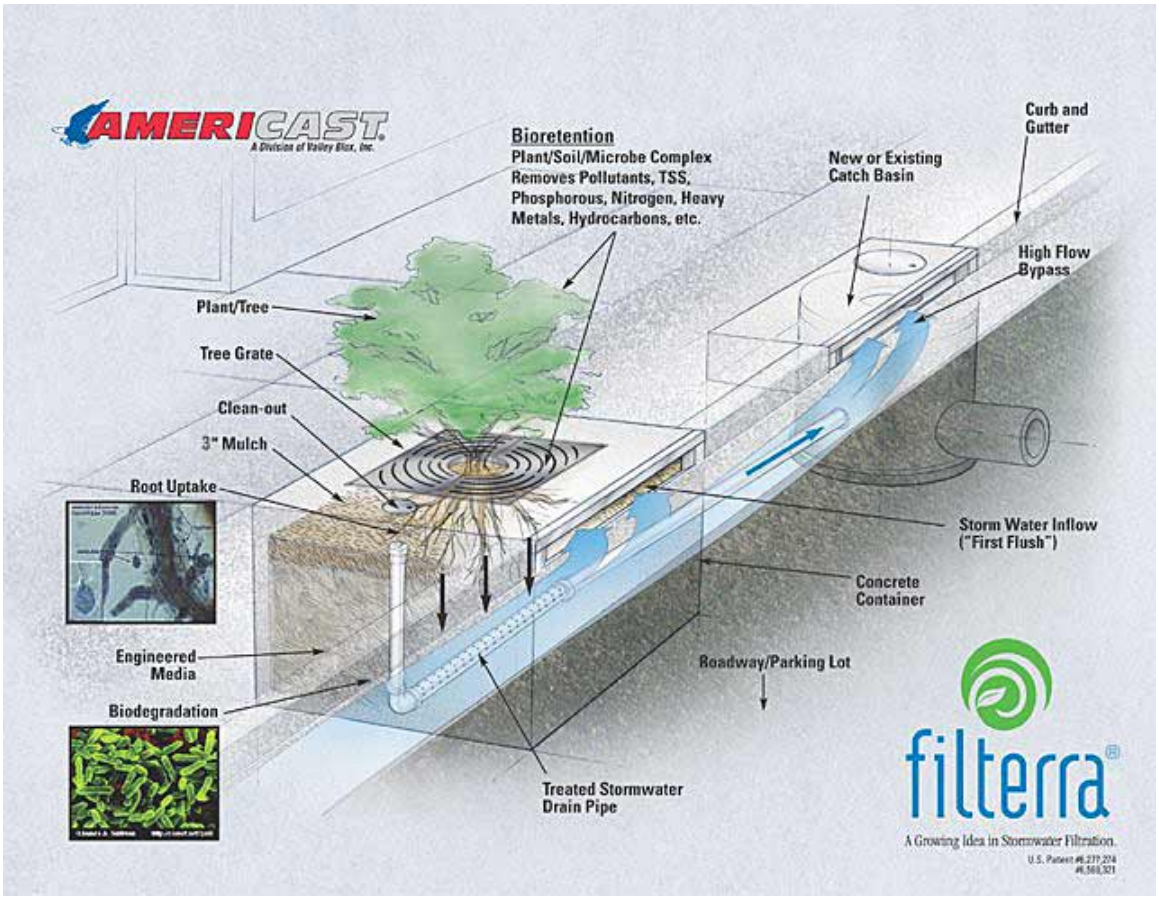

Figure 1.5. Filterra®, a commercially available bioretention area produced by Americast (from Americast, 2004, used with permission).

This research was conducted to examine the pollutant removal performance of a bioretention area located in the Kingsbrooke subdivision of Prince William County, Virginia. Objectives included analyzing the site hydrology and water quality, and determining pollutant removal efficiencies for selected trace metals and nutrients.

2 Literature Review

Because bioretention is a fairly new urban stormwater BMP, relatively few studies have been performed on it until recently. This section summarizes the current design standards from the Prince George's County Bioretention Design Manual (Winogradoff and Coffman, 2002), and results from several other published studies.

Davis (2001, 2003, 2005) conducted laboratory studies and a series of field studies of bioretention using synthetic stormwater runoff. More detailed studies are currently underway on a paired system of bioretention cells at the University of Maryland, but those results are not yet available (Davis, 2005).

Yu (1999, 2001) has reported short-term studies on a bioretention area in Charlottesville, Virginia, and on a combined bioretention area and wet pond in Warrenton, Virginia. In North Carolina, Hunt and Jarrett (2004) monitored water quality from bioretention areas in Greensboro and Chapel Hill. In Pennsylvania, Emerson and Traver (2004) reported hydrology data from the Bio-Infiltration Traffic Island at Villanova University. Plans are underway to initiate water quality sampling at the same location (Emerson and Traver, 2004). Nordberg and Thorolfsson (2004) have reported on plans for a detailed study of the application of bioretention in cold climates.

Rushton (2001) conducted a study of parking areas that involved the incorporation of grassed swales and vegetated areas that functioned similarly to bioretention. On a larger watershed scale, a study is continuing in Prince George's County, Maryland, to evaluate the hydrologic and water quality benefits of applying Low Impact Development strategies, including bioretention, to an entire subdivision (Cheng et al, 2004). Two years of data are currently available from the paired watersheds in that study, in which an older residential development with conventional curb and gutter and lacking BMPs was compared to a newer watershed that was developed using LID techniques.

Christianson, et al. (2004) have reported the development of a model of infiltration and pollutant removal mechanisms in bioretention areas using computer spreadsheets. Lastly, Pitt, et al. (2002) have reported on the effects of soil compaction on infiltration rates in urban areas, particularly with regard to the potential impacts on the effectiveness of an infiltration-based BMP such as bioretention.

2.1 Nitrogen Cycle

Several nitrogen species are commonly present in surface and groundwaters. A basic understanding of these nitrogen species and the transformations between them, shown in Figure 2.1, is necessary for any discussion of bioretention area nutrient removal.

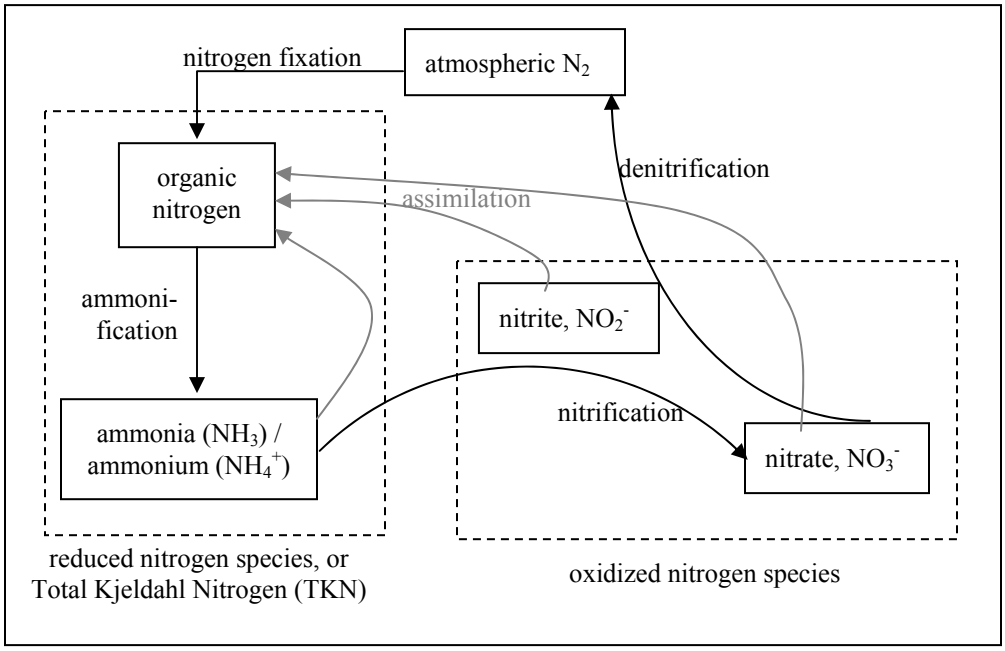

Figure 2.1. A simple nitrogen cycle, based on Metcalf and Eddy (2003).

"Total nitrogen" is the sum of the reduced nitrogen species and the oxidized nitrogen species present in a water sample. The reduced nitrogen species include organic nitrogen and ammonia/ammonium. Of the oxidized nitrogen species, nitrite concentrations are usually insignificant compared to nitrate concentrations. Nitrogen gas is not part of the total nitrogen measurement. Thus, nitrogen "removal" from water generally involves the transformation of all other nitrogen forms into nitrogen gas, followed by the escape of that gas to the atmosphere (Metcalf and Eddy, 2003). Not shown in Figure 2.1, but significant to bioretention processes, is the fact that both organic nitrogen and ammonium can adsorb to organic matter and sediment particles, while nitrate and nitrite are primarily dissolved species. So organic nitrogen and ammonium may also be removed from a water stream through their incorporation with solids (Davis et al., 2001). A reduction in the concentration of a single nitrogen species does not necessarily equal a reduction in the total nitrogen concentration, but may only indicate a transformation to some other aqueous species. Consider the case of a stormwater containing mainly organic nitrogen. In order for this nitrogen to be removed from the water, three different transformations must occur: ammonification to convert it to ammonia, followed by nitrification to convert it to nitrite and then to nitrate, and finally denitrification to convert it back through nitrite to nitrogen gas. Some assimilation of these nitrogen forms into plant organic matter may also occur, and of course the harvesting of those plants would also remove nitrogen from the system. Nitrogen fixation occurs when there is a nitrogen deficit, a condition that is uncommon in stormwater. Nitrification requires an aerobic environment, while denitrification only occurs under anaerobic conditions, so the stormwater must pass through both micro-environments in order for the organic nitrogen to completely transform to nitrogen gas (Metcalf and Eddy, 2003).

2.2 Bioretention Design Principles

The earliest set of design practices identified in this review of the literature is the Bioretention Manual was published by Prince George's County, Maryland in 1993. It has since been modified and expanded in the most current version (2002), and may be accessed through the county website at www.goprincegeorgescounty.com. A brief summary of the relevant information from that document is included here in Section 2.2. Inclusion of an underlying sandbed was recommended in the 1993 guidelines,

but this recommendation has been removed from the 2002 document. The design guidelines allow for a great deal of variation as bioretention features are altered to fit the characteristics of a specific site. It should be noted, however, that the variation in designs has resulted in variation in the pollutant removal efficiencies observed at different bioretention areas. This variation is especially evident in the cases when a single research team has studied multiple bioretention areas, as in Davis (2003) or Hunt and Jarrett (2004).

2.2.1 Size

The bioretention size may be designed either to reduce the post-development runoff volume to the predevelopment volume, or to reduce the post-development peak runoff rate to the predevelopment peak runoff rate, or to treat the regulatory water quality volume. In the best-case scenario, the largest storage volume would be selected to meet all three of these goals. The Prince George's County Manual includes charts based on the TR-55 methodology to help designers determine how much water storage is needed in a single bioretention facility or for a development using many bioretention facilities. Six inches of water storage ponding depth is typical in a bioretention design, but between 3" to 12" may be used under certain site restrictions. Usually the bioretention area should occupy 5 – 7% of the site area, but specific volume calculations may give different results (Winogradoff and Coffman, 2002).

2.2.2 Design of Components

Once the overall size and location of the bioretention area are determined, its components may be designed as discussed below, paraphrased from the Prince George's County Bioretention Design Manual (Winogradoff and Coffman, 2002). The discussion of design principles may be facilitated by reference to Figure 2.2, which is a schematic diagram of the principal layers found in bioretention systems.

2.2.2.1 Inflow Entry

A special inflow scheme is usually not required for bioretention areas located on residential lots; in those cases runoff enters the facility as sheet flow, slowed and filtered by passing first through the surrounding grass lawn. For bioretention areas located adjacent to impervious parking areas, flow may enter through a cut in the curb, gaps under concrete wheel stops, or as sheet flow directly from the pavement or across a grass pre-treatment area. In some cases it may be necessary to slow the inflow velocity and prevent damage to the vegetation by laying gravel just inside the entryway (Winogradoff and Coffman, 2002).

2.2.2.2 Overflow Weir

A broad-crested weir or grass berm around the bioretention area should be designed to control the ponding depth. This berm may be located separately from the inflow point for an on-line bioretention area, or may be the same as the inflow point for the off-line case. The idea behind an off-line bioretention area is that, once the water ponds to the design depth, no more water can enter the facility. When designing a weep garden, the porous gabion wall of the downstream face functions as an overflow weir to regulate ponding depth (Winogradoff and Coffman, 2002).

2.2.2.3 Planting Recommendations

Preferred plantings should be native to the region and tolerant of varying soil moisture conditions. Large trees, under-story trees, shrubs, and groundcover should be combined to simulate the full diversity of a forest. Plants may be selected with aesthetic considerations or to provide food and habitat for wildlife. For aesthetic reasons, noxious weeds should be avoided in the planting soil, mulch, and installed plantings (Winogradoff and Coffman, 2002).

2.2.2.4 Mulch Specifications

Aged, shredded hardwood mulch is preferred to encourage metal adsorption, but fresh mulch may occasionally be substituted to enhance nitrogen removal. Mulch depth should be less than 3" (Winogradoff and Coffman, 2002). Some bioretention applications use grass instead of mulch as the organic layer and groundcover (Rushton, 2001; Christianson, 2004).

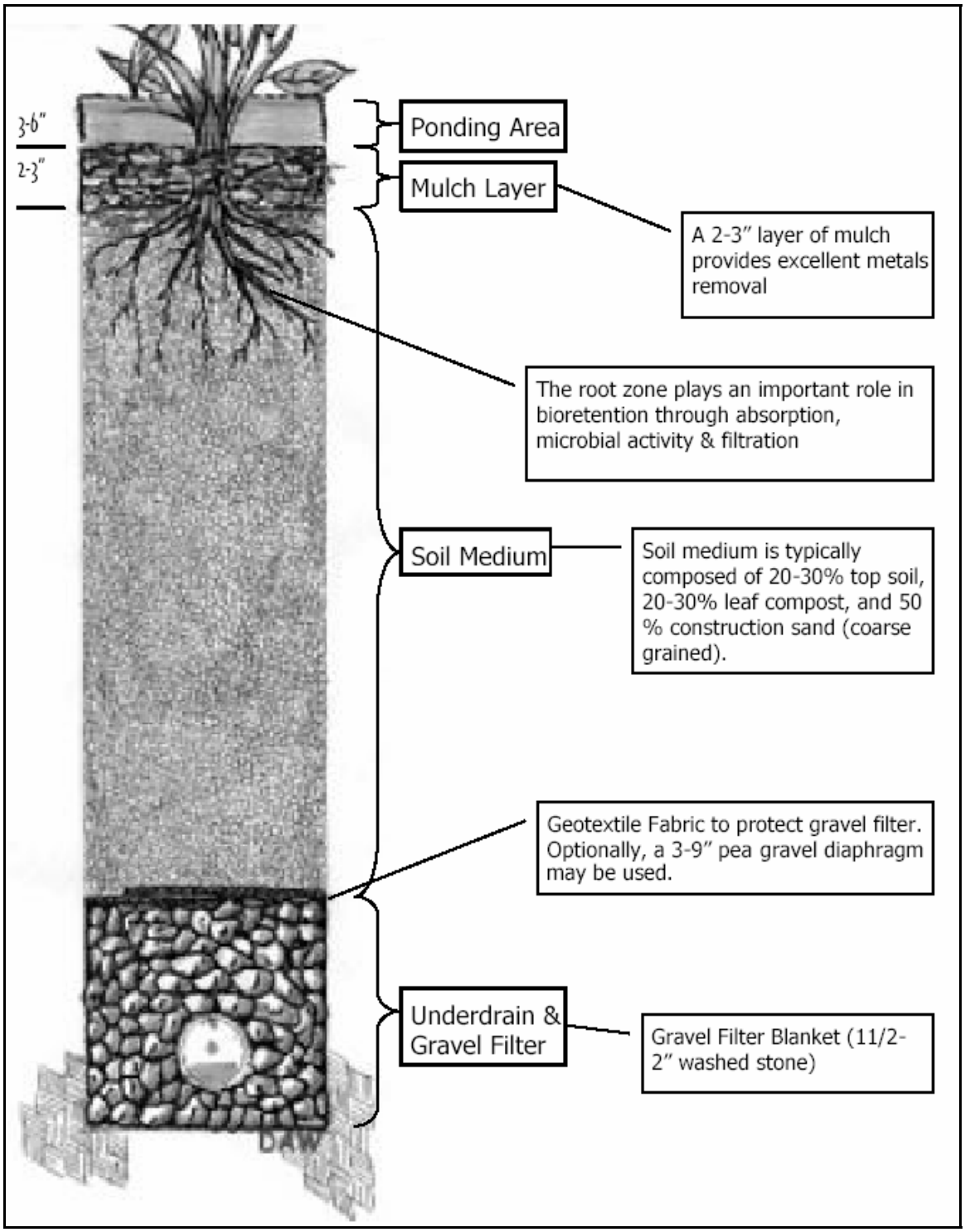

Figure 2. 2. Summary of the layers in a bioretention area (adapted from Winogradoff and Coffman, 2002).

2.2.2.5 Soil Specifications

According to the Prince George's County guidelines (Winogradoff and Coffman, 2002), the planting soil depth should be about 2.5 feet to allow for adequate filtration, pollutant treatment, and plant root growth. Bioretention soil must have an infiltration rate sufficient to draw down the pooled water within 3-4 hours

after a storm event. With the normal 6-inch ponding depth, this corresponds to an infiltration rate of at least 1.5 inches/hour, suggesting that loamy sand, sand, or sandy loam must be used as the planting material. The same guidelines also suggest a mixture of 50-60% sand, 20-30% aged leaf compost, and 20-30% topsoil (sandy loam, loamy sand or loam-textured topsoil). Overall clay content must be less than 5%. Soil compaction should be minimized and allowed to occur naturally rather than mechanically. The detrimental effects of excess soil compaction as detailed by Pitt *et al* (2002) are discussed later in Section 2.12.

2.2.2.6 Underdrain, Gravel Blanket, and Filter Layer

An underdrain is required where the native soils have infiltration rates of less than 1"/hr (except for weep garden design). Perforated PVC pipe is usually used, though other flexible pipe types may be substituted. The manually placed gravel blanket should surround and protect the underdrain to about 12 inches deep with washed stone 0.5 – 1.5" in diameter. To allow for longer water storage times or increased groundwater recharge, a thicker gravel blanket may be used with the underdrain raised above the lower invert of the bioretention area. The saturated anaerobic conditions that would develop in the storage area below the underdrain in that configuration may also result in more efficient denitrification (Winogradoff and Coffman, 2002).

Typically, when a gravel blanket is used then either a layer of geotextile filter fabric or a layer of pea gravel is used above it to prevent soil entry into the gravel blanket and thence to the underdrain. In modern designs, the pea gravel layer is preferred over a geotextile filter fabric because it is less likely to clog. The pea gravel layer should be between 3 and 8 inches thick, extending 2' to either side of the underdrain, with stone sizes of 0.25 – 0.5". Filter fabric is also recommended for lining the sides of the bioretention area that are adjacent to paved areas to prevent water flow sideways under the pavement and to direct the flow downward (Winogradoff and Coffman, 2002).

2.2.2.7 Impermeable Liner

An impermeable liner may be required in some areas to protect against groundwater contamination, for example in places where toxic spills are likely ("hot-spots" such as gas stations) or where the groundwater is protected for drinking water purposes. Use of an impermeable liner requires the addition of an underdrain to ensure soil drainage. In case of a toxic spill, the underdrain may be capped while the facility is pumped out through the connected observation well (Winogradoff and Coffman, 2002).

2.2.3 Facility Maintenance

Although bioretention areas generally require only minimal maintenance, they are not maintenance-free. A few simple steps, followed regularly, should enhance the functioning and aesthetics of any bioretention area (Winogradoff and Coffman, 2002).

- Fertilizer should not be added to bioretention facilities because they are expected to receive excess nutrients with stormwater runoff.
- Weeding is recommended for aesthetic reasons, but is not required for proper functioning.
- Regular plant pruning and harvesting is encouraged to enhance pollutant removal, though for a bioretention area located in a "hot-spot", such trimmings should be landfilled rather than composted.
- Newly installed plants should be watered regularly, but established ones only require watering in drought conditions. Windy, exposed areas such as parking lot islands may be more susceptible to those drought conditions.
- Mulch should be added yearly, not to exceed the maximum total mulch depth of 3 inches.
- Standing water problems indicate that the bioretention area is not functioning properly. Such problems should be corrected as soon as possible.

2.3 University of Maryland Studies

Davis et al. (2001, 2003, 2005) have performed a variety of experiments on various scales of bioretention projects, ranging from laboratory-based column tests to field tests on actual bioretention areas. Currently, a long-term field project is underway, but most previous results have been reported from short-term studies with only a few "storm" events using synthetic lab-prepared runoff (Davis, 2003). Although short-term laboratory and field studies are necessarily limited in their conclusions, they do provide important insights to the pollution removal mechanisms operating in a bioretention area.

2.3.1 Metal Adsorption

A sandy loam agricultural topsoil was used for all of the University of Maryland laboratory studies reviewed herein (Davis et al., 2001). Column sorption studies for trace metals were performed on the soil and on the shredded hardwood mulch used in the experiments. During the sorption studies, more than 800 bed volumes of metal-containing solution were passed through Plexiglas columns containing either soil or mulch. In all cases the effluent metal concentrations remained significantly less than the influent concentrations and breakthrough did not occur. The studies showed that the shredded hardwood mulch had a much higher capacity for sorbing metals than did the sandy loam soil, suggesting that in a full-scale bioretention area a majority of the metal removal would occur by means of adsorption to the surface mulch layer (Davis, et al., 2001).

Davis, et al. (2003) calculated the potential long-term metal accumulation in a bioretention area for the purpose of predicting the facility life span and also for addressing other issues that might arise from maintaining it. Davis used runoff volumes "estimated using 90 cm/a of rainfall, runoff volume of 90% of rainfalls (c = 0.9), and a 30:1 concentration of drainage area to BMP area", and assumed metal concentrations were of 8 μg/L Cd, 80 μg/L Cu, 75 μg/L Pb, and 700 μg/L Zn. In order to ensure a conservative analysis, it was also assumed that 100% of the influent metal load would be removed and stored within the bioretention area. Using EPA limits on biosolids land application (U.S. Environmental Protection Agency (1993) *Standards for the Use or Disposal of Sewage Sludge. Fed. Regist.,* **58,** 32, 40 CFR Part 503.), it was found that the assumed metal application rates would limit the bioretention area's life span to 16 years; after that time the biosolids application rates would be exceeded for both lead and zinc. Many facilities may have a longer life span than that due to having metals removal rates of less than 100%, but the calculation still shows that metal accumulation in bioretention areas is significant and may impact the useful life span of a facility. Harvesting and removal of plants may be useful as a mechanism for continuously removing metals from the facility (Davis et al., 2003).

2.3.2 Small and Large Box Experiments

Davis et al. (2001) have also reported results from two laboratory-scale bioretention prototypes. The systems consisted of a thin gravel bed surrounding perforated drainage pipes, sandy loam soil, hardwood mulch topper, and several creeping juniper plants. One small system and one large system were constructed, measuring respectively 76cm x 107cm with 61cm of soil depth, and 305cm x 152cm with 91cm of soil depth. Both boxes included sufficient freeboard to allow for ponding. Synthetic runoff was applied to the surface at a rate of 4.1 cm/hr over 6 hours for each synthetic storm event, which were repeated every few days. The flowrate was selected to roughly correspond to a 1.5-cm (0.7 inches) total rainfall over 6 hours (which was reported as the average for the Washington, D.C. area). The applied water volume was computed assuming that the bioretention area occupied 5% of the drainage area and the rational runoff coefficient was 0.8. Thus, the total runoff applied in each storm event was approximately 200 L for the small box and 1000 L for the large box. The observed infiltration rates were between 1 and 2 cm/hr for the small box and 0.3 – 0.4 cm/hr for the large box (Davis, et al., 2001)

Samples were taken from ports in the sides of the experiment boxes throughout the simulated storms and as the boxes drained, then were tested for metals and nutrients. Very high pollutant removal efficiencies were observed for metals and for phosphorus, as summarized in Table 2.1. Based on column test data, the removal of metals was found to be due principally to adsorption on the mulch, with most removal occurring above the upper ports and limited removal in the lower soils and by the plants. Phosphorus removal was reported to occur throughout the bioretention depth, probably through sorption onto aluminum, iron, and clay minerals or through precipitation reactions.

Concentrations of nitrogen are also shown in Table 2.1 for both the influent and the sample ports. Although not shown in the table, total nitrogen may be calculated as the sum of the TKN and nitrate concentrations, assuming nitrite to be negligible. So, for the large box the total nitrogen concentration reduced steadily from 3.1 mg N/L in the influent to 2.4 mg/L at the upper port, 2.1 mg/L at the middle port, and 1.2 mg/L of nitrogen at the lower port and in the underdrain effluent. This represents a reduction in total nitrogen concentration of 63% between the influent and the effluent. Nitrate concentrations increased from the influent to the middle port, indicating that nitrification was occurring in the upper soil regions, but then decreased again between the middle port and lower port, indicating that some denitrification also occurred in the lower soil regions. Davis et al. (2001) did not indicate whether the upper soil regions were completely aerobic and lower regions completely anoxic, or whether the nitrification and denitrification zones were simply the result of microenvironments within and around the soil particles. Both the large and small boxes in these studies were allowed to drain fully between experiments. The increase in nitrate concentrations was significantly less than the decrease in TKN, suggesting that adsorption of TKN and ammonium to soil particles played a larger role in instantaneous TKN removal than did nitrification. TKN and ammonium reductions were similar in both the small and the large boxes.

Table 2.1. Chemical data summary from box experiments at University of Maryland (from Davis, 2001, used with permission).

System		Copper, µg/L	Lead, µg/L	Zinc, µg/L	Phosphorus, mg/L	TKN, mg N/L	NH_4^+, mg N/L	Nitrate, mg N/L
Small Box								
	Influent	140	61	600	0.44	3.5	1.2	not measured
Average	upper port (18cm)	12	2.9	43	0.37	1.5	1.3	"
	lower port (60cm)	3.4	< 2	< 25	0.13	0.88	0.48	"
Percent Reduction in Conc.	upper port (18cm)	91%	95%	93%	16%	57%	(-8)%	"
	lower port (60cm)	98%	>98%	>97%	71%	75%	60%	"
Large Box								
	Influent	64	54	590	0.52	2.8	2.4	0.34
Average	upper port (25cm)	7.4	4.1	70	0.49 (1 outlier omitted)	1.7	1.1	0.67
	middle (56cm)	4.5	< 2	< 25	0.14	1.1	0.32	1.0
	lower port (90cm)	4.9	< 2	< 25	0.10	0.9	0.50	0.26
Percent Reduction in Conc.	upper port (25cm)	89%	92%	88%	7% (1 outlier omitted)	38%	54%	(-96)%
	middle (56cm)	93%	>98%	>98%	73%	61%	87%	(-205)%
	lower port (90cm)	92%	>98%	>98%	81%	68%	79%	24%

After 26 synthetic storms, several soil cores, mulch samples, and plant clippings were tested for changes in metal content. Those results, combined with the measured inflow and outflow concentrations and volumes, were used to create a mass balance for copper, lead, and zinc, which is summarized in Table 2.2. Plant uptake in the study's 10 months accounted for less than 5% of the applied influent metals. Most of the applied metals could not be accounted for, so they were assumed to be adsorbed to the soil. The resulting change in the soil's metal concentration would be too small to be measured.

Table 2.2. Small box study, mass balance for metals over 10 months and 26 storms (from Davis, 2001, used with permission).

Parameter		Copper	Lead	Zinc
Influent	cumulative mass of metals applied	540 mg	340 mg	4400 mg
Mulch	increase in metal mass in mulch	110 mg	35 mg	1500 mg
	% of influent sorbing to mulch	20%	10%	34%
Plants	factor of increase in plant metal concentration	6.3 x	77 x	8.1 x

Additional experiments were performed with the flowrate either doubled or halved or with the flow duration either doubled or halved. The additional experiments gave very similar results as the prior studies, with one exception: high flow rates or long flow durations sometimes resulted in overly high ponding depths. In such cases, the inflow rate was reduced to simulate diversion of the inflow around an offline bioretention area, and that diverted inflow was mixed with the outflow in the final mass balance calculations. This operational strategy was found to lower the metal removals for the overflowing storms from a potential 99% reduction to as low as 66% (Davis et al., 2003).

Some experiments were performed to investigate the effects of influent pH and metal concentrations on effluent quality and pollutant removal. The pH was adjusted to 6 or to 8, and several experiments were run in the small box. The metals concentrations were either doubled (small box only) or halved (small and large box experiments). Reductions in metals concentrations from these experiments remained greater than 97%, meaning that moderate changes in pH or influent metal concentration did not significantly impact the pollutant removal efficiency (Davis et al., 2003).

2.3.3 Field Studies

To date, field studies completed by the University of Maryland team (Hsieh and Davis, 2003) have involved spraying synthetic runoff over bioretention areas to simulate storm events and retrieving grab samples of the drainage effluent. One of the purposes of the studies was to investigate the effect that variations in soil composition could have on pollutant removal mechanisms. For example, trace metal adsorption/desorption and phosphorus migration can both be affected by soil characteristics (Hsieh and Davis, 2003).

Initially two sites were tested, one in Greenbelt, MD, and another at Inglewood Plaza in Landover, MD. The Greenbelt facility was constructed in 1992, with approximately 5 cm of mulch, a thick growth of grasses, shrubs, and small trees, and a PVC underdrain at 114-cm depth. The Greenbelt synthetic storm experiment was performed in June, 1997, while the area was still damp from the previous rainstorm 4 days before. The Inglewood Plaza facility in Landover was constructed in 1998 and tested in 1999. It was constructed by the standards current at that time, with soil consisting of 50% sand, 20-30% leaf mulch, and 20-30% topsoil. The Landover facility was dry at the time of testing, but the young plants were frequently watered. Much of the soil surface at Landover was bare mulch. The hydraulic loading for both sites was 4.1 cm/hr for 6 hours, the same as for the initial box tests. The synthetic runoff was applied directly to the surface of the bioretention areas instead of through the curb inlets (Davis, 2005). Table 2.3 summarizes the influent and effluent pollutant concentrations and the calculated pollutant reductions from the Greenbelt and Landover field experiments.

Table 2.3. Pollutant removal summary for Greenbelt and Landover field studies (from Davis, 2003, used with permission).

	Cu (μg/L)	Pb (μg/L)	Zn (μg/L)	P (mg/L)	TKN (mg-N/L)	NH_4^+ (mg-N/L)	NO_3^- (mg-N/L)
Greenbelt Bioretention Area							
Input	66±32	42±35	530±72	0.52	3.5	2.6	0.33
Effluent	2±1	<2	<25	0.18±0.04	1.7±0.23	0.22±0.18	0.67±0.49
% Concentration Reduction	97±2%	>95%	>95%	65±8%	52±7%	92±7%	16±6%
Landover Bioretention Area							
Input	120±27	54±9.4	1100±20	0.83	6.9±0.81	-	1.3±0.05
Effluent	69±9.4	16±7	390±440	0.11±0.02	2.3±0.64	-	1.1±0.15
% Concentration Reduction	43±11%	70±23%	64±42%	87±2%	67±9%	-	15±12%

All metals concentrations were reduced by more than 95% for the synthetic storm at the Greenbelt facility. The effluent volume was not quantified, but was observed to be much less than the influent volume. Metals removals were not as great at the Landover facility, where the concentration reductions varied between 43 and 70%. The differences may have been due to variations in bioretention media (Greenbelt had more soil fines), facility age, plant growth and uptake, antecedent moisture conditions, measured variations in the influent concentrations, and the possible effects of sampling the Landover effluent from a crack in the manhole floor instead of from the underdrain (Davis, 2005).

Later in 2001-2002, six bioretention locations were tested, including one in Greenbelt, MD ("Beltway Plaza"), two in Hyattsville, MD ("NW HS-A" and "NW HS-B"), and three in Largo, MD ("Peppercorn", "Wash. Heights", and "Wash. Bus Park"). The synthetic runoff, whose composition is shown in Table 2.4, that was used for these studies was pumped at a loading rate of 3.2 cm/hr onto the bioretention areas. For each of these sites, the soil was tested for both the upper soil layer (10-15 cm) and the lower soil layer (15-40 cm). For most of the six sites in the 2001-2002 study, the silt/clay content of the upper layer was higher than for the lower layer, possibly limiting the infiltration rates of those bioretention areas. At sites "NW HS-A" and "Wash. Bus Park", the silt/clay contents limited the infiltration to such an extent that ponding occurred during the field studies. Ponding did not occur at the other locations (Hsieh and Davis, 2003).

Table 2.4. Composition of the synthetic runoff used for the field studies (from Davis, et al., 2001 and 2003).

Pollutant	Chemical	Concentration, mg/L
Nutrients		
Nitrate	Sodium Nitrate ($NaNO_3$)	2 (as N)
Organic Nitrogen	Glycine (NH_2CH_2COOH)	4 (as N)
Phosphorus	Dibasic sodium phosphate (Na_2HPO_4)	0.8 (as P)
Trace Metals		
Copper	Cupric sulfate ($CuSO_4$)	0.08
Lead	Lead chloride ($PbCl_2$)	0.08
Zinc	Zinc chloride ($ZnCl_2$)	0.6
Dissolved Solids	Calcium chloride ($CaCl_2$)	120
pH	HCl / NaOH	7.0

Figure 2.3 summarizes the results of the latter set of field studies in term of the reductions in pollutant concentrations. Oil and grease were removed effectively from all six bioretention areas. Suspended solids and lead were also removed fairly well. In the cases in which TSS escaped from a facility, it was found from visual inspection that the solids present in that effluent originated from the bioretention media itself rather than from the influent. Given the high correlation between the removal of lead and the removal of

TSS together with the visual observations, Hsieh and Davis (2003) suggested that most of the influent lead was filtered out along with the influent sediment particles while any lead in the effluent had been sorbed to the soil particles leaking out of the facilities. Phosphorus removal varied between 37 and 99% at the test sites. Efforts to correlate this variation with soil depth and texture failed to produce any significant relationship. However, a promising relationship appeared between phosphorus removal and soil percent organic matter, in which the bioretention areas that had higher soil organic matter content removed more phosphorus. None of the six sites was effective in removing nitrate or ammonium, although "Peppercorn" performed better than most with a 49% reduction in ammonium concentration, the result of either a greater ammonium adsorption to soil particles or a greater nitrification rate (Hsieh and Davis, 2003).

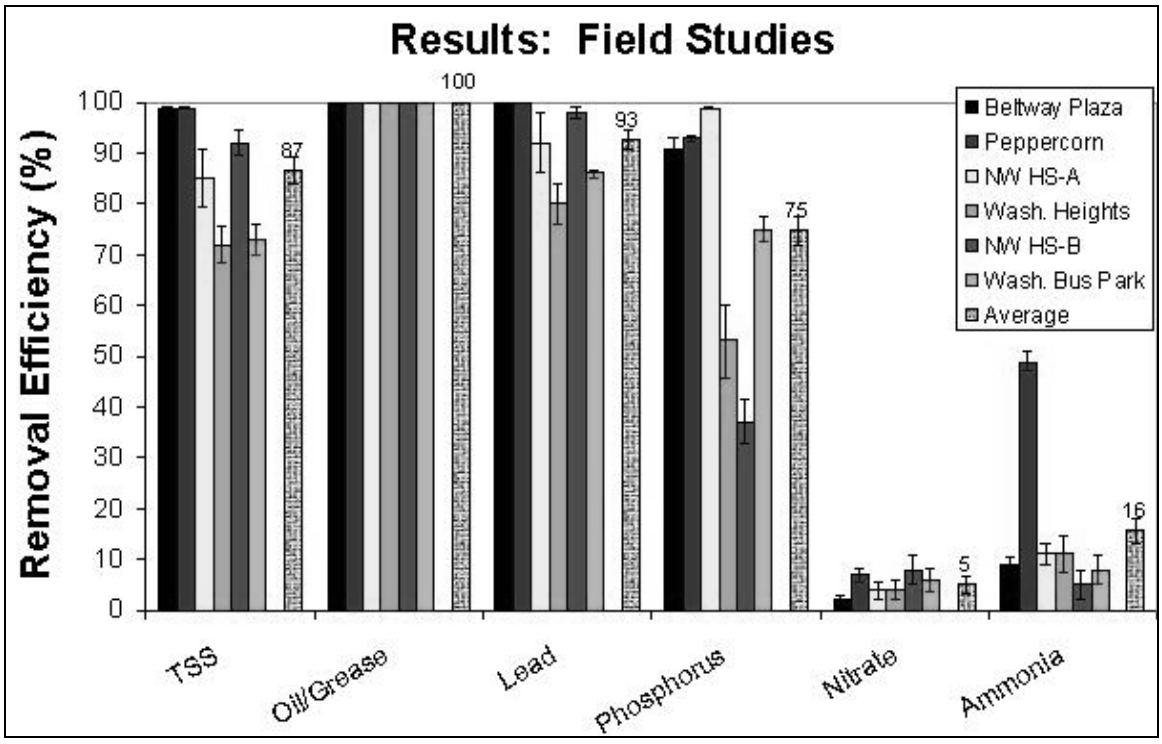

Figure 2.3. Field bioretention studies by the University of Maryland in 2001-2002 (from Davis, 2003, used with permission).

2.3.4 Denitrification in Bioretention Areas

Kim (2003) evaluated a redesigned bioretention area that included an anoxic, continually submerged zone below the underdrain depth that was employed to enhance the removal of nitrate through denitrification. A similar design is recommended by Prince George's County for full-scale bioretention areas that must remove nitrate (Prince George's County, 2001).

In a series of anoxic column studies, Kim compared several organic electron donors (alfalfa, leaf mulch compost, newspaper, sawdust, wheat straw, and wood chips) and a few varieties of elemental sulfur electron donors (large and small sulfur particles, used with and without limestone). The mass of each of the electron donors was based on a stoichiometric relationship between the mass of inflow nitrate and either the mass of total organic carbon present in the organic electron donors or the mass of sulfur for the inorganic electron donors. Following the column experiments, shredded newspaper was selected as the preferred electron donor because it provided excellent nitrate removals but did not degrade so rapidly as to cause the column to become anaerobic and the bacteria to produce sulfides. Shredded newspaper also had the advantages of being very inexpensive and readily available (Kim et al., 2003).

Kim et al. (2003) reported the stoichiometry for the organic electron donors as:

$$25\ CH_2O + 11.06\ NO_3^- + 11.06\ H^+ \rightarrow 1.94\ C_5H_7O_2N + 15.29\ CO_2 + 4.56\ N_2 + 4.3\ H_2O$$

For the sulfur / limestone columns, the stoichiometry was given as:

$$1.667\ S + 1.706\ NO_3^- + 0.32\ CO_2 + 1.04\ H_2O \rightarrow 1.627\ H^+ + 1.667\ SO_4^{2-} + 0.064\ C_5H_7O_2N + 0.821\ N_2$$

…and… $CaCO_3 + H^+ \rightarrow Ca^{2+} + HCO_3^-$

The final set of experiments featured a 76-cm by 40-cm pilot scale bioretention box. An 18-cm deep layer of sand and shredded newspaper served as the denitrification zone, and was underlain by an underdrain that curved upwards such that the sand and newspaper layer remained saturated between experiments. The upper 18-cm deep soil layer was a high-infiltration rate topsoil, partially separated from the lower layer by a plastic baffle to prevent short-circuiting. A series of synthetic storms was applied to the box. Between storm events the anoxic zone was left full of stagnant water to allow for maximum denitrification potential. The nitrate volumetric loading rate was 17 mg/day per liter of anoxic newspaper volume, where the anoxic zone contained 1.3 kg of newspaper mixed with 75 kg of sand. During the column studies, this nitrate loading rate had resulted in the greatest mass removal of nitrogen per day. In the pilot-scale study 70% of the influent mass of oxidized nitrogen ($NO_3^- + NO_2^-$) was removed.

Kim et al. (2003) also reported on several potential problems that appeared during the experiments. Some effluent turbidity appeared at start-up due to washout of the smallest newspaper or woodchip particles. At higher nitrate loadings, not all of the nitrate was reduced to N_2 gas but some was released as NO_2^-. When the nitrate was depleted, such as when fast-degrading alfalfa was used as the electron donor, the bacteria used sulfate as an electron acceptor, reducing it to malodorous sulfides. These sulfur-reducers were reported to be capable of performing "dissimilatory nitrate reduction", reducing the NO_3^- to NH_4^+, thus conserving the nitrogen in the water instead of removing it. When dormancy periods were tested, nitrate removal efficiency was reduced following each dormancy, but generally recovered after 1 to 3 days of re-exposure to nitrate.

2.3.5 Current Work

Davis (2005) is currently conducting a long-term study of a pair of bioretention cells at the University of Maryland in College Park. The inflow and the cell outflows are monitored and sampled automatically, and the cells are protected from groundwater interaction by impermeable membranes. Two novel approaches have been implemented in these bioretention cells, the inclusion of a continually-submerged layer for denitrification and the use of *Thlaspi* plants that are known to accumulate higher metals concentrations than other plants. Although final results have not been published at this writing, more information may be obtained at http://www.ence.umd.edu/~apdavis/Rain%20Gardens.htm.

2.4 University of Virginia Studies

Yu et al. (2001) reported on the results from a study of an off-line bioretention area constructed in 1998 at Monticello High School in Charlottesville, Virginia. The bioretention area was slightly less than 1,100 ft^2, and drained 0.78 acres of impervious parking lot. Vegetation was sparse and young, so much of the surface of the bioretention area was bare mulch, as shown in Figure 2.4 from Estes (1999). Grab samples of influent and effluent were taken during storms between September and November of 1999, and average constituent concentrations computed from simple means. Flow data were not available. Each storm was preceded by at least 72 hours of dry weather and had a minimum rainfall depth of 0.10 inches, based on what the authors claimed were the EPA recommendations for studies of this kind. Reported reductions in constituent concentration were 53% for total suspended solids (TSS), 13% for total phosphorus (TP), 16% for COD, and 66% for oil and grease.

Figure 2.4. Photo of the Monticello High School bioretention area (from Estes, 1999, used with permission).

Yu and Langan (1999) also reported on the results from a study of a combined bioretention area and wet detention pond located along Route 17 in Warrenton, Virginia. The site received drainage from the highway, a local school, and some nearby grassy fields. Drainage flowed into first a small upper pond, then through the bioretention area, and lastly to a small lower pond. Background pollutant concentrations were compared between the upper pond and the lower pond to determine the dry-weather water quality benefits of the bioretention area. Based only on these dry weather observations, it was determined that the bioretention area had no impact on water quality. This may have been due to poor percolation into the bioretention soils and short-circuiting via a channel that had formed in the bioretention area.

2.5 North Carolina State University Studies

Hunt and Jarrett (2004) installed and monitored several bioretention areas in Greensboro, Chapel Hill, and Wilson, North Carolina. Results from 2 of those bioretention areas were included in the proceedings of the 2004 World Water and Environmental Resources Congress.

2.5.1 Greensboro Battleground Crossing Shopping Center

Hunt and Jarrett (2004) reported the study results from one of the bioretention areas constructed at the Battleground Crossing Shopping Center in Greensboro, NC. Local soils were clay loam with very low permeability (0.2 – 0.6 in/hr), so an underdrain was included in the bioretention design to ensure proper drainage. The Greensboro bioretention area was conventionally drained, with no designed saturated zone. During soil testing after construction, isolated pockets of saturated soil were located inside this bioretention area, but no water table formed. Organic sandy soil was used at this site, with a hydraulic conductivity near 15 in/hr and a depth of 4 feet.

Two tipping-bucket rain gages were installed at the Greensboro site. Runoff quantity and quality data were collected at the cell entrance. Automated samplers collected water samples from the underdrain for outflow water quality analysis. Data were collected for almost a year (time periods 6/1/02-7/21/02, 8/17/02-1/9/03, and 2/6/03-5/15/03), including 11 storm events, or about 3 storms per season. Table 2.5 shows the results of the pollutant load analysis.

Table 2.5. Inflow and outflow loadings and percent removals at the Greensboro bioretention area over the one year study period (from Hunt, 2004, used with permission).

Pollutant	Annual Mass In (kg)	Annual Mass Out (kg)	Percent Reduction or Increase
TN	2.53	1.51	40%
NO_3-N	1.194	0.297	75%
TKN	1.22	1.28	-4.9%
NH_3-N	0.595	0.601	-0.99%
TP	0.129	0.442	-240%
Ortho-P	0.048	0.052	-9.3%
Zn	0.459	0.009	98%
Cu	3.68	0.021	99%
Pb	0.016	0.003	81%
Fe	0.128	16.845	-13,000%
TSS	17.9	48.4	-170%

Regarding performance of the Greensboro site, Hunt and Jarrett (2004) concluded the following:.

- This bioretention cell showed good removal efficiencies for metals. Hunt and Jarrett suggest that the slightly lower removal efficiency for lead than for the other metals was related to the very low inflow concentrations of lead.
- Both nitrate reduction and total nitrogen reduction were unexpectedly good, possibly due to denitrification occurring in the isolated pockets of saturated, anaerobic soil that were identified during soil sampling.
- There was little TSS inflow to the bioretention cell because the watershed was stabilized. However, soil particles did leak into the outflow, causing an negative removal efficiency for TSS.
- The fill soil used for the bioretention area had a high phosphorus content. When some of this soil leaked in the outflow, it caused a negative removal efficiency for phosphorus.
- The negative iron removal efficiency may also be explained by iron bound to escaping soil particles, or it may be explained by anaerobic biological processes dissolving iron inside the saturated soil areas.

2.5.2 Chapel Hill University Mall

Hunt and Jarrett also reported the study results from on of the bioretention cells constructed at another shopping center, in Chapel Hill, NC. As with the Greensboro site, native soils in Chapel Hill had very low permeability, so an underdrain was included in the bioretention design. The watershed drainage area was 0.28 ac, and the bioretention area occupied 6.6% of this area. The bioretention cell was backfilled with 2 feet of sandy media that had a permeability of between 1.3 and 3.1 in/hr.

A tipping bucket rain gage was used to measure precipitation at the Chapel Hill site. Inflow quantity and quality were measured at the entrance, and the underdrain flow was sampled automatically. Data were collected for about 10 months from June 2002 to April 2003. The results of a load analysis on that data are shown in Table 2.6.

Table 2.6. Inflow and outflow loads and percent removal over the study period for the Chapel Hill bioretention area (from Hunt, 2004, used with permission).

Pollutant	10-Month Mass In (kg)	10-Month Mass Out (kg)	Percent Reduction or Increase
TN	0.608	0.365	40%
NO_3-N	0.093	0.081	13%
TKN	0.515	0.284	45%
NH_3-N	0.328	0.045	86%
TP	0.139	0.048	65%
Ortho-P	0.059	0.016	69%

Regarding performance of the Chapel Hill site, Hunt and Jarrett (2004) had the following comments:

- In the few storm events for which Chapel Hill TSS was measured, the outflow TSS was observed to be lower than the inflow TSS (unlike the Greensboro bioretention cell). This net removal, rather than addition, of TSS probably accounts for the much higher removal of total phosphorus observed at Chapel Hill compared to Greensboro.
- TKN removal rates were higher for Chapel Hill than for Greensboro, but nitrate removal was lower. Total nitrogen removal was about the same for both sites. Hunt and Jarrett suggest that the differences are explained by the greater sandy uniformity and lower organic matter content of the Chapel Hill soil. Perhaps the Chapel Hill bioretention cell did not have the isolated anaerobic pockets that contributed to the high denitrification rates observed in Greensboro, or perhaps there was not enough organic matter food to support as much denitrification.

2.5.3 Comparison of Seasonal Flow Reductions

Percent flow reductions were compared for storms during each of the four seasons. Both the Greensboro and the Chapel Hill bioretention areas reduced stormwater flow much more during the warm seasons (spring, summer, and fall) than during winter. Because the load-based percent reductions for the pollutants were calculated based on concentration and flow, the seasonal change in flow reduction could be an indication of important seasonal differences in load reduction as well that are not visible in the net annual results.

2.6 Villanova Bio-Infiltration Traffic Island

Emerson and Traver (2004) reported on the retrofit of an existing grassed area in a parking lot on the Villanova University campus to create a bioretention area. Water quality data have not been reported, but hydrologic analysis has been underway for a three year period. The 50,000 square foot watershed consisted of 52% impervious surface, most of which was parking area. The bioretention area was constructed by excavating the existing soil, mixing it with 50% sand, and filling the hole with the altered soil mixture. The surface depression had an average depth of 2 feet, which allowed for up to 1,220 ft^3 of ponded water storage. This site did not include an underdrain or a gravel bed because the existing soil was found to be sufficiently permeable to allow for infiltration through to groundwater.

Infiltration rates, which were measured by the rate of lowering in the ponded water level, were not observed to have any consistent decreasing trends. This suggests that the site has not yet experienced any clogging of the soil pores with fine sediment. However, seasonal variations were observed, with similar results to those seen by Hunt and Jarrett (2004) in North Carolina. During the warm months of late summer, the infiltration rate at the Villanova bioretention area was found to be significantly higher than observed during late fall and spring. Other variations in the infiltration rate were explained by changes in soil moisture content. Infiltration rates ranged between 0.13 and 0.54 in/hr, and generally no overflow from the facility was observed until after at least one inch of rainfall. Computer modeling of the site, assuming an average infiltration rate of 0.22 in/hr, showed that the facility should be capable of reducing the peak flow rate by 27% for a 25-year storm. Computer modeling also predicted that the BMP would reduce the annual watershed runoff volume from 16 inches to 4.8 inches (Emerson, 2004).

2.7 Filterra®, Concrete Bioretention in a Box

A schematic of a Filterra bioretention system was shown previously in Figure 1.5. The Filterra® system has been described as capable of removing up to 95% of total suspended solids, 82% of total phosphorus, 76% of total nitrogen, and 91% of trace metals such as copper. The amount of runoff from a given site that can be so treated may be close to 90-95%, depending on the specific design, watershed characteristics, and the treatment area in proportion to the watershed area (Coffman, 2004).

2.8 Trondheim, Norway

Nordberg and Thorolfsson (2004) of the Norwegian University of Science and Technology detailed a research plan for studying bioretention in cold climates. Trondheim, Norway, (N63°20', E10°18') was reported to have average July temperatures of 13.9°C, average January temperatures of -1.3°C, and was described as occasionally experiencing temperatures of -20°C for a week at a time. Such extreme low temperatures might be expected to significantly reduce the effectiveness of bioretention in removing pollutants during the winter months. The Risvollan watershed, where the planned research will be conducted, was reported to have the advantage of several years' previous hydrologic study and already having much of the necessary equipment in place.

The planned small-scale bioretention area to be studied in Trondheim will consist of a 1 meter by 1 meter box filled with soil and local plants, suspended by the four corners to settle in a hole in the ground. In this way, the box may be adjusted to remain level and may be weighed continuously to monitor the mass of stored water, snow, and ice. Outflow from the underdrain and overflow from large storms will be collected nearby in sheltered tanks whose water levels will also be continuously measured. The measurement of water volumes rather than flow rates is anticipated to enable calculation of an accurate water balance during all seasons of the year (Nordberg and Thorolfsson, 2004).

2.9 Florida Aquarium Study

Rushton (2001) of the Southwest Florida Watershed Management District conducted a study involving the incorporation of vegetated swales and small garden areas into a parking lot at the Florida Aquarium. The swales and garden areas are shown in Figure 2.5. The study results showed that, despite not having been designed for bioretention, the vegetated areas with sandy Florida soils functioned as bioretention areas, and were observed to infiltrate a significant portion of the runoff. The swales and vegetated areas were designed as part of a series of BMPs including a vegetated strand and a wet pond. Part of the objective of the project was to compare several drainage areas, shown in Figure 2.5, using different paving types and either vegetated or non-vegetated swales.

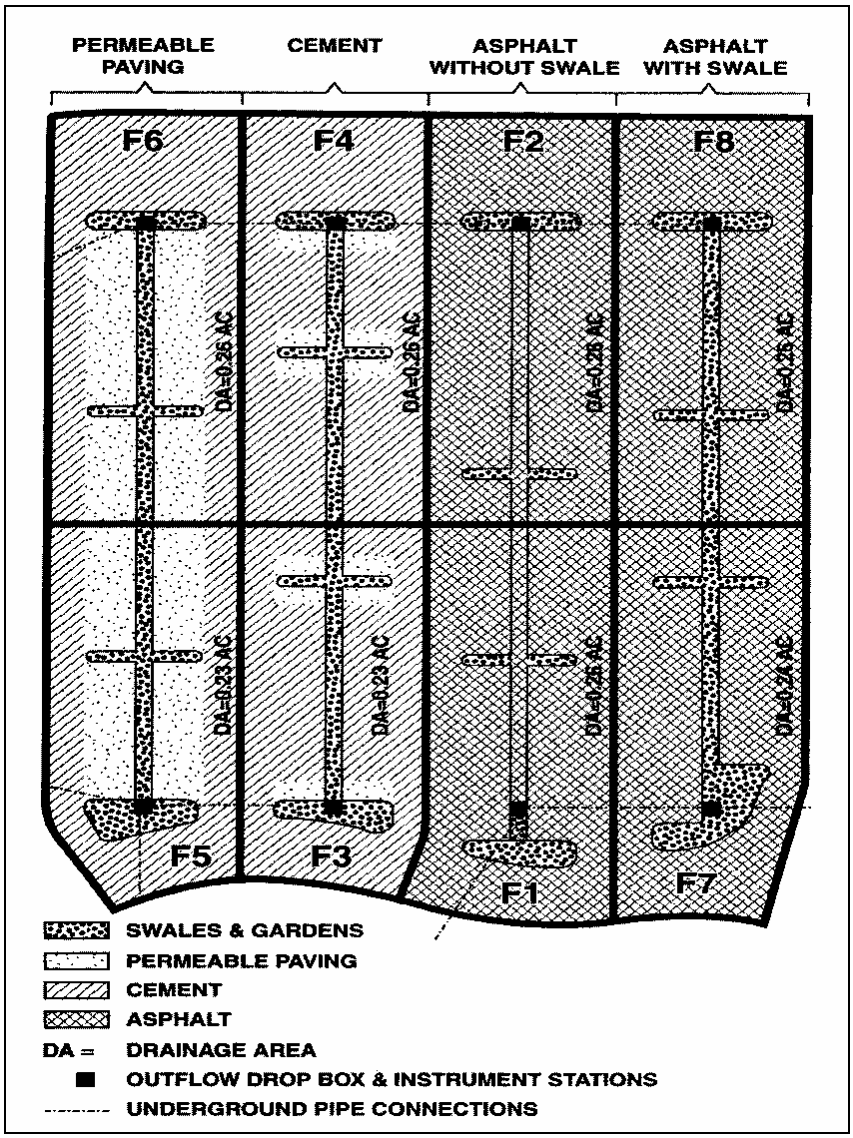

Figure 2.5. Drainage areas for the Florida Aquarium study, showing different pavement types and the use of vegetated swales and gardens (from Rushton, 2001, used with permission).

During the test period, the normal asphalt drainage area (labeled as F2 in Figure 2.5) without vegetated swales converted 55% of rainfall to runoff. The asphalt or concrete drainage areas with vegetated swales only produced 30% of the rainfall as runoff, representing a 38% reduction in flow volume. Adding a larger vegetated area at the end reduced the flow by an additional 50% (the odd-numbered drainage areas in Figure 2.5). Although the soils for the swales and vegetated areas were not modified for bioretention purposes, it should be noted that the local soils were naturally sandy and had high infiltration capacities. As a result, despite not having been designed or named as "bioretention" areas, the swales and vegetated areas helped to perform the same infiltration reduction of stormwater flow (Rushton, 2001).

Results from the first year of the study are shown in Table 2.7 (Rushton, 2001). Rain during the first year was found to be slightly less than average for the region. The second year had similar results, but might not be considered as characteristic because of a severe drought. The vegetated swales were effective in keeping metals pollution close to its source. Sediment tests at the end of the study showed that sediment-bound metals remained stationary and did not migrate downward significantly or contaminate the groundwater. Phosphorus concentrations were actually increased by the vegetated swales. The parking lot runoff itself contained virtually no phosphorus, but the vegetation and soil in the swales did, so presumably the phosphorus measured in those outflows came from the swales themselves.

Table 2.7. Results from Year 1 of the Florida Aquarium Project (from Rushton, 2001, used with permission).

Constituent	Percent Pollutant Load Reduction (compared to area F2, asphalt with no vegetated swale)		
	F8: Asphalt + vegetated swale	**F4: Cement + vegetated swale**	**F6: Porous Pavement + vegetated swale**
Ammonia	46%	73%	85%
Nitrate	44%	41%	66%
Total Nitrogen	4%	16%	42%
Orthophosphorus	-180%	-180%	-74%
Total Phosphorus	-94%	-62%	3%
Suspended Solids	46%	78%	91%
Copper	23%	72%	81%
Iron	52%	84%	92%
Lead	59%	78%	85%
Manganese	40%	68%	92%
Zinc	46%	62%	75%
Reduction in Runoff Coefficient	38%	42%	66%

* Phosphorus loads increased with vegetated swales.

The vegetated parking island areas and swales of the project demonstrated that there are many BMPs that are very similar in function to bioretention but may use different names. Rushton (2001) commented:

> "The garden areas would probably reduce runoff even more if they had been constructed with proper soils according to the low impact development design criteria which are identified by them as bioretention areas (www.lowimpactdevelopment.org). […] The garden areas in our study included existing soil and were only slightly recessed below grade when compared to the surrounding parking lot, instead of the 16 to 20 cm maximum suggested in the [Low Impact Development] manual and the garden depressions were not as deep as the swales."

Even though the design deviated from standard practice, the pollutant load reductions resulting from the swales and vegetated areas were significant. Extra pollutant removal was observed by combining several BMPs in an overall low impact development design, including features such as porous pavement, vegetated swales, a larger vegetated strand, and finally a wet pond (Rushton, 2001). Other areas of the country have also employed vegetated swales to reduced runoff volume and improve water quality. Seattle, Washington, has several low impact development projects underway, including the installation of vegetated swales and terraced cascades to the sides of many roads (Seattle Public Utilities, 2003).

2.10 Somerset Heights Subdivision

Prince George's County, Maryland, has sponsored a study on the effectiveness of Low Impact Development (LID) on stormwater hydrology and water quality (Cheng et al., 2004). In the Somerset Heights Subdivision, two small watersheds, developed using LID and conventional practices, were monitored for both water quantity and quality. At this writing, two years of data have been collected. The subdivision design did not fully follow the now-current standards for Low Impact Development, and the LID watershed had just been constructed and was not fully stabilized at the time monitoring began. Even so, many of the results were very encouraging in terms of the potential LID benefits (Cheng et al., 2004).

The LID watershed contained roughly 36% impervious surface, while the conventional development had only 30% impervious surface, but the more important difference lay in the discontinuity of the impervious areas in the LID development. The conventional watershed had curb-and-gutter with conventional stormwater drainage pipes. The LID site lacked curbs and gutters, and instead employed grassed swales for most drainage, and had bioretention areas on individual lots and along the swales. For the LID watershed, pipes were only used to carry water under driveways and roads and to convey flows that were too heavy to be safely contained by the swales (Cheng et al., 2004).

During the first two years of the study, the LID site had 20% fewer runoff events, 20% less total runoff volume, and an average of a 44% reduction in peak flow rate on a per-acre basis. Reductions in peak flowrate from the LID site were more significant after longer dry periods. The site generally required 24 hours to recover its storage and infiltration capacity during the growing season and even longer during the winter. The LID watershed sometimes continued releasing water for several days after a storm, probably because the gage was located below the ground surface and the flows included not just surface water but also groundwater. The gage for the conventional site was close to ground level and was not impacted by groundwater. By examining the storm hydrographs, the authors determined that 25.5% of the total LID flow came from groundwater or interflow. As a result, while the total flow volume from the LID site was only 20% less than from the conventional site, the surface runoff volume was 40% less than that from the conventional site (Cheng et al., 2004).

In the first two years, about 66% of the conventional runoff and about 69% of the LID runoff were sampled for water quality using automatic composite samplers. Event mean concentrations from these samples were then applied to the total runoff volume to estimate the loading rates for various pollutants, which are shown in Table 2.8 (Cheng et al., 2004).

Table 2.8. Average pollutant loading from the first two study years (from Cheng et al., 2004, used with permission).

Parameter	Conventional Loading (lb/acre)	LID Loading (lb/acre)	% Difference
Total Nitrogen	6.57	6.39	2.74%
Nitrate / Nitrite	1.64	1.07	34.76%
TKN	4.92	5.33	-8.33%
Total Phosphorus	1.11	1.55	-39.64%
TSS	121.86	104.45	14.29%
Copper	0.0184	0.0117	36.41%
Lead	0.0057	0.0045	21.05%
Zinc	0.0682	0.0433	36.51%

Pollutant loadings from the LID site were found to be reduced for metals in comparison to the conventional site, but increased for the nutrients TKN and total phosphorus. The increase was probably due to the fact that the LID subdivision was new while the conventional subdivision was more than ten years old. The authors noted that homeowners in new subdivisions often apply more fertilizers, so the nutrient loading from the LID subdivision is expected to decrease over time as the site becomes more stabilized (Cheng et al., 2004)

Rainfall for the first study year was slightly less than average, and for the second study year was only 63% of average. The data from these dry years may not be indicative of normal or wet years, so it is fortunate that the sampling program is continuing (Cheng, 2004).

2.11 Computer Model at Oklahoma State University

Christianson, et al. (2004) created a spreadsheet-based model for determining the size requirement of a bioretention area in order to meet pollutant removal requirements. The Green-Ampt model (also discussed in Charbeneau, 2000) was used for the infiltration component, and the Freundlich isotherm (also discussed in Watts, 1998) was used to predict pollutant adsorption to soil particles. A series of column adsorption studies are currently underway to generate data for the Freundlich isotherms, while plans are being finalized to validate the model by testing a series of bioretention boxes similar to those used by Davis et al. (2001).

2.12 Effects of Soil Compaction on Infiltration Rates

Field and laboratory tests conducted by Pitt, Chen, and Clark (2002) indicated that the soil compaction typical of urban settings can substantially reduce the infiltration rate. The causes of most of the reduced infiltration capacity in urban settings included construction activities, uses such as pedestrian and motor traffic, and replacement of deep-rooted native plants with shallow-rooted grasses. Soils were reported to

recover some infiltration capacity over time due to root growth and the actions of soil insects and other digging animals, but recovery may take decades.

To compensate for reduced infiltration in urban settings, several varieties of infiltration practices have been implemented. The success of most of these has been limited due to clogging with silt and compaction by foot traffic. Pitt, et al. (2002) concluded that bioretention practices appear to be "a more robust solution", and have the added advantage of allowing soil amendments such as compost. Compost amendments can significantly improve infiltration and help protect groundwater from trace metal pollution. Unfortunately, large quantities of fresh compost can also leach nutrients into the soil water, but using a smaller amount of compost may decrease this risk while providing the same benefits (Pitt et al., 2002).

Infiltration of urban stormwater may present dangers to potable groundwater supplies. For several potential groundwater pollutants, Pitt, et al. (2002) considered potential mobility through soils, typical abundance in stormwater, and capacity to be removed by initial filtration of the stormwater. They concluded that stormwater salts and enterovirus pathogens had a high potential for reaching groundwater after infiltration of stormwater through a bioretention area. A moderate potential for groundwater pollution was presented by other pathogens, some organics, and nitrate. Trace metals were considered to have a low potential for groundwater pollution through bioretention areas due to their low mobility through soils.

Pitt, et al. (2002) also performed a series of tests in the field to compare the infiltration rates at several sites. Infiltration rates were compared by soil classification: clayey versus sandy, degree of compaction, and degree of soil water saturation. When comparing dry, noncompacted soils, clayey soils had slightly lower average infiltration rates than sandy soils. The degree of compaction had a significant effect on both sandy and clayey soils, reducing the average infiltration rate by more than 90%. Interestingly, the degree of water saturation had a significant effect on clayey soils but not on sandy soils, lowering the average infiltration rate by more than 90% for both compacted and noncompacted clays. These results offer yet another reason to avoid using clays in bioretention areas; the frequent saturated conditions found there would severely reduce the infiltration rate of any clays found in the bioretention soils.

2.13 Summary of Pollutant Removal Results

There was tremendous variation between the pollutant removal rates observed in each study. Significant removal efficiencies were observed at many sites, while at other sites negative pollutant removal occurred. The results from each study are briefly summarized in Table 2.9.

The measurement methods used in these studies were divided between calculating a concentration reduction and a mass load reduction. Most removal rates were positive, indicating that the bioretention areas significantly improved water quality for that compound. However, in some cases negative removal rates were calculated, for example in Hunt and Jarrett (2004), Rushton (2001), and Cheng et al. (2004), meaning that more of certain pollutants were carried out of those bioretention areas than entered them. Table 2.9 demonstrates the wide ranges of both positive and negative removals that have been observed at a variety of bioretention areas and LID sites, and the virtual impossibility of selecting any single value as the *typical* bioretention removal efficiency.

Table 2.9. Summary of pollutant removal rates from several water quality studies.

Study	Researchers	Measurement Method	Nitrogen	Phosphorus	Trace Metals	Other	Comments
Filterra ® Laboratory Experiments	Coffman and Siviter (2004), and Americast (2004)	mass load reduction	76% TN	82% TP	91% Cu	95% TSS	No information was given about the experiment methods.
Small Box Lab Experiments	Davis, Shokouhian, Sharma, and Minami (2001)	concentration reduction	75% TKN 60% NH_4^+	71% TP	98% Cu >98% Pb >97% Zn		Study of several storms with artificial runoff in a laboratory setting.
Large Box Lab Experiments	Davis, Shokouhian, Sharma, and Minami (2001)	concentration reduction	68% TKN 79% NH_4^+ 24% NO_3^-	81% TP	92% Cu >98% Pb >98% Zn		Study of several storms with artificial runoff in a laboratory setting.
Greenbelt, MD	Davis (2003)	concentration reduction	52% TKN 92% NH_4^+ 16% NO_3^-	65% TP	97% Cu >95% Pb >95% Zn		Study of 1 storm with artificial runoff.
Inglewood Plaza, Landover, MD	Davis (2003)	concentration reduction	67% TKN 15% NO_3^-	87% TP	43% Cu 70% Pb 64% Zn		Study of 1 storm with artificial runoff.
Other MD Sites	Hsieh and Davis (2003)	concentration reduction	5 – 49% NH_4^+ (16% average) 2 – 7% NO_3^- (5% average)	37 – 99% TP (75% average)	80 – 100% Pb (93% average)	100% Oil & Grease 72 - 99% TSS (87% average)	Study of 1 storm at each of 6 sites with artificial runoff. Range of concentration reductions and average.
Nitrate Removal Laboratory Bioretention Box	Kim (2001)	mass load reduction	70% NO_3^-				Incorporating shredded newspaper with an anoxic zone into a bioretention box in a laboratory setting.

Study	Researchers	Measurement Method	Nitrogen	Phosphorus	Trace Metals	Other	Comments
Charlottesville, VA	Yu (2001)	concentration reduction		13% TP		53% TSS 16% COD 66% Oil & Grease	field study over 3 months
Warrenton, VA	Yu (1999)	There was no measurable pollutant reduction in this bioretention area due to poor infiltration and short-circuiting.					
Greensboro, NC	Hunt and Jarrett (2004)	mass load reduction	-1% NH_4^+ -5% TKN 75% NO_3^- 40% TN	-9% OP -240% TP	99% Cu 81% Pb 98% Zn	-170% TSS -13,000% Fe	1 year (11 storms) of field study
Chapel Hill, NC	Hunt and Jarrett (2004)	mass load reduction	86% NH_4^+ 45% TKN 13% NO_3^- 40% TN	69% OP 65% TP			10 months of field study
Florida Aquarium Project, vegetated swales	Rushton (2001)	mass load reduction	45% NH_4^+ 44% NO_3^- 9% TN	-180% OP -94% TP	23% Cu 59% Pb 40% Mn 46% Zn	46% TSS 52% Fe	Comparison of load reduction from the addition of vegetated swales to an asphalt parking area.
Somerset Heights Subdivision, LID study	Cheng, Coffman, Zhang, and Licsko (2004)	mass load reduction	-8% TKN 35% NO_3^- 3% TN	-40% TP	36% Cu 21% Pb 37% Zn	14% TSS	New LID subdivision versus an older conventional subdivision. New homeowners frequently use more fertilizers.

3 Methods and Materials

3.1 Site Description

The Kingsbrooke bioretention area was designed and constructed in 1993-94 as one of the first applications of the bioretention concept in Prince William County. The site is located in Bristow, Virginia, just outside the city of Manassas. The area is designed in a weep garden configuration (refer to Figure 1.3) with three 3-foot high terraces separated by gabion walls. Flow is intended to filter into the soil of each terrace and then flow out through the gabion wall. The design plans state the total drainage area as 13.83 acres and the bioretention area as 11,713 square feet (Dewberry & Davis, 1994). Thus the bioretention area takes up less than 2% of the total drainage area. The design plans acknowledge that the site was under-designed and was intended to only treat a portion of the runoff. Figures 3.1 and 3.2 show two views of the bioretention area, an overview of the entire site with instrumentation and a closer view of one of the gabion walls. The H-flume for the outflow gage and its associated equipment shed are plainly visible in the foreground of Figure 3.1. Figure 3.2, a closer-range photograph taken in late summer of 2004, gives a good indication of the vegetative cover present at the site: mostly grass with sparse trees and bushes.

Figure 3.1. A view of the Kingsbrooke bioretention area in early spring of 2004, soon after the first three lysimeters were installed.

Figure 3.2. One of the 3-foot high gabion walls separating the bioretention terraces.

3.1.1 Soils

There were several discrepancies between the official design recommendations from Prince George's County (Winogradoff and Coffman, 2002), the design plans for the Kingsbrooke bioretention area (Dewberry & Davis, 1994), and the actual site conditions found at Kingsbrooke. Although discrepancies were found in several areas, including the use of mulch as a groundcover and the care of plant materials in the bioretention area, the changes in soil composition had the greatest impact on the site performance as a BMP.

3.1.1.1 Prince George's County Bioretention Manual

The current bioretention design recommendations from the Prince George's County manual call for a homogeneous soil mix composed of 50% construction sand, 30% topsoil (with less than 5% clay content), and 20% leaf compost (Winogradoff and Coffman, 2002). A principal goal of these recommendations was to ensure that the soil had a high infiltration capacity.

3.1.1.2 Kingsbrooke Design Plans

The design plans for the Kingsbrooke bioretention specified:

> "a planting soil having a composition of at least 10 to 25 percent clay and […] of sandy loam or loamy sand texture. Loamy soils may be utilized for the planting soil but must consist of 35% sand. In addition, the furnished planting soil shall be of uniform composition, free of stones, stumps, roots, or similar objects larger than one inch." (Dewberry & Davis, 1994).

The design plans also called for 3 feet of topsoil above a 1-foot sand layer. Also specified was a mulch layer of "shredded hardwood or shredded wood chips or similar product […], well aged, uniform in color, and free of foreign material" (Dewberry & Davis, 1994). Dewberry & Davis (1994) also required that the planting soil meet the following criteria:

pH range:	5.5 – 6.5
Organic mater:	1.5 – 3.0%
Magnesium – Mg:	35 lbs./acre
Phosphorus – P_2O_5:	100 lbs./acre
Potassium – K_2O:	85 lbs./acre
Soluble salts:	not to exceed 500 ppm

Construction specifications called for soil to be "placed in lifts less than 18 inches and lightly compacted (minimal compactive effort) by tamping with a bucket from a dozer or a backhoe." (Dewberry & Davis, 1994)

3.1.1.3 Actual Site Conditions

No mulch was present at the site, and the groundcover was grass instead of ivy. Litter was also an unfortunate feature at this bioretention area, as it was found to travel through the storm sewer and be deposited on the upper terrace.

Soil samples were retrieved on July 12, 2004 using a hand auger. Both at that time and during installation of lysimeters, three distinct soil layers were encountered: (1) a brown clayey topsoil layer, (2) a reddish sand layer, and (3) a crushed bluestone layer. Bluestone is a trade term referring to a type of fine-grained arkosic or feldspathic sandstone (Bourget Flagstone Company, 2005). The hand auger could not penetrate beyond the crushed bluestone layer, suggesting that the bioretention area is underlain by fractured bedrock. A photo of those soil layers is shown in Figure 3.3, as they were encountered during lysimeter installation.

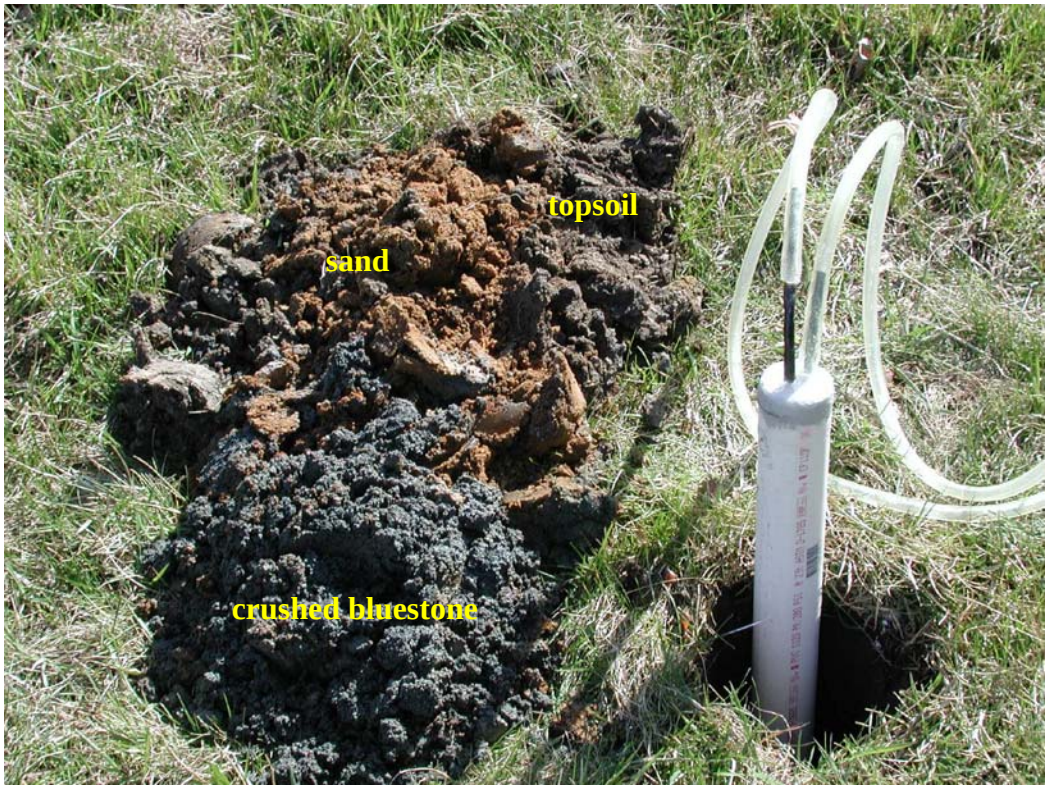

Figure 3.3. A photo of the soil layers encountered during installation of the lysimeter on the middle terrace.

Figure 3.4 shows a diagram of the estimated extent of the soil layers based on a visual assessment during the July 12 sampling. Table 3.1 gives the results of the mechanical soil tests performed by the Prince William County Department of Public Works Materials Laboratory (from the Report on Sample of Soil on July 28, 2004), and in Table 3.2 are the standard methods that were used during the Virginia Tech soil chemical analysis (results of which are shown later in the Results section).

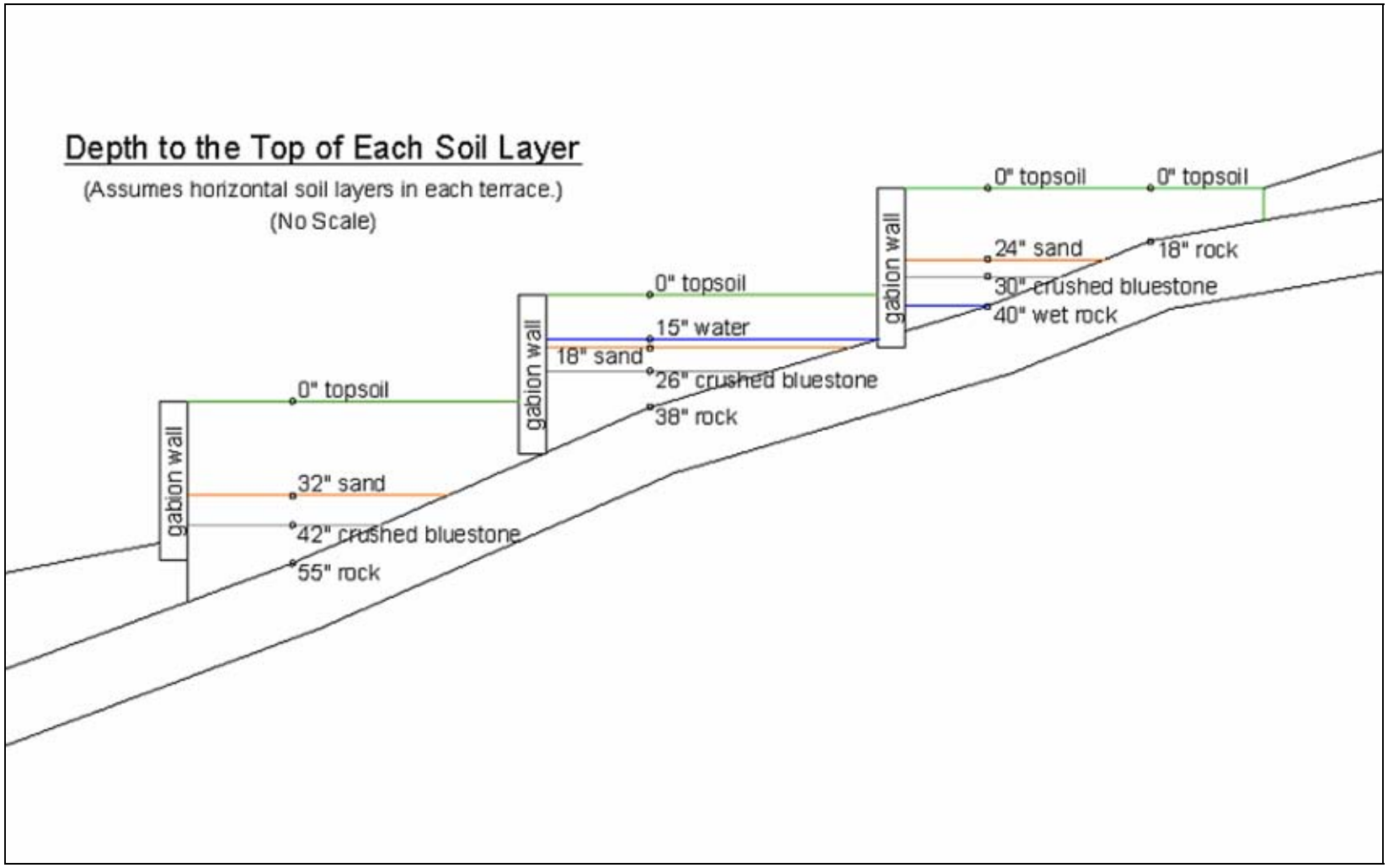

Figure 3.4. Estimated soil profile of the Kingsbrooke bioretention area, based on sampling performed July 12, 2004 with a hand auger.

The soil classifications given in Table 3.1 show that the topsoil at the Kingsbrooke bioretention area had a much higher clay content than is recommended by the current design recommendations (Winogradoff and Coffman, 2002). This high clay content must limit the infiltration capacity of the site, especially under wet conditions (Pitt, 2002).

Table 3.1. Results of mechanical soil tests performed by the Prince William County Department of Public Works on July 28, 2004.

Terrace:		**upper terrace, 1**			**middle terrace, 2**		**lower terrace, 3**						
sample depth (in.):		12	24	35	22	38	12	24	38	42	48	55	
sieve #	**size (μm)**	**% mass retained…**											**particle class**
20	850	6.0%	39.2%	51.5%	2.6%	45.7%	11.7%	13.1%	17.7%	22.4%	47.3%	17.7%	very coarse sand
40	425	3.5%	26.2%	15.9%	5.0%	18.0%	11.4%	7.8%	18.9%	17.0%	17.3%	12.1%	coarse sand
60	250	5.0%	12.0%	10.7%	13.3%	13.2%	14.6%	9.1%	11.7%	13.0%	12.0%	8.6%	medium sand
80	180	5.2%	4.7%	5.0%	9.7%	5.7%	7.7%	6.4%	5.6%	6.6%	5.6%	5.2%	fine sand
100	150	4.8%	2.9%	3.3%	7.7%	3.5%	5.0%	4.9%	4.0%	4.5%	3.6%	4.4%	fine sand
200	75	21.1%	7.6%	7.9%	26.2%	7.8%	18.8%	21.4%	19.2%	14.2%	8.6%	17.1%	very fine sand
smaller		54.3%	7.4%	5.7%	35.5%	6.1%	30.9%	37.3%	22.8%	22.2%	5.5%	34.7%	silt / clay
Revised Public Roads System Classification		silt clay A-6	granular sand A-1-8	sand granular A-1-8	silt clay A-7	granular sand	granular material A-2-6	clayey silt clay A-6	granular A-2-7	granular A-2-7	sand granular A-3	granular A-2-6	
Liquid Limit		31	non-plastic	non-plastic	53.4	non plastic	35.4	38.7	40.8	40.7	non-plastic	33.5	
Plastic Limit		19.3			30.5		23.3	24.7	26.7	25.3		22.4	
Plasticity Index		11.7			22.9		12.1	14	13.9	15.4		11.1	

Some of the soil samples collected in July of 2004 were analyzed chemically by Virginia Tech. Results of this analysis are shown in section 4.2, and the standard methods used are summarized here in Table 3.2.

Table 3.2. The following standard methods were used for the soil chemistry analysis (from personal communication with M.L. Daniel of the Occoquan Watershed Monitoring Laboratory in April, 2005).

Chemical Abbreviation	Chemical Name	Analytical Method	Reference
TP	Total Phosphorus	GLERL – SED NUTRIENT – 96	Standard Operating Procedures for Determining Total Phosphorus, Available Phosphorus, and Biogenic Silica Concentrations of Lake Michigan Sediments and Sediment Trap Material, NOAA/Great Lakes Environmental Research Lab, Ann Arbor, MI.
TN	Total Nitrogen by Combustion	ThermoFinnigan, FlashEA™1112 Operating Manual, 2001. ThermoFinnigan, Milan, Italy.	
TC	Total Carbon by Combustion		
TOC	Total Organic Carbon by Combustion Following Treatment with HCl		
NH3_N & OX_N	Ammonia and Nitrate (extraction)	Carter Martin R., Soil Sampling and Methods of Analysis, 1993, p.26. Lewis Publishers, Boca Raton, FL	
NH3_N	Ammonia (analysis)	EPA350.1	Methods for Chemical Analysis of Water and Wastes, EPA-600/4-79-020, Revised March 1983, USEPA, Washington, DC
OX_N	Nitrate (analysis)	EPA353.1	
	% Total Solids	SM2540G	Standard Methods for the Examination of Water and Wastewater 20th Edition, 1998. American Public Health Association, Washington, DC
EPB	Total Recoverable Lead	EPA 3050B Acid Digestion of Sediments, Sludges, and Soils, 1996.	
EZN	Total Recoverable Zinc		
ECU	Total Recoverable Copper		

3.1.2 Plants

The plants and groundcover actually identified at the Kingsbrooke bioretention site were significantly different than those specified in the design plans (Dewberry & Davis, 1994). Table 3.3 details those differences. Specifically, fewer trees and bushes were present on the site, and instead of using shredded hardwood mulch and ivy the site had mown turf grass. In addition, several trees on the site appeared to be unhealthy or were leaning sideways, as pictured in Figure 3.5. Fewer healthy trees would logically lead to a lower evapotranspiration rate than would have been anticipated in the design. The use of grass rather than mulch may have slightly increased the possibility of soil compaction as the grass was mowed regularly.

Table 3.3. Plants specified and plants found at the Kingsbrooke bioretention area.

Plant Common Name	Number Specified in Design Plans (Dewberry & Davis, 1994)	Number Found on Site	Comments
Trees			
Black Gun	17	11	
Eastern Red Cedar	41	10	a couple of cedars are tilted, almost falling over
Red Maple	61	6	
Willow Oak	13	4	
Sycamore	13	8	several appear unhealthy
Shrubs			
Witch-Hazel	22		
Winterberry	44		
Inkberry	58		
Japanese Bayberry	42		
Summersweet Clethra	39		
Arrow-Wood	30		
Nannyberry Viburnum	27		
Creeping Juniper	66	16	overgrown with long grass and weeds
total shrubs	328	79	
Ground Cover			
English Ivy	1800	-	
Turf Grass	-	everywhere	

The original design (Dewberry & Davis, 1994) called for fertilization at planting time with fertilizer tablets at the bottom of the tree and shrub planting pits and as a wet application for the groundcover. Fertilization was not called for as part of the regular maintenance schedule. These recommendations aligned well with the Prince George's County Bioretention Manual (2002). A representative of the landscape company engaged to maintain the Kingsbrooke site stated that no fertilizers were being applied to the site (from telephone communication with DH Custom Scapes in March, 2004). The landscaper also stated that grass clippings from mowing were not bagged, but were left on the surface of the bioretention area. Logically, this would mean that the clippings must ultimately decompose on the site, re-releasing their associated pollutants, including any nitrogen, phosphorus, and trace metals that had been incorporated into the grass biomass. Removing the plant clippings, as suggested by Davis et al. (2003) would be expected to increase the useful life of the bioretention area.

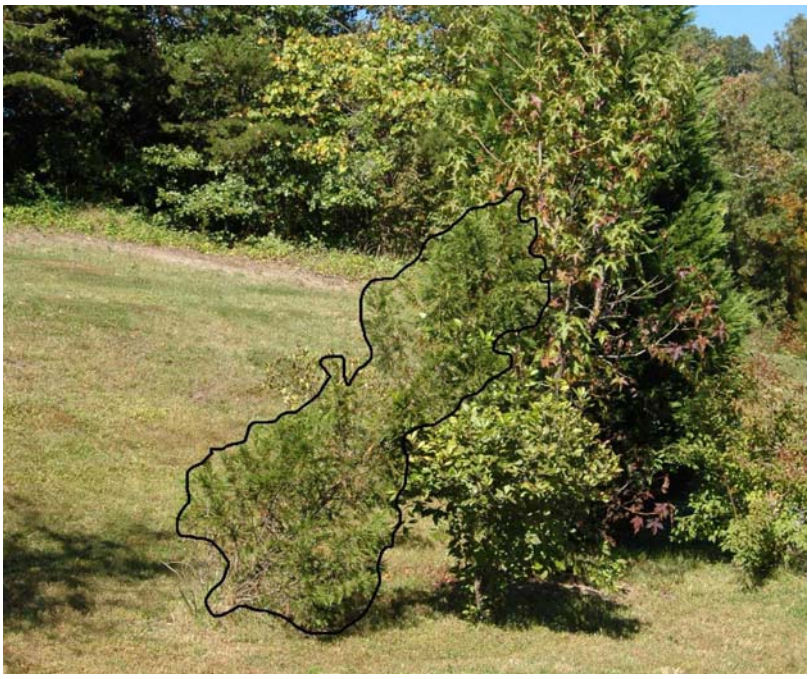

Figure 3.5. Photograph showing a partially-fallen tree at Kingsbrooke, demonstrating the poor health of some of the plants on the site.

3.2 Hydrologic Measurements

Inflows and outflows were measured using 3-foot H-flumes (U.S. Dept. of Agriculture, 1979) constructed locally at Dixie Sheet Metal in Falls Church, Virginia, coupled with continuously recording flowmeters (model 8210 by Sutron of Sterling, VA). H-flumes were chosen as the primary control devices at this site because of their ability to measure wide ranges of flowrates accurately without retaining sediment (Accura-Flo, 2005). The inflow gage H-flume is shown in Figure 3.6. The water depth in the H-flumes, used to find the flowrate, was measured using pressure transducers ($KPSI_{TM}$ by Pressure Systems, Inc. of Hampton, VA), capable of measuring up to 5psi with a ±0.05 ft accuracy in water depth measurements.

Figure 3.6. A photograph of the inflow gage H-flume and equipment shed.

Each gage was considered to be in a storm runoff condition when the stage exceeded 0.05 ft., and then to have returned to baseflow when the stage dropped back below 0.05 ft. At regular intervals, date/time, stage, flowrate in cfs (FLO), cumulative storm flow volume in cubic feet (TOTFLO), and any events such as storm beginning/ending or the collection of an automatic sample were recorded to a microcomputer data file maintained by the flowmeter. Table 3.4 shows an example of data from the outflow gage. Data were recorded at hourly intervals during low-flow conditions, once every 10 minutes during storm conditions, whenever a storm began or ended, and whenever an automatic sample was collected. During storms, flow-weighted composite samples were created by combining several individual water samples, each of which was collected automatically after a standard volume of stormwater had passed through the gage. Samples were collected automatically using a Manning VST portable vacuum sampler (model VST by Manning of Georgetown, TX). The standard flow volume between samples could be changed from one storm to another depending on, for example, how much rain was expected, with common values being 500 ft^3, 1000 ft^3, or 2000 ft^3 of stormwater. Hydrology measurements were taken from 11/10/03 to 12/18/03 and from 2/1/04 to 10/31/04, for a total of about 10 months data.

The recording precision was improved twice. When flow measurements restarted in February of 2004, the precision of the FLO column was increased from 0.01 cfs to 0.001 cfs. This improvement aided in calculating the low baseflow volumes. On March 19, 2004, the storm measurement recording frequency was increased from every 10 minutes to every 5 minutes, and for total storm volume the TOTFLO column precision was increased from 10 ft^3 to 1 ft^3. In both cases the electronic equipment had already been measuring to the higher precision, but only the lower precision had been written to the computer records. The higher precision numbers occupied more disk space, but greatly improved accuracy in computing the flow balance.

Table 3.4. A sample of some hydrology data collected at the outflow gage. Column definitions are shown below the table.

DATE1	TIME1	STAGE	FLO	TOTFLO	STORMDUR	SAMPLE	SKNT
12/14/2003	11:00	0.02	0.01	0.00	0.00	0	0
12/14/2003	12:00	0.03	0.01	0.00	0.00	0	0
12/14/2003	13:00	0.04	0.01	0.00	0.00	0	0
12/14/2003	13:13	0.05	0.01	0.00	0.00	1	0
12/14/2003	13:20	0.06	0.01	10.00	0.13	0	0
12/14/2003	13:30	0.08	0.03	20.00	0.30	0	0
12/14/2003	13:40	0.08	0.03	30.00	0.47	0	0
12/14/2003	13:50	0.11	0.04	50.00	0.63	0	0
12/14/2003	14:00	0.13	0.05	80.00	0.80	0	0
12/14/2003	14:10	0.15	0.07	120.00	0.97	0	0
12/14/2003	14:20	0.16	0.08	160.00	1.13	0	0

Column definitions for Table 3.4:

DATE1 and TIME1 are the date and time of the flow measurement.
STAGE is the depth (feet) of water in the H-flume.
FLO is the current flowrate (cfs).
TOTFLO is the cumulative flow over the storm. TOTFLO was reset to zero at then end of the storm or whenever a sample was collected.
STORMDUR is the cumulative duration of the storm (hours).
SAMPLE is a code indicating either the start of a storm (1), the end of a storm (3), or the automatic collection of a water quality sample (2).
SKNT is the cumulative number of water samples that have been collected so far during the storm.

When the water balance and pollutant loads were calculated, TOTFLO provided a more accurate measurement of cumulative flow volume during storms than did the FLO column because TOTFLO was calculated by the gage every minute while FLO was only printed every 10 minutes. However, the FLO column had to be used in calculating baseflow volumes. Taking extra care in deciding which column to use helped to ensure accuracy in the flow balance.

Rainfall data for the site was obtained from a nearby tipping-bucket rain gage operated by OWML at the water treatment plant on Lake Manassas. An additional tipping-bucket rain gage (model 6011 tipping bucket by Qualimetrics/Weather Measure of Sacramento, CA, and model 2107 recorder by telog of Victor, NY) was also installed at the Kingsbrooke site and began operation on June 23, 2004. Rain depth measurements were recorded to within ±0.01" every 10 minutes at both locations. Other weather data; including barometric pressure, air temperature, humidity, windspeed, and average cloud cover; were collected at the Occoquan Watershed Monitoring Laboratory in Manassas and at Dulles International Airport (NOAA, 2004) and were used to estimate evapotranspiration.

3.3 Chemical Measurements

Water chemistry data were collected for a total of about 8 months, from 11/10/03 to 12/19/03 and from 4/1/04 to 10/31/04. The constituents measured are listed below along with the standard abbreviations employed herein:

- ortho-phosphate phosphorus (OP)
- total phosphorus (TP)
- total nitrogen (TN), *directly measured only during October, 2004*
- ammonia plus ammonium nitrogen (NH_3 & NH_4^+, jointly abbreviated here as NH3_N)
- total Kjeldahl nitrogen (TKN)
- oxidized nitrogen (OX_N), *equal to nitrate + nitrite. However, nitrite concentrations were assumed to be negligible (Metcalf & Eddy, 2003), so effectively the oxidized nitrogen concentration equaled the nitrate concentration.*
- chemical oxygen demand (COD)
- total organic carbon (TOC)
- total suspended solids (TSS)
- soluble calcium (SCA)
- soluble magnesium (SMG)
- extractable lead (EPB)
- extractable zinc (EZN)

"S*oluble" metals were measured from a filtered water sample, while "extractable" metals were measured from an unfiltered sample that was treated with hydrochloric and nitric acid to solubilize metals that were associated with the sediments.*

The computerized flowmeters automatically collected flow-weighted composite samples during storm events. For one storm, the flow may be sampled after every 2000 ft^3, while another storm may have been programmed to sample every 500 ft^3. The frequency of sampling was sometimes changed between storms based on experience or on expected rainfall depths. In the Results section and the Appendices these storm samples and their event mean concentrations (EMC) are designated as I1 for inflow storms and O1 for outflow storms. Baseflow samples (designated O2) were collected in the outflow flume as grab samples once a week while water was present. A second set of baseflow samples were occasionally collected from the seepage that bypassed the flume and sprung up in the rip-rap just down-slope of it (sample type O3). This second baseflow sampling location is shown in Figure 3.7.

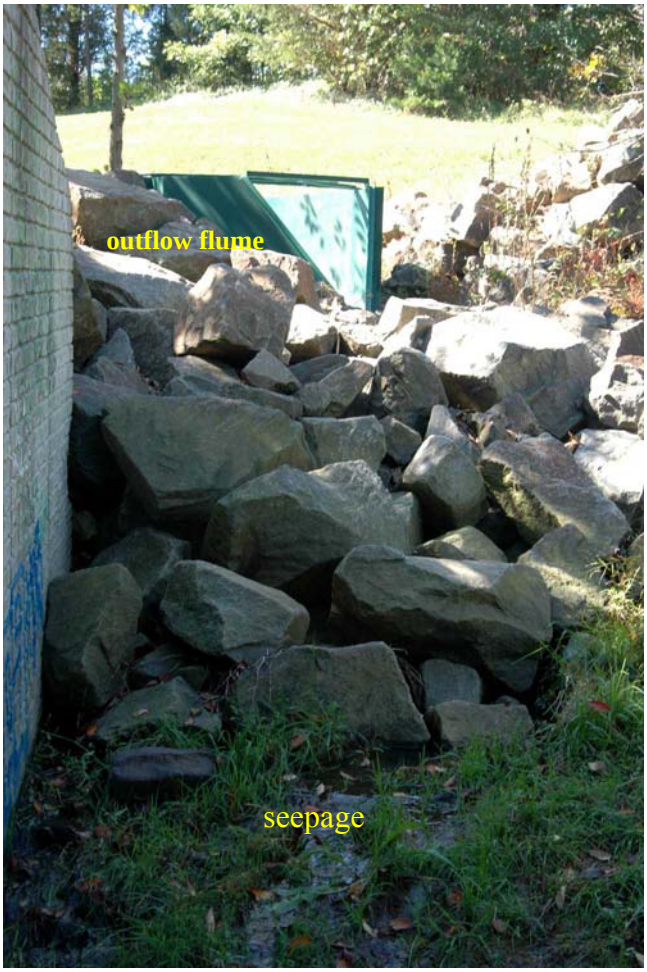

Figure 3.7. Location of the second baseflow sampling point.

Soil pore water in the bioretention area was sampled using suction cup lysimeters. The devices were constructed by Virginia Tech staff at the Occoquan Watershed Monitoring Laboratory (from personal communication with H. Post and G. Underwood or the Occoquan Watershed Monitoring Laboratory in May, 2005). Ceramic filter cups (Soilmoisture Equipment Corp., Santa Barbara, CA) at the end of each lysimeter were attached to PVC pipe and plastic tubing using epoxy glue. After the lysimeter holes were bored, each completed lysimeter was installed and surrounded with a silica flour mixture (Soilmoisture Equipment Corp., Santa Barbara, CA) to aid soil adhesion.

Initially three lysimeters were installed, one in each terrace. However, it was later discovered that the lysimeter in the lower terrace reached into a different soil layer than the others and samples collected from it had a significantly different chemistry. The upper two lysimeters (L1 and L2) reached into the crushed bluestone layer, but the third lysimeter (L3clay) reached into the clayey topsoil layer. Therefore, an additional, deeper lysimeter (L3) was installed on the lower terrace to reach into the crushed bluestone layer. Sampling from the first three lysimeters began on April 6, 2004, and from the L3 lysimeter on August 23, 2004.

A summary of all sampling locations and their abbreviations is shown in Figure 3.8. I1 referred to the inflow, and the lysimeter locations were abbreviated as shown. O1 referred to storms sampled at the outflow gage, while O2 referred to baseflow samples from the outflow gage and the O3 baseflow samples were taken from the rip-rap below the gage.

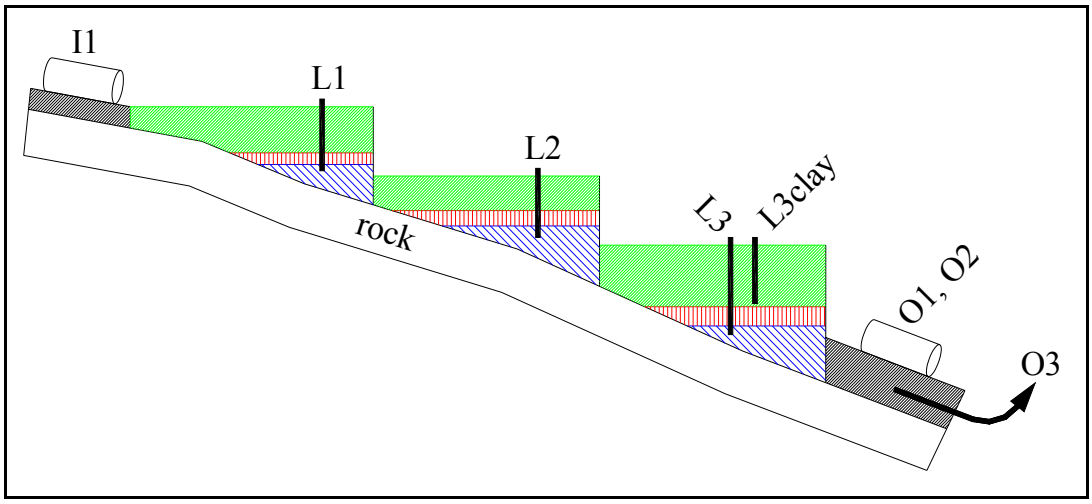

Figure 3.8. Diagram of locations for chemical sampling.

Table 3.5 summarizes the methods used for chemically analyzing the water samples. The quality assurance methods that were used are detailed in the *Quality Assurance Plan for the Occoquan Watershed Monitoring Laboratory* (OWML, 2001).

Table 3.5. The following standard methods were used in determining water chemistry (from personal communication with M.L. Daniel of the Occoquan Watershed Monitoring Laboratory in April, 2005).

Chemical Abbreviation	Chemical Name	Analytical Method	Reference
OP	Orthophosphate, OP	EPA 365.3	Methods for Chemical Analysis of Water and Wastes, EPA-600/4-79-020, Revised March 1983, USEPA, Washington, DC
TP	Total Phosphorus	EPA 365.4	
NH3_N	Ammonia	EPA 350.1	
OX_N	Nitrate + Nitrite Nitrogen	EPA 353.1	
TKN	Total Kjeldahl Nitrogen	EPA 351.2	
TURB	Turbidity	EPA180.1	
PH	pH	EPA150.1	
COND25	Conductivity	EPA120.1	
TN	Total Nitrogen	USGS I-4650-03	United States Geological Survey, National Water Quality Lab, Denver, CO
COD	Chemical Oxygen Demand	SM5220D	Standard Methods for the Examination of Water and Wastewater 20th Edition, 1998. American Public Health Association, Washington, DC
TSS	Total Suspended Solids	SM2540D	
THARD	Total Hardness (by calculation)	SM2340B	
TALK	Total Alkalinity	SM2320B	
SCA	Calcium (analysis)	ASTM D6919-03	Annual Book of ASTM Standards, Volume 11.02, 2004. ASTM International, West Conshohocken, PA
SMG	Magnesium (analysis)		
EPB	Total Recoverable Lead	EPA 200.7	Methods for the Determination of Metals in Environmental Samples, EPA-600/4-91-010, 1991. USEPA, Washington, DC
EZN	Total Recoverable Zinc		
EFE	Total Recoverable Iron		

3.4 Statistics

Two problems were encountered in determining certain pollutant concentrations. Firstly, several sample concentrations were below the method detection limits, requiring special consideration during the data analysis. Secondly, during some time periods, flow volumes could be calculated accurately but no water quality samples were collected, so those pollutant concentrations were unknown and had to be estimated based on the samples that were collected at other times. The methods used to address these problems are discussed in Sections 4.3.1 through 4.3.3; this section gives an introduction to some of the equations and terminology that were used. Most of the information here in Section 3.4 was taken from Berthouex and Brown, *Statistics for Environmental Engineers* (1994).

3.4.1 Detection Limit

In the chemical measurements for this project, concentrations were frequently below the method detection limit (MDL), especially for lead and zinc. The method detection limit is the value below which concentrations measurements lose their accuracy. Such measurements must be "censored", meaning that their actual values are not known but can only be stated as being less than the MDL concentration. For most of the comparisons of individual data, such low concentrations were approximated as equal to half of the MDL. Berthouex and Brown (1994) warn that this method is known to introduce bias, but it was used in a few cases for the sake of simplicity. For other statistical analyses, however, Berthouex and Brown recommend the following methods for dealing with data below the limit of detection or otherwise censored.

3.4.1.1 Median

The median is unaffected by censoring, as long as less than half of the samples are censored. For normally distributed data, the median may be used to estimate the mean. For log-normally distributed data, the median estimates the geometric mean of the data (Berthouex and Brown, 1994).

3.4.1.2 Probability Plots

There are methods for "trimming" points from datasets in order to estimate the mean and standard deviation, but they will not work in cases when more than half of the concentrations are censored for being below the MDL because they involve removing from the upper end of the dataset the same number of datapoints that were censored for being less than the MDL (Berthouex and Brown, 1994). However, graphical methods such as probability plots may provide useful information in most cases. In a typical probability plot, the concentration value for each datapoint is plotted versus that point's cumulative probability on a special probability scale. In an alternate method, each datapoint's z-score may be plotted instead of the probability value.

$$z_i = F^{-1}(p_i) = F^{-1}\left(\frac{i-0.5}{n}\right) \tag{3.1}$$

where z_i is the z-score of datapoint i, and
F^{-1} is the inverse cumulative normal probability distribution
p_i is the cumulative probability of the datapoint,
i is the rank of the datapoint,
such that the minimum has a rank of 1 and the maximum has a rank of n, and
n is the total number of datapoints.

For a normal distribution, z is the distance of a datapoint from the distribution mean in terms of standard deviations. When a normal distribution is graphed on a probability plot, the datapoints align on a straight line of equation…

$$x = \bar{x} + s \cdot z \tag{3.2}$$

where x_i is the value (concentration) of datapoint i,
$\bar{x}$ is the mean (concentration), and
s is the standard deviation of the sample values.

When data are censored for being below the MDL, the first point on the probability plot is at the MDL concentration and has a probability corresponding to the number of censored points. Even with a majority

of the data censored, a probability plot may still provide useful information such as suggesting whether the data are normally or lognormally distributed. Regression may even be used on such datasets to estimate the mean and standard deviation, although such calculations will increase the weight given to data at the upper tail of the distribution. As a result, any small uncertainties or measurement inaccuracies in those upper data points may have a large impact on the regression results. Appendix C shows a series of probability plots for the Kingsbrooke chemistry data, which may be useful in visualizing and comparing the distribution of concentration values for each pollutant.

3.4.2 Confidence Limits on the Mean for a Normal Distribution

For a given sample distribution, the mean of the actual population distribution has a certain probability of being found within certain confidence limits. For a normally-distributed dataset, those confidence limits on the mean may be calculated as follows:

$$\bar{x} \pm \frac{t \cdot s_x}{\sqrt{n}} \tag{3.3}$$

where $\bar{x}$ is the mean, s_x is the standard deviation, n is the number of datapoints, and t comes from the Student's t distribution for the desired significance level and dataset size (Berthouex and Brown, 1994).

3.4.3 Confidence Limits on the Mean for a Lognormal Distribution

Environmental data are often lognormally distributed, such that there are many small values and a few very large values. If a set of concentration data (x_i) are lognormally distributed, then the transformed dataset $y_i = \ln(x_i)$ is normally distributed. If the dataset were graphed on a probability plot as described previously, an exponential function would result:

$$\bar{x} = \exp\left(\bar{y} + s_y z\right) \tag{3.4}$$

in which $\bar{y}$ is the mean and the median and s_y is the standard deviation of the transformed y dataset. It may be shown that $\left[\exp\left(\bar{y}\right)\right]$ corresponds to both the median and the geometric mean of the x dataset, but not the arithmetic mean. Berthouex and Brown (1994) write that the arithmetic mean of a lognormal distribution may be estimated from parameters $\bar{y}$ and s_y as

$$\hat{\mu} = \exp\left(\bar{y} + \frac{s_y^2}{2}\right) \tag{3.5}$$

The upper and lower confidence limits on that mean may be estimated by

$$\hat{UCL}_{1-\alpha} = \exp\left(\bar{y} + \frac{s_y^2}{2} + \frac{s_y H_{1-\alpha}}{\sqrt{n-1}}\right) \quad \text{and} \quad \hat{LCL}_{\alpha} = \exp\left(\bar{y} + \frac{s_y^2}{2} + \frac{s_y H_{\alpha}}{\sqrt{n-1}}\right) \tag{3.6}$$

A computer program developed by Lyon and Land (2005) through the National Cancer Institute calculates those confidence limits with input of $\bar{y}$, s_y, n, and α (http://conflimit.nci.nih.gov/index.shtml). The online version of the program was used to estimate confidence limits for average pollutant concentrations at the Kingsbrooke bioretention area. The previous equations may be combined to find that…

$$\frac{s_y H_{1-\alpha}}{\sqrt{n-1}} = \ln\left(\hat{UCL}_{1-\alpha}\right) - \ln\left(\hat{\mu}\right) \quad \text{and} \quad \frac{s_y H_{\alpha}}{\sqrt{n-1}} = \ln\left(\hat{LCL}_{\alpha}\right) - \ln\left(\hat{\mu}\right) \tag{3.7}$$

In the Kingsbrooke project, confidence limits were estimated around the flow-weighted average pollutant concentrations of the storms and the simple arithmetic average pollutant concentrations of the baseflow and lysimeter samples. It was assumed that these averages, calculated directly from the data rather than through theoretical distribution parameters, were more accurate than the $\hat{\mu}$ calculated in equation 3.5. It was also assumed that the difference between the natural logs of the confidence limits and the mean from

equation 3.7 was valid for both the estimate confidence limit and mean and the actual confidence limit and mean. Given the foregoing, the confidence limits on the mean μ may be calculated as…

$$\ln\left(UCL_{1-\alpha}\right) - \ln\left(\mu\right) = \frac{s_y H_{1-\alpha}}{\sqrt{n-1}} = \ln\left(\hat{UCL}_{1-\alpha}\right) - \ln\left(\hat{\mu}\right) \quad \text{, and likewise for } LCL_{1-\alpha}. \tag{3.8}$$

Therefore,

$$UCL_{1-\alpha} = \hat{UCL}_{1-\alpha}\frac{\mu}{\hat{\mu}} \qquad \text{and} \qquad LCL_{\alpha} = \hat{LCL}_{\alpha}\frac{\mu}{\hat{\mu}} \tag{3.9}$$

This method was used to calculate the confidence limits around the average pollutant concentrations for the various Kingsbrooke sampling locations. The values for $\hat{UCL}_{1-\alpha}$ and $\hat{LCL}_{\alpha}$ were calculated using the NIH website, the values for μ were the flow-weighted or simple arithmetic averages of the sample concentrations, and the values for $\hat{\mu}$ were calculated using equation 3.9.

4 Results and Discussion

4.1 Hydrology

As discussed previously, inflow and outflow hydrologic measurements for the Kingsbrooke bioretention area were based on the discharge relationships of H-flumes equipped with pressure transducers to sense stage. Tipping bucket rain gages at Lake Manassas and at Kingsbrooke were used for precipitation measurements, and other weather information was obtained from meteorological stations at the Occoquan Watershed Monitoring Laboratory and Dulles International Airport (NOAA, 2004).

4.1.1 Climate

The study period had both average rainfall and average temperature. Figure 4.1 shows a comparison between normal monthly rainfall at Dulles International Airport and the monthly rainfall occurring from November, 2003 to October, 2004. Total precipitation during the period was 41.3 inches, which was within 1% of the normal annual precipitation. Monthly precipitation, however, varied between 31% of normal in October, 2004 and 157% of normal in April, 2004.

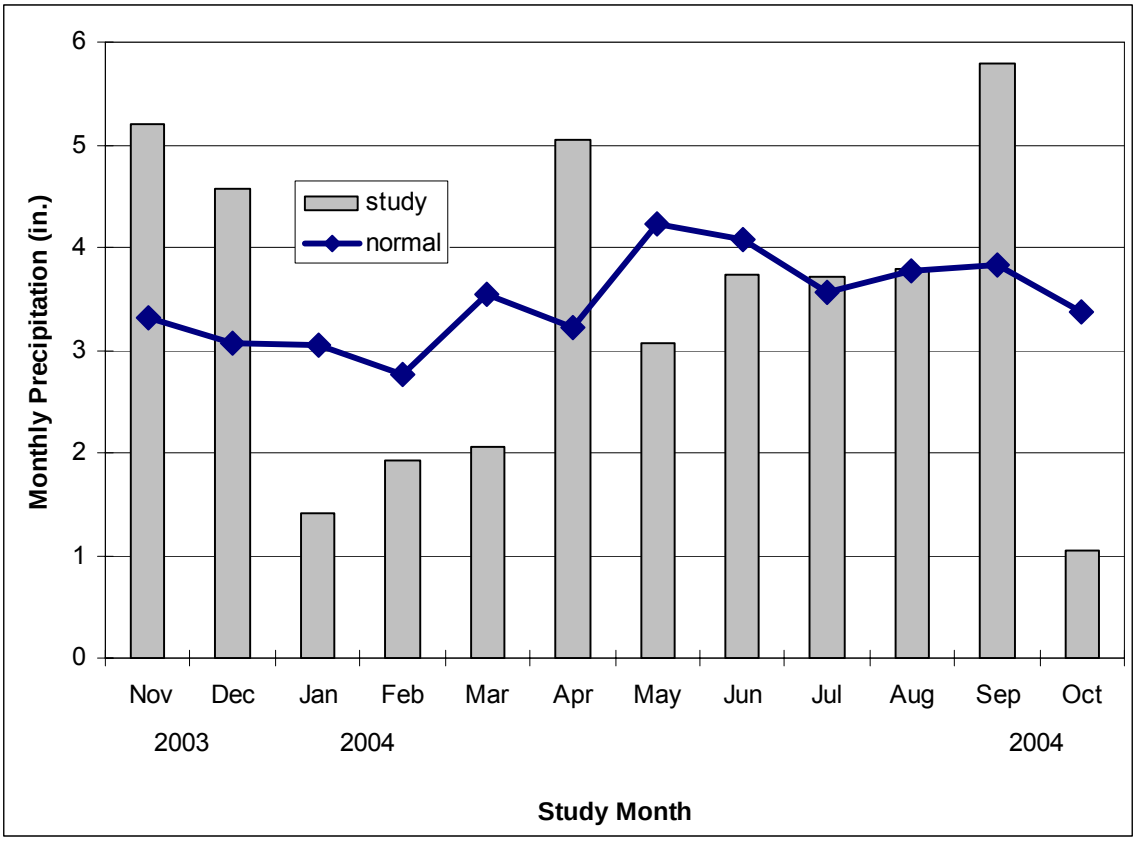

Figure 4.1. A comparison of local precipitation during the study period and during an average year. The rainfall data comes from Dulles International Airport (NOAA, 2004).

4.1.2 Typical Hydrology

Figure 4.2 shows the rainfall and resulting runoff hydrograph for a small storm at the site.

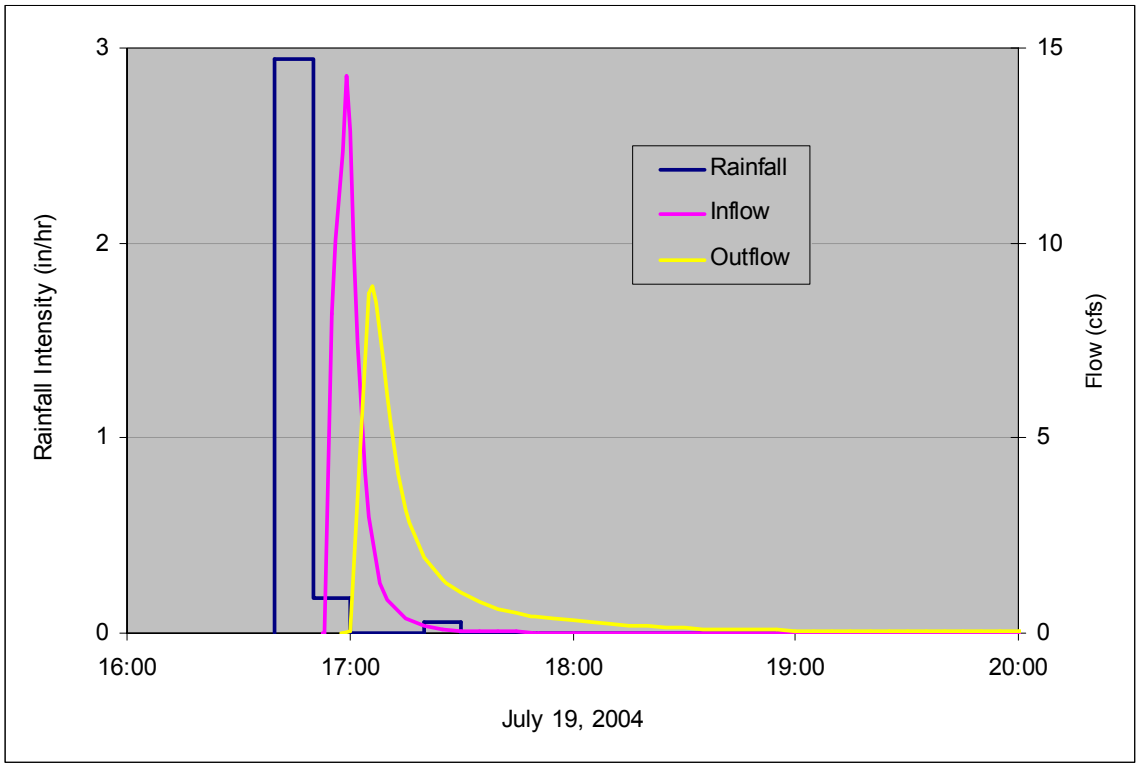

Figure 4.2. Example of a hydrograph resulting from about half an inch of rainfall.

As may be seen from Figure 4.2, the peak outflow occurred 7 minutes after the peak inflow. For the small storm shown, the peak flowrate was reduced by more than 30% between the inflow and outflow gages. For larger storms, however, the inflow and outflow often had close to the same peak flowrate. For most storms, including the one illustrated in Figure 4.2, the total outflow volume was greater than the total inflow volume, demonstrating that the Kingsbrooke bioretention area (as constructed) did a relatively poor job of infiltrating the stormwater runoff.

- Rainfall = 0.53 inches * 13.83 acres = 26,608 ft^3
- Gaged Inflow = 6,966 ft^3
- Total Inflow (assuming an ungaged:gaged drainage area ratio of 0.159) = 8,232 ft^3
- Gaged Outflow = 9,113 ft^3

The hydrograph shown in Figure 4.3 illustrates the diurnal fluctuations that were observed in the outflow baseflow measurements and how those fluctuations may relate to plant transpiration and groundwater flows. The daily variations in outflow baseflow showed no relationship to any flows through the inflow gage. Although the transpiration rates also showed diurnal variations, the variations in outflow exceeded the transpiration rates predicted inside the bioretention area. This may be explained by considering that plants outside the bioretention area were also transpiring and changing the groundwater table elevation. These changes in groundwater table elevation would be expected to cause diurnal changes in groundwater flow into the bioretention area, resulting in the fluctuations seen in the outflow baseflows. No tests were performed to ascertain the source of this apparent influx of subsurface flow to the bioretention area; these flows may originate either with groundwater from below the water table or with interflow that never reached the water table. In this report the subsurface influx of flow is referred to as "groundwater", even if it does not meet the formal groundwater definition.

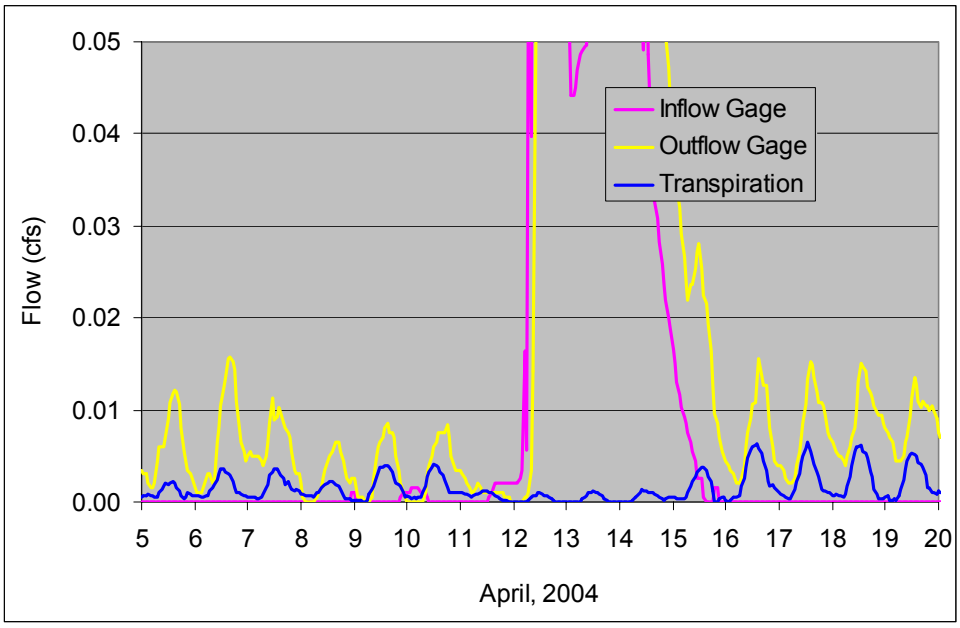

Figure 4.3. An illustration of daily flow variations indicative of groundwater influence.

4.1.3 Measurement Issues

Hydrologic measurements on the site were found to be subject to two classes of error that required manual data correction. First, during the cold months ice occasionally formed in the gage stilling wells, resulting in an increase in head sensed by the pressure transducers and causing false stage (and discharge) readings. Several examples of this are shown in Figure 4.4, which compares inflow and outflow data for February, 2004. Secondly, ponding around the inflow gage created backwater to sit on the H-flume, preventing it from draining properly and thereby distorting the inflow readings. Figure 4.5 shows a time series of the inflow and outflow for a storm in March, 2004 when this problem was discovered. A drainage ditch was dug at about 1:00 PM on March 9 to correct the backwater problem, and its effect is easily visible in Figure 4.5 as the measured flowrate decreased immediately.

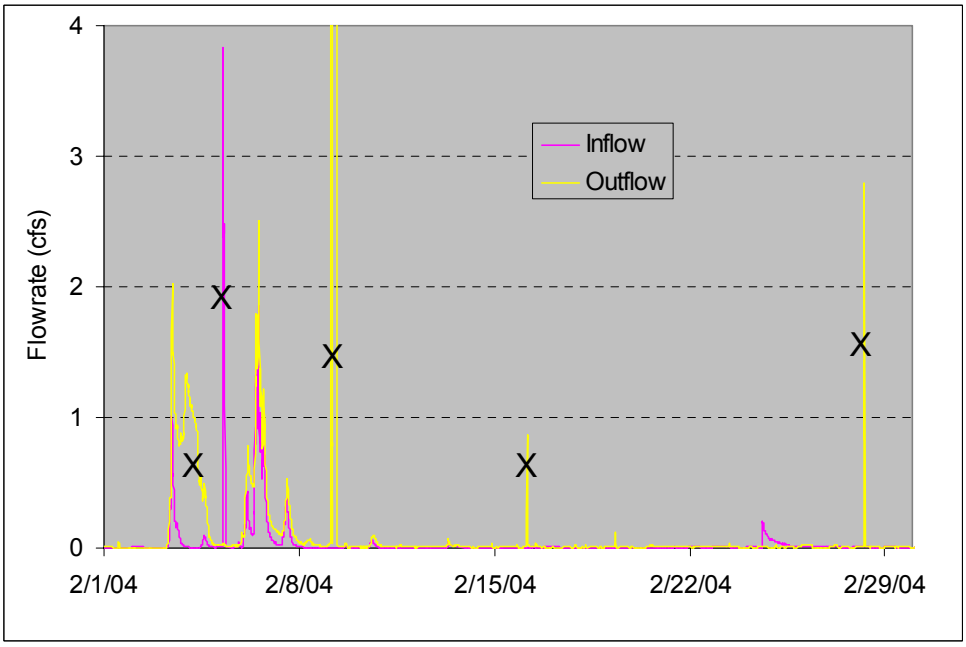

Figure 4.4. A graph showing the effects if ice pressure on the flow gages.

The two measurements problems were corrected during data processing by visual examination of the hydrographs. For the first problem, the flow measurements that were artificially caused by ice pressure were set to zero. For the second problem, the declining limb of the inflow storm hydrographs were manually estimated.

The abnormal peaks in Figure 4.4 (marked with "X") indicate times when the water froze in the gage stilling wells. These peaks were generally identified by high flows in either the inflow or outflow gage no flow appearring in the opposite gage. These points had to be removed from the data set. As shown in Figure 4.4, the outflow gage froze during the storm on February 4. Adjusting the flows to zero, as was done during other times when freezing was experienced at the gages, was not suitable in this case because a storm should produce some outflow. Lacking a more reliable calculation method, that storm was simply omitted from the data analysis. As a result, even though the flow gages resumed operation on February 1 after a month-and-a-half long winter break, the water balance calculations did not restart until February 5. Problems with ice in the pressure transducers occurred several times in the months of December, 2003 and February, 2004.

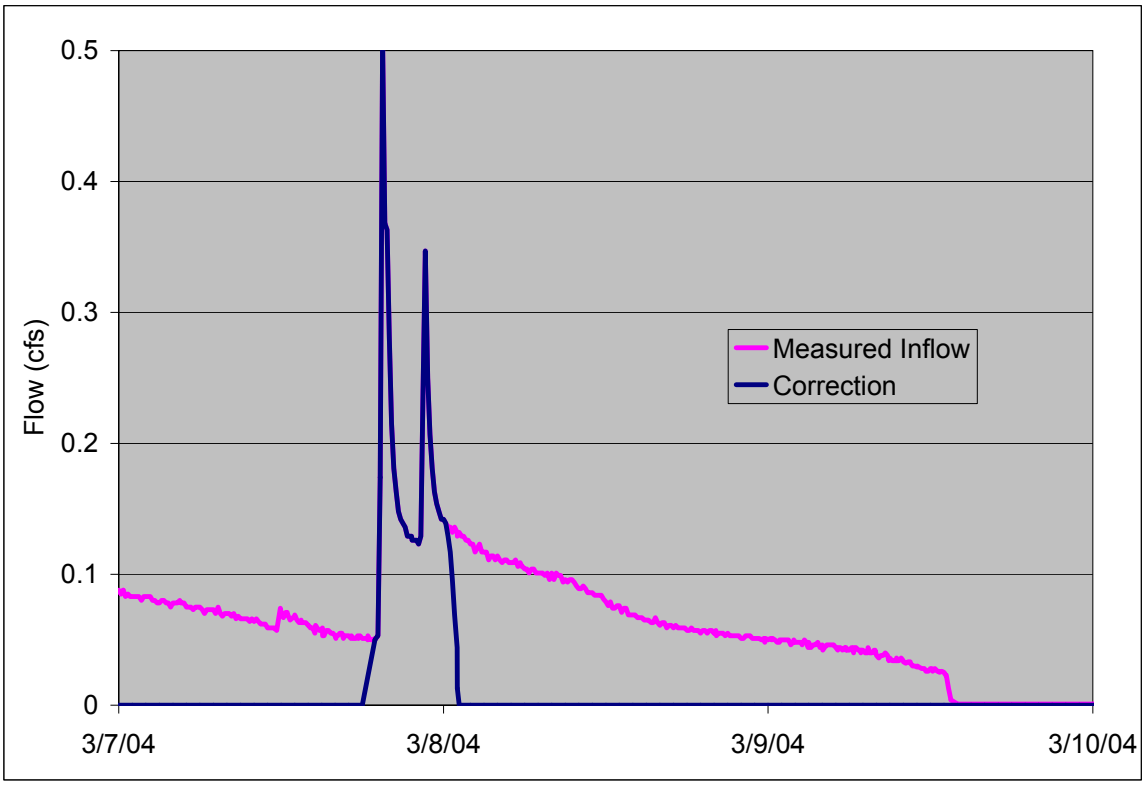

Figure 4.5. Hydrograph on an inflow storm showing backwater effects.

The long tail on the hydrograph in Figure 4.5 was caused by backwater standing in the flume. At about 1:00 PM on 3/9/04, a ditch was dug to help drain the water away from the flume; the pink line in Figure 4.5 drops off sharply at that time. The dark blue line is a graphical estimate of how the inflow hydrograph should have appeared. The inflow data for several storms in February and March had to be similarly corrected. Backwater problems at the inflow gage were noticeable during late February and early March of 2004. Because no storm chemistry samples were taken in February or March, the manual corrections to both the ice problems and the backwater problems had only a minimal impact on the calculation of the pollutant removal efficiency.

4.1.4 Water Balance

In order to calculate the water balance for the Kingsbrooke bioretention area, several flow volumes were required, as shown schematically in Figure 4.6. Some of those flows were directly measured, but the rest had to be estimated. Due to the uncertainties involved in those estimations, the water balance and load

calculations were repeated many times using a series of uncertainty factors, thus arriving at a range of probable results. This section discusses the water balance calculations in the order in which they were performed, including simplifying assumptions, hydrology uncertainty factors, and the final calculated volumes for flows into and out of the bioretention area. The abbreviations that will be used in this section are shown in parentheses in Figure 4.6.

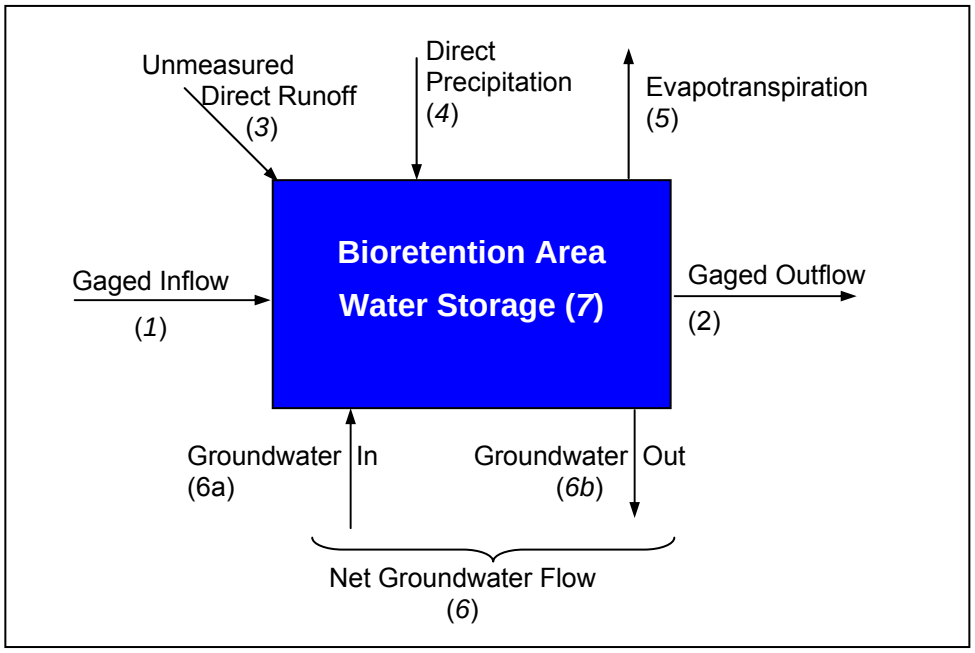

Figure 4.6. A summary of the required inflows and outflows for calculating a water balance for the Kingsbrooke bioretention area.

To begin the water balance analysis, gaged inflow and outflow were directly measured. The total gaged inflow over the entire time period was 5.02 million gallons, and the gaged outflow was 6.73 million gallons.

The next-most important flow, direct overland runoff that did not enter through the storm sewers, could not be measured. Its volume was estimated based on the ungaged:gaged drainage area ratio, as measured on the construction plans using a planimeter. The total drainage area was given on the plans to be 13.83 acres (Dewberry & Davis, 1994) and the ungaged drainage area was measured with a planimeter to be 1.90 acres, so the ratio of ungaged to gaged inflow area was calculated as [1.90 / (13.83 – 1.90)] = 0.159. The area estimation involved significant uncertainty, as did the assumption of a direct relationship between the concentrated gaged inflow and shallow overland ungaged inflow. To account for these uncertainties, the actual ratio of flow volumes was assumed to be somewhere within ±25% of the calculated ratio of 0.159. Therefore, the ungaged:gaged drainage area ratio was applied in the sensitivity analysis as "parameter A", and was given a uniform distribution between (0.159 * 0.75) = 0.119 and (0.159 * 1.25) = 0.199. As a result, the final ungaged inflow volume was calculated to be between (5.02 MG * 0.119) = 0.61 MG and (5.02 MG * 0.199) = 0.96 MG.

Direct precipitation onto the bioretention surface was easily calculated from rainfall depth and BMP area. The volume of precipitation directly onto the surface of the bioretention area was calculated using rainfall depth and the bioretention surface area (11,713 feet^2). Rainfall depth was measured at Kingsbrooke starting on 6/23/04. Prior to that date, rainfall depths were estimated based on measurements from a gage located at the Lake Manassas water treatment plant. A comparison between the rainfall depths at Kingsbrooke and at Lake Manassas as shown in Figure 4.7, revealed some differences between the two locations. Based on the observed differences, the unmeasured Kingsbrooke rainfall between November, 2003 and June, 2004 was conservatively assumed to be within ±50% of the Lake Manassas rainfall during those months. Again a uniform distribution was used, for the sake of simplicity in calculation. Each of the data points in the Figure 4.7 corresponds to the rainfall depth from a one-month period, such as 6/24/04 – 7/24/04 or 8/3/04 – 9/3/04, etc.

The pink lines indicate the values used for parameter "F", a multiplier that was varied in the sensitivity analysis to account for probable differences between the rainfall measured at Lake Manassas and what actually fell at Kingsbrooke. The method used for choosing these values is a suitable example of how parameter values were chosen from a uniform distribution for use in the sensitivity analysis. To choose five possible values, the distribution was first split into five equal sections (0.5 to 0.7, 0.7 to 0.9, … , and 1.3 to 1.5). Each of these sections was considered to have an equal probability of containing the true value. Then the midpoint of each section was chosen, i.e. the value 1.0 was chosen for the section from 0.9 to 1.1, and so on. That single value then represented its entire section of the distribution in the analysis, and each of the five representative values was used equally in the Monte Carlo sensitivity analysis.

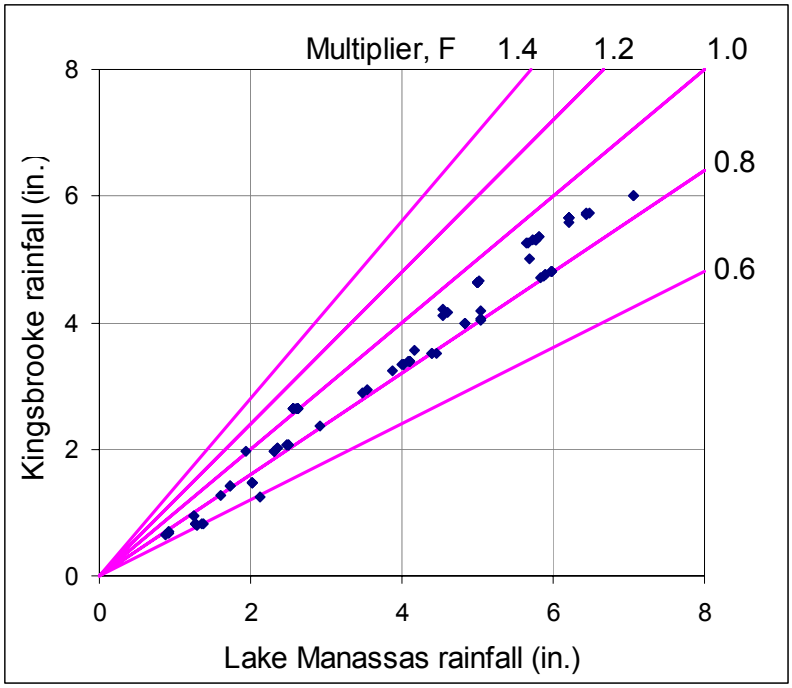

Figure 4.7. A comparison between monthly Kingsbrooke rainfall depths and Lake Manassas rainfall depths, along with values used for sensitivity parameter *F*.

Evapotranspiration was estimated based on local weather conditions using the Penman-Monteith equations (Allen et al., 1998), which are summarized in Appendix E. The "crop type" used in the equations was turf grass. The actual evapotranspiration may have been higher due to the presence of trees at Kingsbrooke, or lower because the site is sunken below the surrounding terrain. To account for these uncertainties, the reference evapotranspiration was assumed to vary uniformly between ±25% of the originally calculated reference evapotranspiration volume of 54,489 cubic feet, or 0.41 million gallons. Crop coefficients were applied as discussed in Appendix E.

The remaining unknowns for the water balance included the water storage volume, the groundwater inflow, and the groundwater outflow. Their calculation is discussed here. The numerical identifiers in parentheses refer to the key(s) in Figure 4.6.

The mass balance equation for water may be given as…

$$(1) - (2) + (3) + (4) - (5) + (6a) - (6b) = d(7) / dt \qquad (4.1)$$

By assuming that …

- Net groundwater flow *(6)* equals groundwater inflow minus outflow, or *(6) = (6a) – (6b).*
- The net change in storage *(7)* over some time period *t* is zero, i.e. $(7)_t - (7)_0 = 0$.
- The net groundwater flowrate *(6)* is constant over time period *t*,

Then the previous equation may be manipulated so that…

$$(6) = \frac{-\int_0^t [(1)-(2)+(3)+(4)-(5)]dt}{t} \tag{4.2}$$

For this project, the groundwater was averaged over each month, i.e. $t \approx 30$ days. This time period was chosen arbitrarily, knowing that groundwater flow is relatively steady but can vary seasonally. Figures 4.8 and 4.9 illustrate the effects on average groundwater flowrate and the storage volumes based on starting the month-long averaging on different dates. For Figure 4.8, storage was set to zero on the 2nd of each month, and the groundwater flowrate was averaged until the 2nd of the next month. In Figure 4.9, the 14th was used instead of the 2nd.

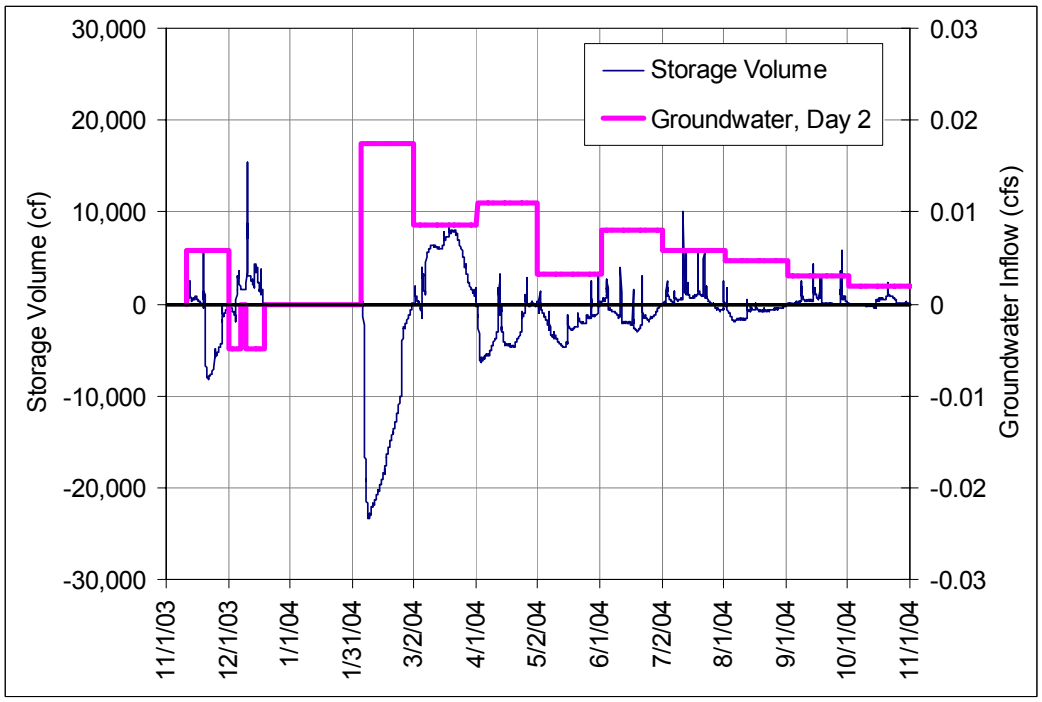

Figure 4.8. An illustration of groundwater averaging and storage volume calculations, based on setting storage to zero on the 2nd of each month.

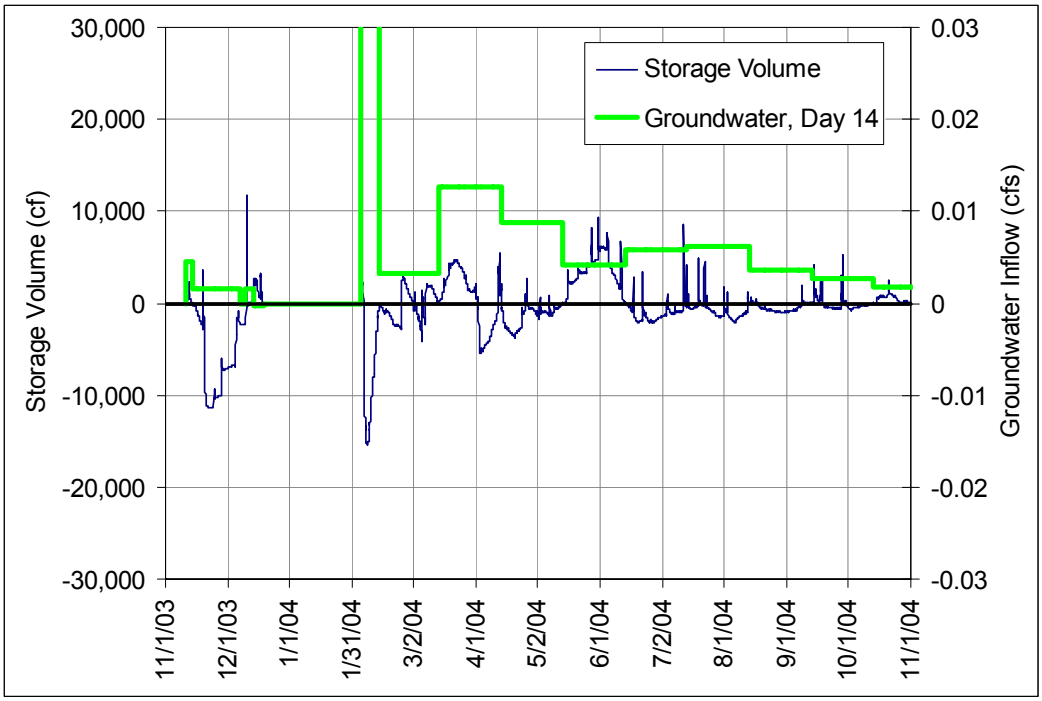

Figure 4.9. An illustration of groundwater averaging and storage volume calculations, based on setting storage to zero on the 14th of each month.

As illustrated in Figures 4.8 and 4.9, the calculated groundwater flowrate was dependent on the beginning and ending times for the averaging period, even when in both cases the groundwater flows were averaged over a month-long period. During the data analysis, 30 different cases were considered, with the monthly averages taken between the 1st of one month and the 1st of the next month, between the 2nd and the 2nd, the 3rd and the 3rd, and so on.

The water balance and groundwater flowrates were calculated for the entire period of flow records from November through December of 2003 and from February through October of 2004. The total flow volumes are shown below for that time period and also for the shorter time period during which water quality samples were taken, from November through December of 2003 and from April through October of 2004.

Table 4.1 gives the results of the water balance, including uncertainty resulting from variation in parameters A, B, E, and F as discussed previously. The spaces that state "between *a.aa* and *b.bb*" mean that in the sensitivity analysis the volume was allowed to vary within a uniform distribution between those points. The spaces that state "*c.cc* ± *d.dd*" mean that the mean of the calculated probable volumes was *c.cc* and their standard deviation was *d.dd*. The spaces that give only a single volume were directly measured by the flow gages and did not involve uncertain estimations.

Table 4.1. Water balance for Kingsbrooke, with volumes in millions of gallons.

	entire time period	chemistry data time period (excludes Feb.-Mar. 2004)
Inflows		
Gaged Inflow	4.93	4.33
Ungaged Inflow	between 0.61 and 0.96	between 0.53 and 0.84
Direct Precipitation	between 0.20 and 0.33	between 0.18 and 0.30
Groundwater Inflow	1.27 ± 0.12	0.81 ± 0.11
Total Inflows	7.25 ± 0.07	6.06 ± 0.08
Outflows		
Outflow Storms	6.30	5.57
Outflow Baseflow	0.43	0.32
Evapotranspiration	between 0.37 and 0.61	between 0.35 and 0.58
Groundwater Outflow	0.03 ± 0.03	0.03 ± 0.03
Total Outflows	7.25 ± 0.07	6.07 ± 0.07

The pie charts shown in Figure 4.10 on the next page illustrate the make-up of the volumes of inflow and outflow for the entire monitoring period, and for the period during which chemistry data were available. The percentages shown in Figure 4.10 come from the averages of the volume ranges in Table 4.1. It may easily be seen in Figure 4.10 that a majority of both the inflow volume and the outflow volume originated in gaged storm flows. The chemistry data for storm flows is considered to be more accurate than for baseflows or groundwater flows because it was based on flow-weighted composite samples. This fact, and the fact that a majority of the storms were sampled for water quality, helped to ensure the reliability of the pollutant load and removal efficiency calculations.

4.2 Soil Chemistry

Table 4.2 shows the results of the chemical tests that were performed on the soil samples collected on July 12, 2004. The data from the upper terrace samples had several distinguishing features. The silt-clay topsoil had higher ammonia and organic carbon content than the sand or the crushed bluestone, probably due to a higher organic matter content. The crushed bluestone had the highest phosphorus and the highest copper concentrations, suggesting that it came from phosphate- and copper- containing rock. It should be noted that the copper concentration of the water samples was never tested. Lead levels did not vary greatly between the soil layers, but the sand layer had almost twice the zinc concentration as the other soil layers.

Samples from the middle and lower terraces did not capture the same image of the soil profile that was seen in the upper terrace samples. In the middle terrace, for example, the first two soil samples (1.0 and 2.0 foot depths) had chemical characteristics that were intermediate between those of sand and silt-clay (as compared to the upper terrace). Some of this variation may have been caused by the fact that the soil samples were retrieved with a hand auger, and may have intermingled with each other, but it is also possible that the soil compositions of the three terraces were truly different from each other. In comparing the data from Table 4.2 with the water quality data, the most important thing to note is that lysimeters L1, L2, and L3 reached into the crushed bluestone layers of each terrace at depths of 3', 3', and 4', respectively, but the L3clay lysimeter reached into the silt-clay layer of the lower terrace at a depth of 3'.

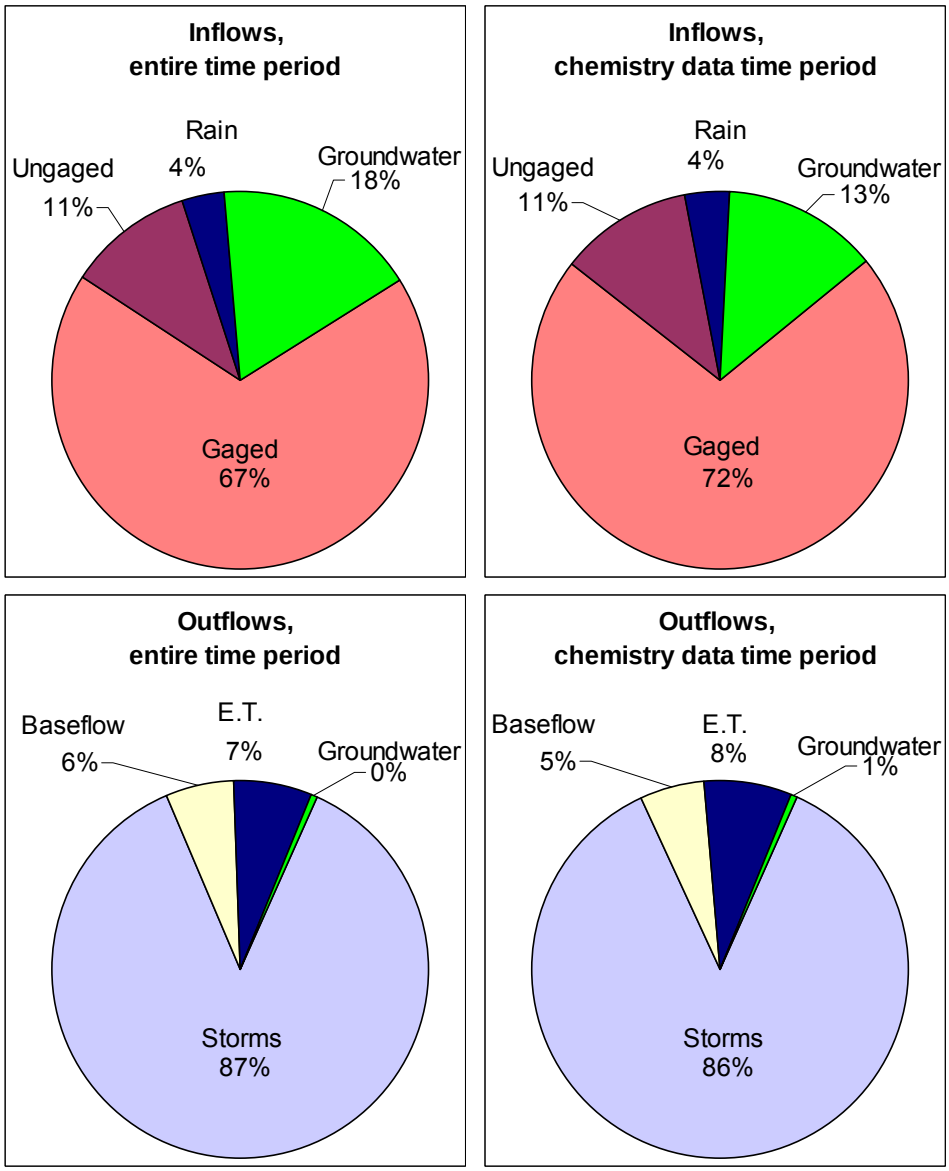

Figure 4.10. Pie charts illustrating relative inflow and outflow volumes.

Table 4.2. Results of chemical tests on soil samples taken on July 12, 2004.

Depth (ft)	Soil Layer	Pollutant Concentration (mg per kg of soil)							
		Total Phosphorus, TP	Ammonia Nitrogen, NH3_N	Total Nitrogen, TN (≈TKN) [a]	Total Organic Carbon, TOC	Total Carbon, TC	Lead	Zinc	Copper
Upper Terrace									
1.0	silt clay	164	56.10	608	7,780 [c]	7,240 [c]	14.8	21.5	4.0
2.0	sand	341	1.98	< 250	< 100	120	13.3	55.5	39.3
2.9	crushed bluestone	608	0.53	< 250	< 100	397	8.7	33.2	85.4
3.3	bottom dregs [b]	245	5.35	308	2,020	3,150	11.9	28.7	31.0
Middle Terrace									
1.0	silt clay / sand	233	1.13	454	3,870	5,240	11.7	35.6	24.4
2.0	silt clay / sand	140	1.71	302	1,700	1,990	14.5	66.7	35.1
3.2	crushed bluestone	548	0.10	< 250	< 100	457	7.7	36.2	59.7
Lower Terrace									
2.0	silt clay	160	25.40	789	7,760	9,940	15.6	32.7	14.1
3.2	silt clay	255	45.60	695	8,840 [c]	8,720 [c]	11.9	30.6	31.8
3.5	crushed bluestone	518	0.28	< 250	< 100	251	8.0	31.1	61.2
4.6	bottom dregs [b]	203	17.00	332	2,460 [c]	2,200 [c]	11.8	26.8	35.1

[a] The concentration of oxidized nitrogen (NO_3^- and NO_2^-) for all soil samples was less than the detection limit of 0.015 mg-N / kg-soil, therefore the total nitrogen concentration was approximately the same as the concentration of total Kjeldahl nitrogen, TKN.

[b] The soil taken from the bottom of each hole, referred to as "bottom dregs" in the table, had a chemistry that was intermediate between the crushed bluestone and the silt clay layers. These soil samples were likely a mixture between the lowest observed soil layer (crushed bluestone), the native soil (silt loam, according to the county website (Prince William County, 2004)), and any bits of soil that remained on the hand-auger from previous layers.

[c] The total carbon concentration should be greater than the organic carbon concentration; these datapoints indicate the magnitude of the concentrations but probably not their exact values.

4.2.1 Iron

The extractable iron concentration was measured in water samples from lysimeters L1, L2, and L3clay on May 3 and May 10, 2004. At L1 the average iron concentration was 104 μg/L, and for L2 it was 478 μg/L. However, for the clay lysimeter (L3clay) the average was 22,000 μg/L. As samples were retrieved from the L3clay lysimeter, they were observed to be colorless but had a slight odor. Following a few minutes of exposure to the air, the water would turn rust-colored. Most likely there was a reducing environment inside the clay layer and the iron was present in the reduced (Fe^{+2}). Upon exposure to atmospheric oxygen, the iron was quickly oxidized to the Fe^{+3} state. This was not observed to happen for any of the other lysimeter samples, all of which had low iron concentrations. Only the L3clay lysimeter withdrew water from the silt clay topsoil layer. It is uncertain what effect the high iron concentrations may have had on the adsorption of lead and zinc to the topsoil particles.

4.3 Pollutant Concentrations and Loads

The tables in Appendix B present the original chemistry data at all sample locations. Note that the sample locations O3 (outflow baseflow collected from the rip-rap below the outflow gage) and L3clay (lysimeter water samples from the clay layer of the lower terrace) were not used in calculating the pollution removal efficiencies. One of the samples for O3 was removed from the analysis because it was an outlier for most parameters. That sample, retrieved on 09/28/04 from the rip-rap below the outflow gage, was from one of the highest flows sampled at O3 in the course of the study. Most of the chemical constituents for that sample were substantially different from those normally observed at that location, with concentrations closer to storm flows than to the usual O3 baseflow concentrations.

Appendix C gives summary statistics and probability plots for the constituents that were routinely tested at all water sampling locations. Suggested probability distributions for the measured constituents are also plotted in Appendix C to aid in visualization and for comparison purposes. Information on the preparation of the plots is given in Appendix C.

4.3.1 Load Calculation Methodology

Using the following equation, removal efficiencies were calculated for phosphorus, nitrogen, suspended solids, lead, and zinc. Removal efficiencies were also calculated for COD, total organic carbon, calcium, and magnesium. Although these latter constituents are not usually considered to be pollutants in urban storm runoff, analysis of their behavior may help understand the basic mechanisms controlling the bioretention area.

$$Removal\ Efficiency = \frac{Inflow\ Load - Outflow\ Load}{Inflow\ Load} \tag{4.3}$$

Where…

$$Load = \Sigma[(Flow\ Volume)*(Concentration)] \tag{4.4}$$

The direct rainfall and the evapotranspiration were considered to be free of any pollutant loads. So,…

$$\begin{aligned} Inflow\ Load = {} & \Sigma[(Gaged\ Inflow\ Volume)*(Gaged\ Inflow\ Concentration)] \\ & + \Sigma[(Ungaged\ Inflow\ Volume)*(Ungaged\ Inflow\ Concentration)] \\ & + \Sigma[(Groundwater\ Inflow\ Volume)*(Groundwater\ Inflow\ Concentration)] \\ Outflow\ Load = {} & \Sigma[(Outflow\ Storm\ Volume)*(Outflow\ Storm\ Concentration)] \\ & + \Sigma[(Outflow\ Baseflow\ Volume)*(Outflow\ Baseflow\ Concentration)] \\ & + \Sigma[(Groundwater\ Outflow\ Volume)*(Groundwater\ Outflow\ Concentration)] \end{aligned} \tag{4.5}$$

Composite storm concentrations were obtained for most, but not all, inflow and outflow storms. Concentrations were also available from grab samples over several weeks for both outflow baseflow and for the soil pore water. Table 4.3 shows a summary of the inflow and outflow storm flow volumes sampled and also the number of weeks during the study (Nov-Dec of 2003 and Apr-Oct of 2004) for which flow data (overall), outflow baseflow sample data, and lysimeter grab sample data were available. The outflows were separated into storm flows and baseflows based on stage recorded in the outflow flume. A stage of

less than 0.05 feet was considered baseflow and a greater stage indicated a storm. This is the same separation point that was used by the automatic flowmeters and samplers in determining when a storm started and ended.

Table 4.3. Summary of water volumes sampled at inflow, outflow, and groundwater.

Volume of Sampled Inflow Storms:	436,364 cf	= 3.26 MG	= 75% of gaged inflows	
			or 65% of gaged + ungaged inflows	
Volume of Sampled Outflow Storms	529,262 cf	= 3.96 MG	= 75% of outflow storms	
Number of weeks of…			lysimeter 1 samples:	30 weeks
flow data:	36 weeks*		lysimeter 2 samples:	30 weeks
outflow baseflow samples:	17 weeks*		lysimeter 3 samples:	10 weeks

* These time durations exclude any data from February or March of 2004 because those months were not considered in the load calculations.

As shown in Table 4.3, 25% of storm inflow and outflow volume were not sampled, and 19 weeks of baseflow concentrations and between 6 and 26 weeks of lysimeter concentrations were also unknown. In order to calculate pollutant loads for unsampled storms, baseflow, and groundwater flow, concentrations were estimated based on the observed data from samples taken at other times. Inclusion of estimated concentrations for the unsampled volumes made it possible to compute removal efficiencies for the constituents of interest for the entire study period.

- For storm events for which composite samples were not available, the flow-weighted average of the sampled storms was used as an estimator for the pollutant concentrations. As part of the sensitivity analysis, this average was allowed to vary within some confidence interval, whose calculation was performed as described in sections 3.5.2 and 3.5.3.

- None of the ungaged overland inflow entering the bioretention area was sampled. In order to estimate the impact of this source on the overall pollutant balance, the chemical make-up was assumed to exactly match the gaged inflow. It may be recalled from the water balance discussion in section 4.3.4 that the ungaged inflow was assumed to be the same as the gaged inflow multiplied by the drainage area ratio. Combining these two assumptions means that the ungaged overland pollutant load is equal to the gaged pollutant load multiplied by the drainage area ratio, and the total overland inflow load was estimated as …

$$\frac{Overland}{Inflow\,Load} = \frac{Gaged}{Inflow\,Load} * \left(1 + \frac{Ungaged : Gaged}{Drainage\,Area\,Ratio}\right) \tag{4.6}$$

- Samples of baseflow were collected as grab samples rather than flow composites. In the loading computations, each of the 17 baseflow chemistry samples was assumed to be valid for the baseflows in the week in which it was taken. For the remaining weeks of pollutant load calculations, the simple arithmetic average of all 21 baseflow samples was used (this average included 4 samples taken during March of 2004). As was done for the storm sample average concentrations, for the baseflow load sensitivity analysis, the average concentration was allowed to vary within a confidence interval, as described in sections 3.5.2 and 3.5.3.

- The exact locations through which groundwater enters and leaves the Kingsbrooke bioretention area soils were unknown. For this study, the groundwater flow was assumed to be distributed across the bioretention area, and divided equally between the three terraces. This assumption allowed the groundwater pollutant concentration to be calculated as the average of the concentrations from lysimeters 1, 2, and 3 (L1, L2, and L3). The shallower lysimeter in the third terrace (L3clay) was ignored because its chemistry differed significantly from the others and because very little groundwater flow was likely to occur through the clayey soil in that layer in comparison to flows through the crushed bluestone layer. As was done for the baseflow grab samples, the chemical results from each lysimeter sample were assumed to be valid for the week

in which the sample was taken. When no lysimeter sample was available for a given week, then the value was estimated from the arithmetic average of the sampled concentrations. Again, confidence intervals were applied to the mean concentrations in the sensitivity analysis.

- Some sample pollutant concentrations were found to be below the method detection limit (<MDL) of the analytical methods employed. Because it would not be valid to simply replace those unknown concentrations with any single value, and they could not be simply removed from the analysis, the sensitivity analysis was modified to include a methodology for estimating the concentrations of constituents below the detection limit. In the sensitivity analysis, the concentration for any datapoint that was censored due to a <MDL concentration was replaced with a value chosen from a uniform distribution of concentrations between 0 and the MDL. In this way, all possible values between 0 and the MDL were considered in the final data analysis.

4.3.2 Sensitivity Analysis

During the calculations several of the parameters included a great deal of uncertainty. The six major areas of uncertainty are listed below, including the volumes of ungaged overland inflow, evapotranspiration, and rainfall, the method for calculating average monthly groundwater flowrates, the constituent concentrations of unsampled flows, and how to account for concentrations that were less than the method detection limit. To account for these uncertainties, a Monte Carlo analysis was employed in which a series of possible values were randomly used in the calculations. Two main classes of parameters were varied for each load calculation: hydrologic parameters and concentration parameters. The individual loads (overland inflow, groundwater inflow, outflow storms, outflow baseflow, and groundwater outflow) were then combined to calculate a series of as many as 2.5 billion possible pollutant removal efficiencies. When two loads were combined, they may have been calculated using different values for the concentration parameters, but they were required to use the same values for all hydrologic parameters.

The hydrologic parameters were:
(The selection of these hydrologic parameter ranges was discussed in Section 4.1.4.)

A. Drainage **A**rea ratio for the ungaged:gaged overland inflows; varied uniformly between 0.119 and 0.199.

B. Day for **B**eginning/ending the groundwater averaging calculations; thirty values were used, between the 1st of the month and the 30th.

E. Multiplier for **E**vapotranspiration; varied uniformly between 0.75 and 1.25.

F. Lake Manassas Rain**F**all multiplier; varied uniformly between 0.5 and 1.5.

The concentration parameters were:

C. **C**oncentration used for unsampled storms or for periods when the baseflow or lysimeters were not sampled; varied based on the calculations for confidence limits of averages, as discussed in sections 3.5.2. and 3.5.3.

D. Assumed value for any concentrations that were less than the method **D**etection limit (MDL); varied uniformly between 0 and 1 multiplied by the MDL.

For each parameter, a set of values was chosen to represent the entire distribution. For instance, if 5 values were chosen to represent a uniform distribution between 0 and 100, then the numbers would have been 10 (representing the range between 0 and 20), 30 (for the range 20 through 40), 50, 70, and 90. If 10 values had to be chosen from the same distribution, then the numbers chosen would have been 5, 15, 25, 35, 45, 55, 65, 75, 85, and 95. Table 4.4 lists the values used in the calculations.

Table 4.4. Parameter values used in the calculations and in the sensitivity analysis.

Parameter	Number of Values	List of Values
A	10	0.123, 0.131, 0.139, 0.147, 0.155, 0.163, 0.171, 0.179, 0.187, 0.195
B	30	1, 2, 3, 4, 5, 6, 7, 8, 9, 10, 11, 12, 13, 14, 15, 16, 17, 18, 19, 20, 21, 22, 23, 24, 25, 26, 27, 28, 29, 30
C	5	10%, 30%. 50%, 70%, 90%
	10	5%, 15%, 25%, 35%, 45%, 55%, 65%, 75%, 85%, 95%
	(as a cumulative percent probability of the possible distribution of values)	
D	5	0.1, 0.3, 0.5, 0.7, 0.9
	10	0.05, 0.15, 0.25, 0.35, 0.45, 0.55, 0.65, 0.75, 0.85, 0.95
	(these values *MDL) This parameter was not applicable in all cases; sometimes there were no <MDL values.	
E	5	0.8, 0.9, 1.0, 1.1, 1.2
F	5	0.6, 0.8, 1.0, 1.2, 1.4

For each of the types of constituent loads, the parameters were varied as follows:

Overland Inflow (I1): varied A 10 times, C 10 times, and D 10 times (if applicable). So the total number of overland inflow loads calculated for each chemical was 1000.

Outflow Storms (O1): varied C 10 times and D 10 times, for a total of 100 outflow storm loads.

Outflow Baseflow (O2): varied C 5 times and D 5 times, for a total of 25 outflow baseflow loads. The outflow baseflow was given fewer calculations because it had less effect on the final pollutant removal efficiency.

Groundwater: The groundwater inflow (Gin) and the groundwater outflow (Gout) were each calculated 1000 times. Parameter A was varied 10 times. For each value of parameter A, 10 random combinations were selected for parameters B, E, and F, giving 10*10, or 100, sets of values calculated for the hydrologic parameters. For each of those sets, parameter C was varied 5 times. For each variation of parameter C, 2 random values were selected for parameter D for groundwater inflow and 2 random D values for groundwater outflow. Ultimately, 10*10*5*2, or 1000 sets of parameters were used to calculate 1000 values for groundwater inflow and outflow. If all of the possible parameter values had been used from Table 4.4, there would have been 10*30*5*5*5*5, or 187500 values, which would have been too cumbersome to accommodate in calculating the percent removal efficiencies. Only a small error (less than 1%) was introduced by limiting the calculation set to 1000 loads rather than 187500.

Total Inflow: For total inflow, the parameter estimates were calculated using: 10 for A, 10 for [B,E,&F], 10 for C_{I1}, 5 for C_{Gin}, 10 for D_{I1}, and 2 for D_{Gin}, for a total of 10*10*10*5*10*2, or 100000 total inflow calculations.

Total Outflow: For total outflow, the parameter estimates were calculated using: 10 for A, 10 for [B,E,&F], 10 C_{O1}, 5 C_{O2}, 5 C_{Gout}, 10 D_{O1}, 5 D_{O2}, and 2 D_{Gout}, for a total of 10*10*10*5*5*10*5*2, or 2500000 total outflow calculations.

Percent Removal Efficiency (PRE): The parameter variations in the final PRE calculations were 10 for A, 10 for [B,E,&F], 10*5*10*5*5 for C for the 5 different load types, and 10*2*10*5*2 for D (when applicable), for a total number of 2,500,000,000 calculations. Fortunately, most of the D parameters did not have to be varied, because most constituents did not have any <MDL analytical results. In such cases, far fewer calculations were required.

The possible values for the individual loads I1, Gin, O1, O2, and Gout were calculated as described above, and listed in a series of text files. However, the sheer number of calculated total inflow and outflow loads

and pollutant removal efficiencies made it impractical to list them individually. Instead, the values were sorted into set ranges of values (bins), as for a histogram, and the number of values in each bin was determined. The mean and standard deviation of the values were calculated simultaneously; those values presented later in the results Tables 4.8 and 4.9.

All calculations were performed using Microsoft Excel 97 and Microsoft Visual Basic for Applications, version . Appendix D contains more detailed information on load calculations and removal efficiencies, including the actual confidence limits on the averages used to substitute for non-sampled concentrations.

The calculations for total nitrogen were preformed in a slightly different manner. Total nitrogen loads were calculated as the sum of the oxidized nitrogen and TKN loads. Removal efficiency calculations for total nitrogen, therefore, depended on A, B, E, and F, on C and D for the various oxidized nitrogen loads, and on C for the various TKN loads. Parameter D was not used with relation to the TKN loads because there were no <MDL concentrations for TKN. The organic nitrogen loads were similarly calculated by subtracting ammonia from the TKN loads, while varying all the appropriate parameters for each. Because the total nitrogen and organic nitrogen calculations each involved combining the loads from two different chemicals, they required more calculation effort as a greater number of combinations existed for the variation in appropriate parameters.

4.3.3 An Example: Pollutant Removal Calculations for Total Phosphorus

This section will detail the steps used to calculate the pollutant removal efficiency and the sensitivity analysis for total phosphorus.

Because there were no <MDL total phosphorus concentrations for the samples from I1, O1, or O2, there was no need to vary D_{I1}, D_{O1}, or D_{O2}. In other words, for total phosphorus the number of variations in D_{I1} = D_{O1} = D_{O2} = 1. The resulting number of possible pollutant removal efficiencies was then calculated as A*[B,E,&F]*C_{I1}*C_{Gin}*C_{O1}*C_{O2}*C_{Gout}*1*D_{Gin}*1*1*D_{Gout} = 10*10*10*5*10*5*5*1*2*1*1*2 =5,000,000.

Consider the calculation for one of those 5 million PRE values…

- Pick specific values for A, B, C_{I1}, C_{Gin}, C_{O1}, C_{O1}, C_{Gout}, D_{Gin}, D_{Gout}, E, and F:
    - The drainage area ratio, A = 0.123.
    - Use the 12th as the date for groundwater averaging calculations (B).
    - Use the 15% cumulative probability concentration for C_{I1}, 30% for C_{Gin}, 45% for C_{O1}, 70% for C_{O2}, and 90% for C_{Gout}. This means, for example, that the non-sampled inflow storms will be assigned a concentration of
      0.301 mg/L = (0.342 mg/L)*(0.278 / 0.316).
      The above values may be found in Appendix D for the inflow storm TP values of the flow-weighted average, the theoretical lower 70% confidence limit, and the theoretical mean for the lognormal distribution.
    - Variations in D_{I1}, D_{O1}, and D_{O2} are not applicable here because there were no <MDL concentrations among the I1, O1, or O2 samples. For D_{Gin} use 0.5*MDL and for D_{Gout} use 0.9*MDL. With the method detection limit equal to 0.01 mg/L, this means that any non-detectable concentrations at lysimeters L1, L2, and L3 will be set to 0.003 mg/L for calculating the groundwater inflow loads and then to 0.007 mg/L for calculating the groundwater outflow loads.
    - For E, use a multiplier of 0.9 on the original evapotranspiration.
    - For F, use a multiplier of 1.4 on the Lake Manassas rainfall.
- Calculate Loads:
    - Overland Inflow Load, I1 = 6.115 kg phosphorus
    - Groundwater Inflow Load, Gin = 0.099 kg P
        - Total Inflow Load = I1 + Gin = 6.214 kg P

- Outflow Storm Load, O1 = 4.400 kg P
- Outflow Baseflow Load, O2 = 0.095 kg P
- Groundwater Outflow Load, Gout = 0 kg P
    - Total Outflow Load = O1 + O2 + Gout = 4.495 kg P

- Pollutant Removal Efficiency = (Inflow Load – Outflow Load) / Inflow Load = 27.67%

The calculation illustrated above was performed a total of 5,000,000 times. The possible values of the pollutant removal efficiency were sorted into 1000 bins (where "bin" means a set range of values, normally used for one bar on a histogram) between a minimum of 22.64% and a maximum of 40.02% in order to generate the cumulative distribution illustrated in Figure 4.11. The average of those 5,000,000 removal efficiency values was 31.68%, and the standard deviation was 2.78%. The cumulative number of possibilities and the cumulative probabilities were plotted for both the actual calculations and for a theoretical normal distribution based on their average and standard deviation.

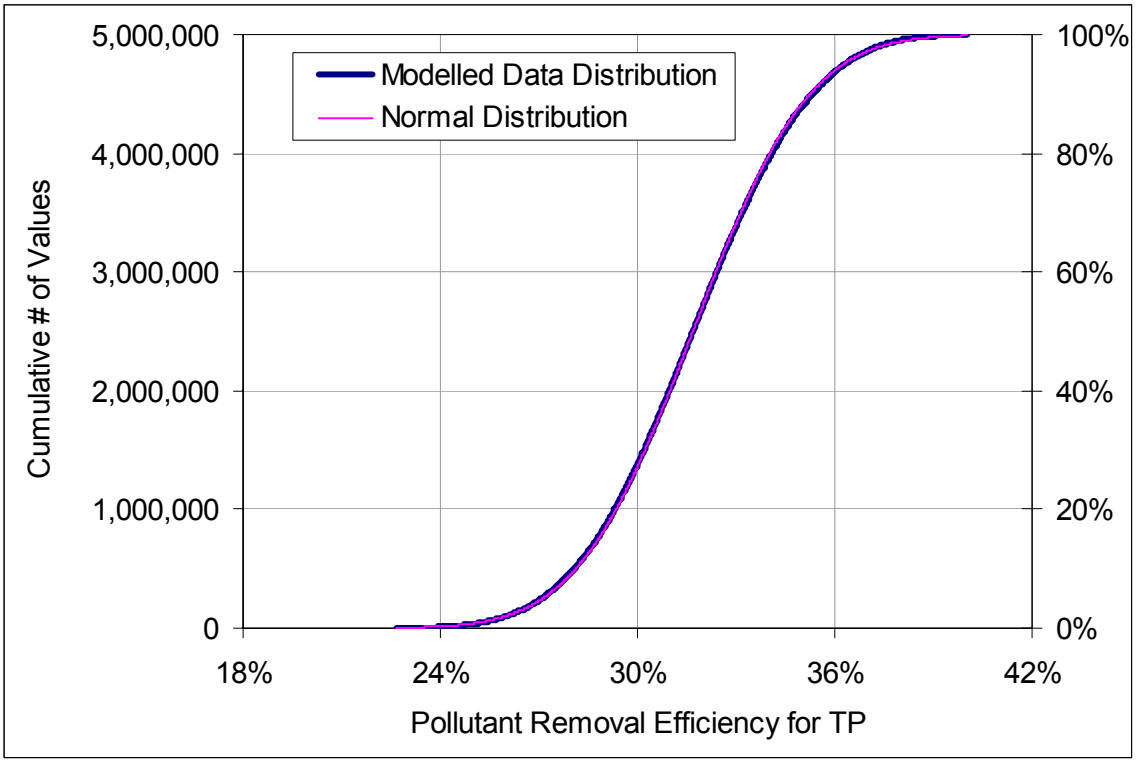

Figure 4.11. Results from calculating possible removal efficiencies for total phosphorus.

During the load calculations it was also possible to analyze the sensitivity of the calculations to variations in the parameters A, B, C, D, and E. Table 4.5 demonstrates this by listing the average total phosphorus loads for variations in two different parameters: A (gaged:ungaged drainage area ratio), and C_{O2} (which concentration to use for non-sampled baseflows).

Table 4.5. Example of sensitivity analysis calculations for total phosphorus, parameters A and C_{O2}.

Parameter	Value	Average of Calculated Loads (kg)					Pollutant Removal Efficiency	Standard Deviation
		I1	Gin	O1	O2	Gout		
A	0.123	6.312	0.127	4.422	0.092	0.001	29.88%	1.23%
	0.131	6.356	0.123			0.002	30.31%	
	0.139	6.401	0.119			0.002	30.73%	
	0.147	6.446	0.115			0.003	31.15%	
	0.155	6.491	0.111			0.004	31.56%	
	0.163	6.535	0.107			0.005	31.96%	
	0.171	6.580	0.103			0.006	32.36%	
	0.179	6.625	0.099			0.007	32.76%	
	0.187	6.669	0.095			0.008	33.15%	
	0.195	6.714	0.092			0.010	33.53%	
C_{O2}	10%	6.513	0.109	4.422	0.084	0.005	31.89%	0.11%
	30%				0.088		31.83%	
	50%				0.091		31.77%	
	70%				0.095		31.72%	
	90%				0.102		31.61%	

The standard deviations calculated by this method may not be statistically accurate, but are useful for comparing the sensitivities of the final pollutant removal efficiencies to variations and uncertainties in the calculation parameters. For example, it may be deduced from Table 4.5 that the ungaged:gaged drainage area ratio (parameter A) has a greater impact on the calculations than does the concentration used for the unsampled baseflow periods (parameter C_{O2}). The standard deviations calculated by this method are listed for all parameters and all pollutants in Table 4.14 at the end of the Results section.

4.3.4 Solids and Turbidity

Turbidity (TURB) and total suspended solids (TSS) were measured for samples from the inflow storms (I1), outflow storms (O1), and outflow baseflow (O2 and O3). The suspended solids concentration of the groundwater flows was assumed to be zero for the load calculations. Average TSS concentrations are illustrated below in Figure 4.12. Flow-weighted averages are shown for the storm samples, I1 and O1, and simple arithmetic average for the baseflow samples.

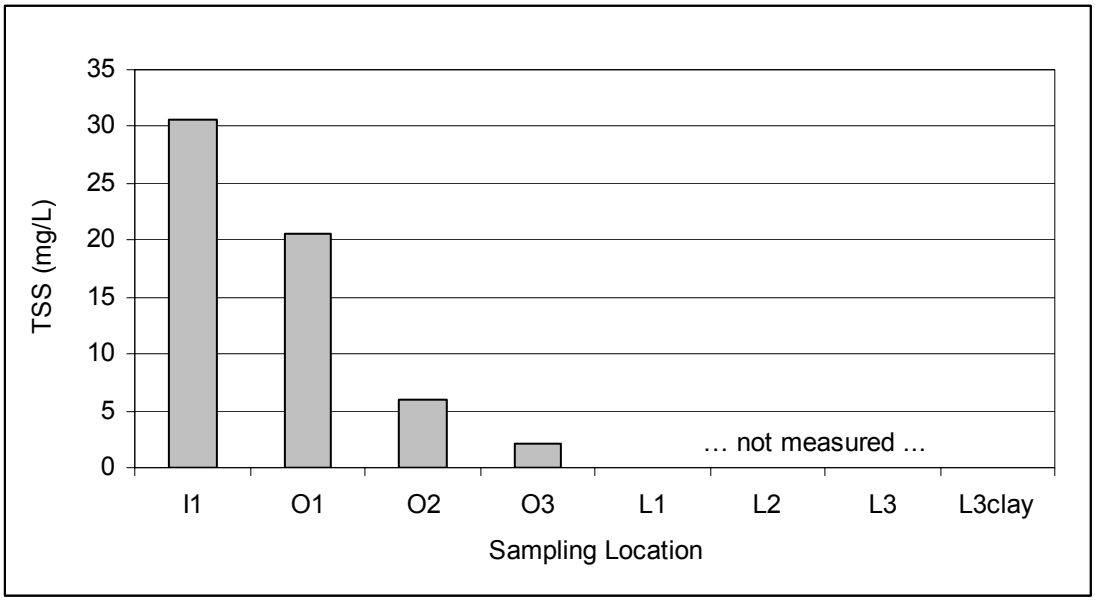

Figure 4.12. Comparison of TSS concentration for each sampling location.

Table 4.6 gives not only the average concentrations for TSS and TURB, but also the calculated inflow and outflow loads for total suspended solids and the average calculated removal efficiency. The concentrations shown in Table 4.6 are all simple arithmetic averages except for the storm concentrations for TSS, for which the flow-weighted averages are shown.

Table 4.6. Average TSS concentrations, loads, and removal efficiencies.

Total Suspended Solids and Turbidity				
Sampling Station	TURB (NTU)	TSS Conc. (mg/L)	TSS Load (kg)	Flow Type
I1	33.5	30.7	+ 585	Inflow Storms
O1	19.1	20.6	- 412	Outflow Storms
O2	8.4	6.0	- 6	Outflow Baseflow
O3	9.5	2.2		
L1	-	-	+ 0 - 0	Groundwater Flows
L2	-	-		
L3	-	-		
L3clay	-	-		
Removal Efficiency			28.4%	

The data for both turbidity and TSS from all locations were lognormally distributed (refer to the plots in Appendix C). The storm samples generally had higher turbidity and TSS values than did the baseflow samples. In fact several of the baseflow samples had TSS values lower than the detection limit. For both turbidity and TSS, the inflow storm average exceeded the outflow storm average and showed greater variability. The turbidity values for O2 and O3 were almost interchangeable, but in general the TSS concentrations for the O2 baseflow samples were higher than for the O3 baseflow samples.

Removal of TSS is important because many other pollutants are associated with sediment, including trace metals and phosphorus. The average mass load reduction for TSS of 28% is less than most of the reductions cited in the literature for other bioretention areas. For most of the literature-cited bioretention

areas, however, the discharge sediment came from bioretention soil leaking into the underdrain while nearly all of the influent sediment was removed by filtration. At Kingsbrooke, the high clay content of the topsoils reduced the infiltration capacity, so the sediment removal was probably due to sedimentation rather than filtration by the topsoil.

If the site could be altered so that the stormwater retention times were increased, infiltration increased, and the average effluent concentration reduced to the observed baseflow (O2) concentration, the removal efficiency of TSS would be closer to [(30.7 – 6.0) / 30.7] = 80% removal. Currently, however, there are no plans to retrofit the site to enhance its bioretention function. The low average concentration of the baseflow TSS indicates, however, what removals might be possible from flows allowed to infiltrate more slowly through the site.

4.3.5 Nutrients

4.3.5.1 Phosphorus

Both ortho-phosphate phosphorus (OP) and total phosphorus (TP) were measured for all 8 sampling locations. The average concentrations are shown graphically in Figure 4.13. Ortho-phosphate phosphorus is shown as black hatch marks, while the total phosphorus concentration includes the entire bar. The flow-weighted averages are shown for the storm concentrations, I1 and O1, and simple arithmetic averages for the baseflow and lysimeter concentrations.

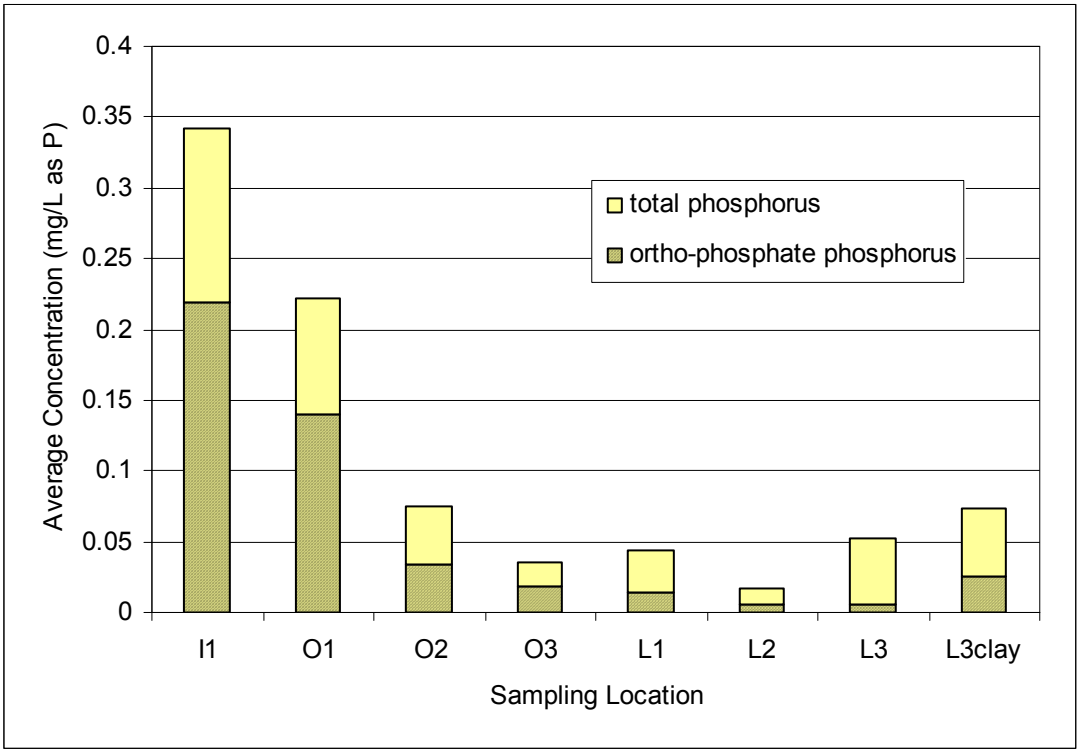

Figure 4.13. Comparison of phosphorus concentrations for the different sampling locations.

The average inflow storm concentrations for both orthophosphate and total phosphorus were greater than the average outflow storm concentration, leading to the calculation of pollutant removal efficiencies of 33% and 32%, respectively. Phosphorus is frequently associated with sediment particles, so its removal at Kingsbrooke was probably affected by settling of TSS and adsorption to the on-site soil particles.

The baseflow and lysimeter phosphorus concentrations were all found to be much less than the storm concentrations. The clay lysimeter (L3clay) did have slightly higher phosphorus concentrations than the other lysimeters, a result opposite to what was observed during the soil tests. In the soil tests, the silt clay topsoil had significantly lower phosphorus concentrations than the crushed bluestone layer. The

phosphorus contained in the crushed bluestone media may have been intrinsic to the soil particles, while more of the phosphorus in the upper soil layers was loosely bound to the soil surfaces or dissolved. For the baseflow concentrations, the values at O2 were more similar to the storm samples than were the O3 values, meaning that the O2 concentrations were generally slightly higher than the O3 concentrations. Table 4.7 lists the average phosphorus concentrations for all sampling locations. Again, the flow-weighted average concentrations are shown for storms and the simple arithmetic averages are shown for the baseflow and lysimeter samples.

Table 4.7. Average phosphorus concentrations and loads.

Phosphorus Species					
Sampling Station	Conc. (mg/L)		Load (kg)		Flow Type
	OP	TP	OP	TP	
I1	0.22	0.34	+ 4.21	+ 6.51	Inflow Storms
O1	0.14	0.22	- 2.79	- 4.42	Outflow Storms
O2	0.03	0.07	- 0.04	- 0.09	Outflow Baseflow
O3	0.02	0.03			
L1	0.01	0.04	+ 0.02 - 0.00	+ 0.11 - 0.00	Groundwater Flows
L2	0.01	0.02			
L3	0.01	0.05			
L3clay	0.03	0.07			
Removal Efficiency			33.0%	31.7%	

The variation within each sample set is not shown in either Figure 4.13 or Table 4.7, but is illustrated in the plots in Appendix C. The inflow and outflow storm concentrations showed more variation than did the other samples. The O2 baseflow samples showed more variation than the O3 samples because they were more influenced by storm flows. L1 and L3clay displayed more variability in phosphorus concentration than did L2 or L3, suggesting that those lysimeters were located farther from the groundwater table and received occasional influence from the more-variable overland inflow.

4.3.5.2 Nitrogen

Ammonia (NH3_N), total Kjeldahl nitrogen (TKN), and oxidized nitrogen (OX_N) were measured routinely for all water samples. For the last few samples in this study, OWML switched from measuring TKN to measuring Total Nitrogen (TN), and then calculating TKN from TN and OX_N. Total nitrogen may be related to TKN and OX_N through…

$$TN = TKN + OX\_N \tag{4.7}$$

The organic nitrogen (Org_N) concentration was calculated from TKN and ammonia using the following…

$$TKN = NH3\_N + Org\_N \tag{4.8}$$

Figure 4.14 compares the average concentrations of nitrogen species for each sampling location.

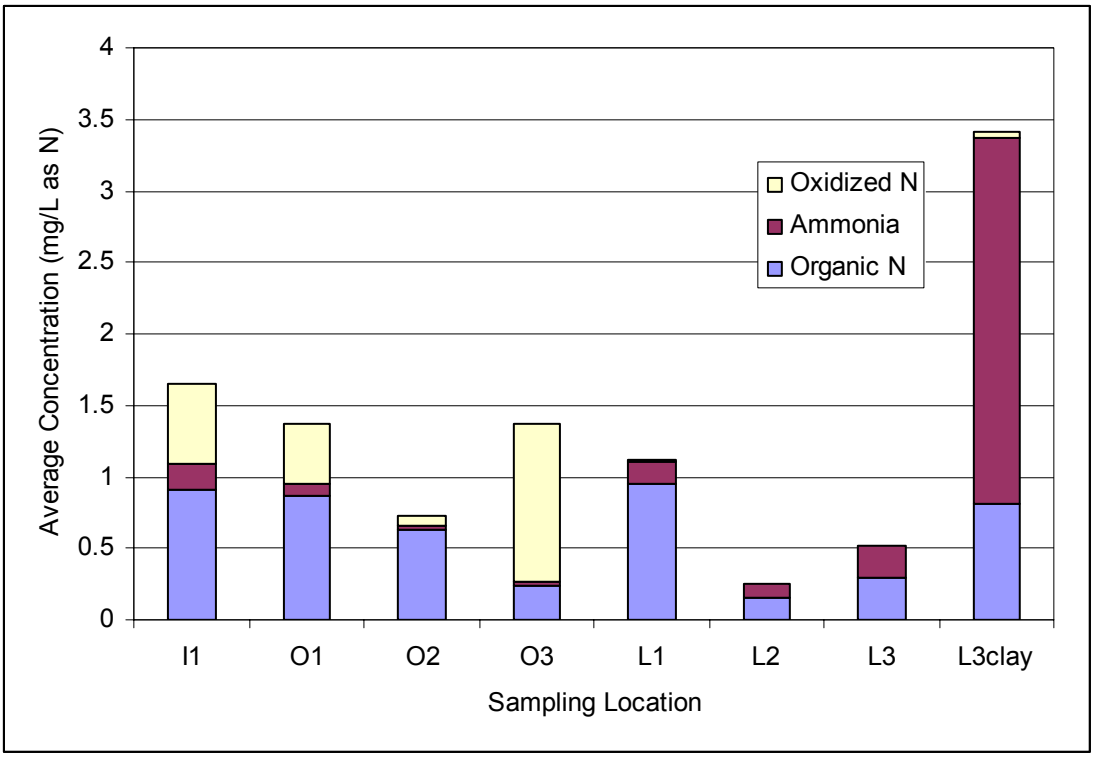

Figure 4.14. Comparison of average or flow-weighted average concentrations for nitrogen at each sampling location.

The inflow storms exhibited slightly higher average concentrations for all nitrogen species than did the outflow storms, and much higher standard deviations of concentration. Even though the average inflow and outflow storm chemistry data were similar, the concentrations for the other sample locations showed significant differences. Those differences may best be understood by considering the biological processes of nitrification and denitrification.

Ammonia in the soil water may, under aerobic conditions, be oxidized biologically to nitrate. The high nitrate and low ammonia concentrations for the O3 baseflow could be explained by the activity of nitrifying bacteria living where the soil water (with high ammonia concentrations as for L3clay) exited the soil into the more aerobic conditions of the rip-rap. In contrast to O3, the O2 baseflow samples taken from the outflow gage itself had higher TKN concentrations that were more similar to the storm flows, and very low nitrate concentrations. The O2 baseflows probably passed through a different oxidation-reduction environment in the soil and surface water than did the O3 flows.

In contrast to the baseflows or storm flows, the lysimeter samples all had measurable ammonia and TKN concentrations but often very little oxidized nitrogen. The low values of nitrate may indicate its use as an alternate electron acceptor in anoxic zones of the soil, a process called dissimilatory denitrification. Ammonia concentrations were comparable for lysimeters L1, L2, and L3, but were extremely high for the clay lysimeter, L3clay. The soil chemistry tests (Section 4.2) gave similar results, also showing significantly higher ammonia concentrations in the silt-clay topsoil than in the lower soil layers. Ammonium, being a cation, may be sorbed to soil particles via ion exchange for various metal ions. Accumulation of ammonium in the clayey topsoil was, therefore, one possible mechanism for nitrogen removal in the BMP. Other possible mechanisms included denitrification within the flooded soils and nitrogen uptake by plants, although plant decay could ultimately be expected to return that nitrogen to the environment. Table 4.8 lists average concentrations and loads for ammonia, organic nitrogen, TKN, oxidized nitrogen, and total nitrogen at each sampling location.

Table 4.8. Average nitrogen concentrations and loads.

Nitrogen Species											
Sampling Station	Conc. (mg/L)					Load (kg)					Flow Type
	NH3_N	Org_N	TKN	OX_N	TN	NH3_N	Org_N	TKN	OX_N	TN	
I1	0.19	0.91	1.10	0.55	1.65	+3.5	+17.3	+20.8	+10.5	+31.3	Inflow Storms
O1	0.08	0.87	0.95	0.42	1.37	- 1.6	- 17.3	- 18.9	- 8.4	- 27.3	Outflow Storms
O2	0.02	0.63	0.65	0.07	0.72	- 0.0	- 0.8	- 0.8	- 0.2	- 1.0	Outflow Baseflow
O3	0.02	0.24	0.27	1.11	1.37						
L1	0.16	0.95	1.11	0.01	1.11	+ 0.5 - 0.0	+ 1.4 - 0.1	+ 1.9 - 0.1	+ 0.0 - 0.0	+ 1.9 - 0.1	Groundwater Flows
L2	0.09	0.16	0.25	0.01	0.26						
L3	0.22	0.30	0.52	0.01	0.52						
L3clay	2.56	0.81	3.37	0.03	3.41						
Removal Efficiency						59.9%	2.9%	13.0%	17.9%	14.6%	

4.3.6 Metals

Adsorption to soils is the primary mechanism for the removal of metals in most bioretention areas (Davis, 2001). In the column adsorption studies done at the University of Maryland, lead sorbed more readily to sandy loam soil and to mulch than did zinc (Davis, 2001). In his textbook *Hazardous Wastes: Sources, Pathways, Receptors*, Watts (1998) compared the selectivity of common soil sorbents for divalent metals. The tables in that book show that in most cases lead sorbs more strongly to soil particles than does zinc. Those same tables also show that calcium generally sorbs more readily than does magnesium, but whether calcium/magnesium are more sorbable than lead/zinc varies depends on the soil's makeup. No adsorption studies were performed on the soils from the Kingsbrooke bioretention area. The high concentrations of calcium and magnesium in the groundwater may have interfered with adsorption of the trace metals, including lead and zinc, present in the inflowing stormwater, possibly limiting the function of this bioretention area.

4.3.6.1 Calcium and Magnesium

The lysimeter samples consistently exhibited high concentrations of hardness (250 – 500 mg/L as $CaCO_3$), while samples from the inflow and outflow storms usually had very low hardness values of less than 50 mg/L as $CaCO_3$. This large difference between soil water chemistry and overland stormwater chemistry showed yet again that the Kingsbrooke bioretention area was strongly influenced by groundwater. The groundwater may have picked up soluble calcium and magnesium by dissolving minerals in the bedrock. Figure 4.15 compares both calcium and magnesium hardness values, expressed as mg/L as $CaCO_3$ for all sampling locations, and Table 4.9 lists the actual calcium and magnesium concentrations and calculated loads.

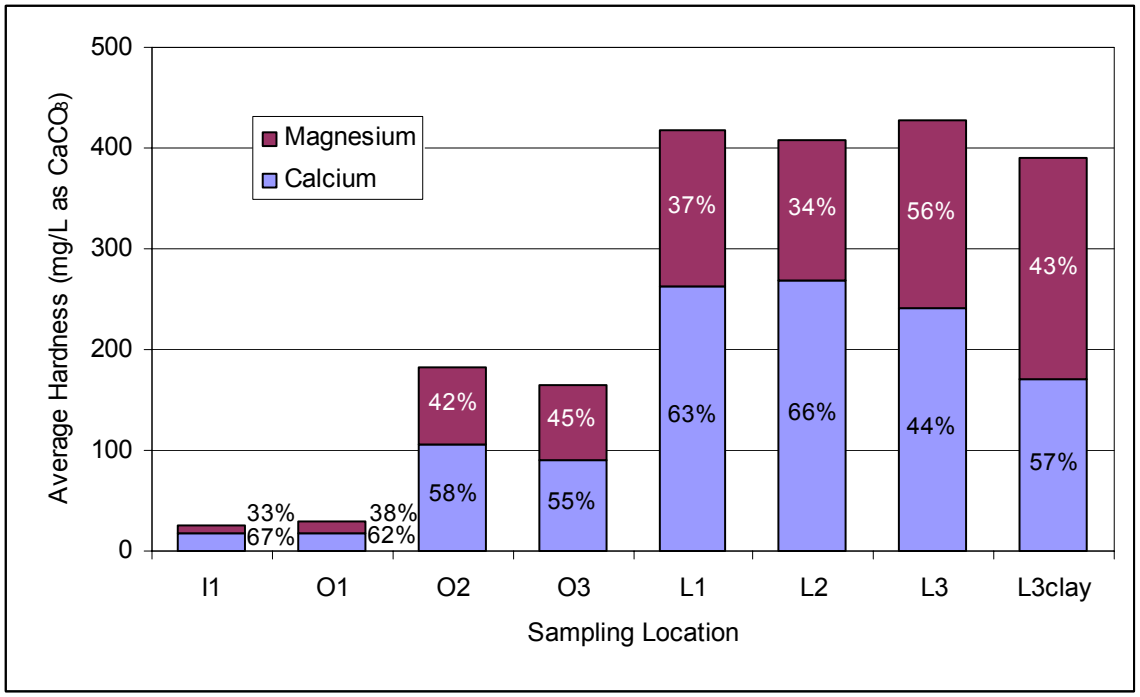

Figure 4.15. Comparison of average calcium and magnesium concentrations.

Although Figure 4.15 and Table 4.9 illustrate the average concentration differences between the sampling locations, they do not show the differences in standard deviation. Appendix C provides more information about all of the concentration distributions. As was usually observed, O2 had a larger standard deviation than O3 while L1 and L3clay had larger standard deviations than L2 or L3 because those locations were more often influenced by intermittent surface stormwater.

Table 4.9. Average concentrations and loads for calcium, magnesium, and total hardness.

Hardness Species						
Sampling Station	Conc. (mg/L)			Load (kg)		Flow Type
	SCA (as Ca)	SMG (as Mg)	THARD (as $CaCO_3$)	SCA (as Ca)	SMG (as Mg)	
I1	6.7	2.0	21	+ 128	+ 39	Inflow Storms
O1	7.2	2.6	26	- 143	- 52	Outflow Storms
O2	42.6	17.9	168	- 47	- 21	Outflow Baseflow
O3	44.6	18.2	186			
L1	104.9	36.5	413	+ 316	+ 115	Groundwater Flows
L2	107.5	32.6	402	- 12	- 4	
L3	96.5	43.6	420			
L3clay	68.1	51.7	384			
Removal Efficiency				54.2%	48.7%	

Removal efficiencies were calculated for calcium and magnesium because the data were available, but it should be noted that these cations are generally not considered to be pollutants. They were included in the analysis, however, in order to understand the impact of groundwater inflow on the soil chemistry and

because of the concern that high calcium and magnesium concentrations in the soil might reduce the availability of soil sorption sites for lead and zinc.

4.3.6.2 Lead and Zinc

Lead and zinc concentrations were measured for all locations whenever the sample volume was sufficient to allow the analysis. Often, the lead and zinc concentrations were found to be below the method detection limits of 3 μg/L for lead and 15 μg/L for zinc. The large number of datapoints that were less than the MDL increased the uncertainty in the data analysis. Although the probability plots and distributions shown in Appendix C were intended to help visualize trends in the data, they were of only limited utility in this case. Table 4.10 lists the fraction of lead and zinc samples from each location that had a <MDL concentration, and an estimate of the average concentrations and overall loads. The average concentration estimates were calculated by substituting a value of one-half the MDL for all censored sample concentrations (*e.g.*, 1.5μg/L for EPB and 7.5μg/L for EZN).

Table 4.10. Estimated average lead and zinc concentrations and loads, and the fraction of samples with <MDL concentrations.

Trace Metals							
Sampling Station	# <MDL Samples / # Total Samples		Average Conc. (μg/L)		Load (g)		Flow Type
	EPB	EZN	EPB	EZN	EPB	EZN	
I1	23 / 30	14 / 30	2.5	14.1	+ 48	+ 268	Inflow Storms
O1	24 / 30	16 / 30	2.0	12.1	- 41	- 241	Outflow Storms
O2	20 / 21	8 / 21	1.6	17.1	- 2	- 19	Outflow Baseflow
O3	15 / 15	15 / 15	1.5	7.5			
L1	12 / 12	12 / 12	1.5	7.5	+ 5	+ 23	Groundwater Flows
L2	25 / 29	29 / 29	1.8	7.5	- 0	- 1	
L3	9 / 10	10 / 10	1.7	7.5			
L3clay	12 / 22	20 / 22	3.0	8.9			
Removal Efficiency					16.4%	6.8%	

For lead, L3clay had a lower percentage of <MDL points than did the other sampling locations. Only 55% of the samples tested for lead from L3clay had concentrations less than the minimum, compared to between 77 and 100% of the samples from the other locations. The higher concentrations of extractable lead in the L3clay samples suggested that lead had adsorbed to the clay particles and was concentrating in the clay layer, as expected based on the findings by Watts (1998). Zinc behaved differently, with its highest concentrations found in samples from I1, O1, and O2. Because zinc does not adsorb to soil particles as readily as lead (Watts, 1998), this may explain the lower accumulation in the topsoil.

Samples from the crushed bluestone lysimeters L1, L2, and L3 almost always had lead and zinc concentrations below the detection limits. Because they are fairly immobile in pH-neutral soils, lead and zinc are very rarely found as pollutants in groundwater (Pitt, 2002). Most of the soil water sampled at L1, L2, and L3 originated as groundwater, explaining its low concentrations of those trace metals.

The overland stormwater samples frequently did have measurable lead and zinc concentrations, as would be expected for urban stormwater runoff. Concentrations for the inflow storms were slightly higher than for the outflow storms. The calculated removal efficiencies had very high uncertainties due to the high percentage of censored (<MDL) samples. After the sensitivity analysis, the ranges of probable pollutant removals were calculated as 16 ± 33% for lead and 7 ± 27% for zinc. Most of the limited lead and zinc removal at Kingsbrooke probably occurred by adsorption either to suspended solids followed by sedimentation or by adsorption to clay particles in the bioretention area topsoils.

4.3.7 Organic Matter: COD and TOC

Organic matter concentrations, in the forms of chemical oxygen demand (COD) and total organic carbon (TOC), were measured at all sampling locations. Table 4.11 lists average concentrations and loads for three different measures of organic matter content: COD, TOC, and organic nitrogen. The organic nitrogen loads shown are the same as in the previous Table 4.8. As before, the concentrations listed for the I1and O1 storm flows were calculated using a flow-weighted average, while the baseflows and lysimeter values were computed as simple arithmetic averages.

Table 4.11. A comparison COD, TOC, and organic nitrogen concentrations and loads.

Organic Matter Measurements							
Sampling Station	Conc. (mg/L)			Load (kg)			Flow Type
	COD	TOC	Org_N	COD	TOC	Org_N	
I1	23.5	6.6	0.91	+ 447	+ 126	+17.3	Inflow Storms
O1	22.4	7.5	0.87	- 446	- 150	- 17.3	Outflow Storms
O2	21.7	8.8	0.63	- 28	- 11	- 0.8	Outflow Baseflow
O3	7.2	3.3	0.24				
L1	43.6	9.8	0.95	+ 56	+ 17	+ 1.4	Groundwater Flows
L2	6.9	3.7	0.16	- 2	- 1	- 0.1	
L3	6.7	3.0	0.30				
L3clay	33.5	23.6	0.81				
Removal Efficiency				5.3%	-13.4%	2.9%	

As shown in the table, there was practically no removal of COD, TOC, or organic nitrogen. Whether each removal efficiency was positive or negative seemed to be determined by whether the inflow or outflow storm concentration was greater. Fortunately, none of these constituents is considered to be a major component of urban nonpoint source pollution, so their removal at a bioretention area is less important than the removal of nutrients or trace metals. Figure 4.16 further illustrates the low organic matter removal by showing the similarities in I1 and O1 concentrations. In order to put the different organic content measurements on the same scale, they were normalized with respect to the average inflow concentration.

The high relative concentration of organic matter at L3clay is consistent with the results from the soil tests, which showed that the silt clay layers contained very high concentrations of organic carbon. The L2 and L3 lysimeters showed low organic matter concentrations, as expected, and were matched by the O3 baseflow. What was less expected was the high concentrations at L1. It was suggested previously that soil water at L1 may have been more influenced by surface infiltration than the other lysimeters because it was situated at a greater distance from the groundwater table. Such infiltration may have carried organic matter down from the silt clay topsoil to the L1 lysimeter. If L2 and L3 received more steady groundwater inflows, as previously suggested, then they must have also received less percolating organic matter from their silt clay topsoil layers.

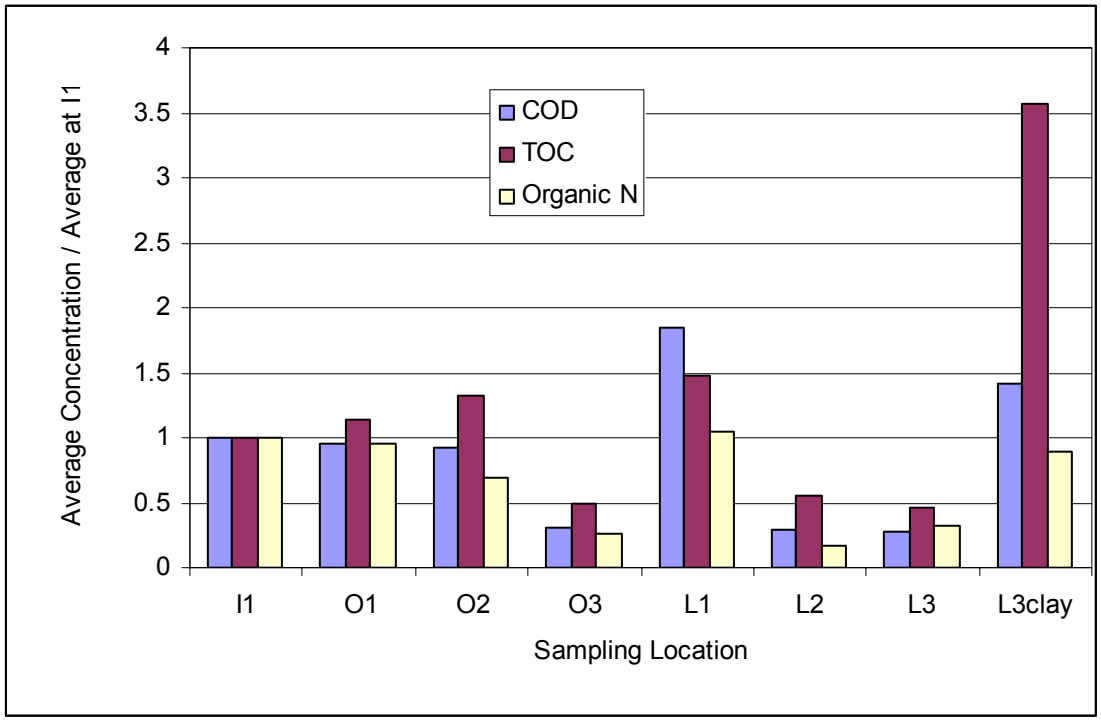

Figure 4.16. A comparison of organic matter at each sampling location, normalized with respect to the I1 concentration.

4.3.8 Other Measurements

Several chemical measurements were taken that did not lend themselves to load analysis. Dissolved oxygen and alkalinity were measured for the outflow baseflow samples at sites O2 and O3. Conductivity and pH were measured for the storm flows and for the baseflows. None of these parameters were measured for the lysimeter samples.

4.3.8.1 Dissolved Oxygen

Dissolved oxygen was only measured for the baseflow samples. The baseflow that passed through the outflow gage, O2, exhibited a much higher median concentration and a higher standard deviation than did the baseflow seeping up through the rip-rap. The higher variation for O2 may be explained by the greater influence of flow variations and the fact that the O2 flows were sampled for a longer period, from March through October. If the O3 flows had been sampled in the cold March weather, then they likely would have also had more high DO values and a higher standard deviation. Sampling at O3 did not begin until late June. The highest dissolved oxygen concentration for O2 was 16 mg/L, which occurred on a day in March when the water temperature was only 3 degrees Celsius. When both the O2 and O3 baseflows were sampled on the same day, the O3 samples had lower dissolved oxygen concentrations, probably because the O3 baseflow seeped up from deeper, more anaerobic soil environments and was less influenced by surface water. Also, as mentioned previously in the nitrogen section, bacteria at the O3 sampling location may be converting ammonia to nitrate. Biological nitrification, and possibly other biological oxidation processes, would be expected to deplete the oxygen contained in the O3 baseflow. Figure 4.17 compares the percent oxygen saturation values for baseflow samples from both locations, plotted versus the flowrate measured at the outflow gage. Figure 4.17 illustrates the difference in oxygen concentrations between the two locations, as well as the apparent independence of those concentrations to flowrate, at least during non-storm periods.

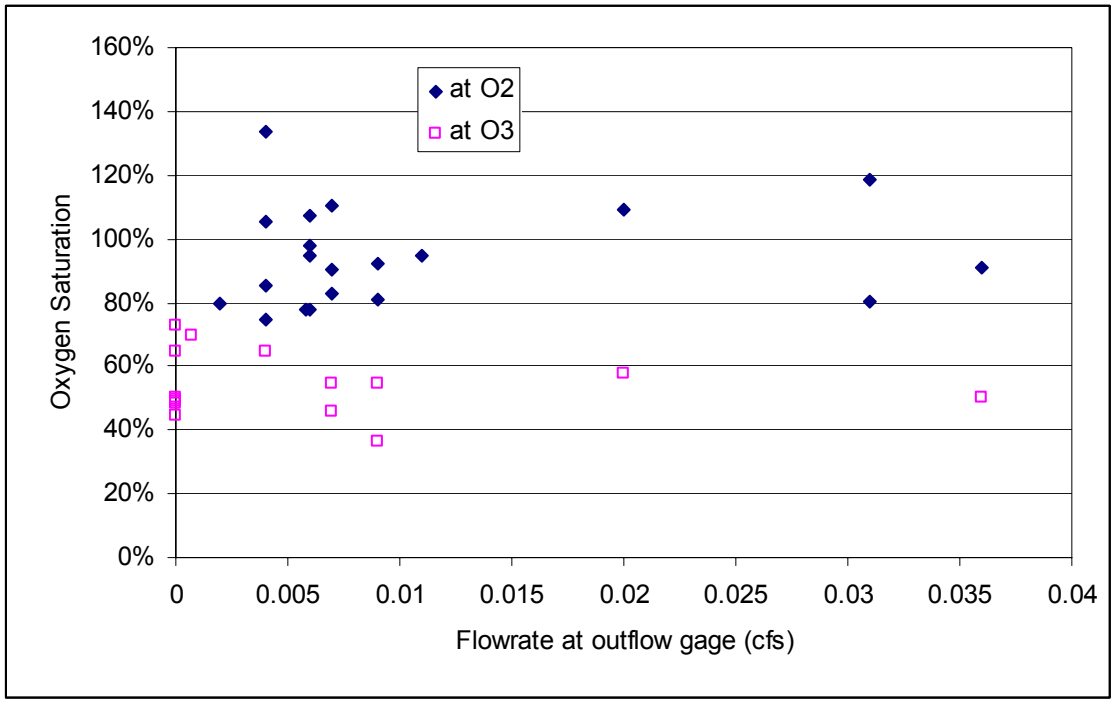

Figure 4.17. Comparison of dissolved oxygen for both types of baseflow.

4.3.8.2 pH

The pH was measured in the field for the O2 and O3 baseflows and in the laboratory for the I1 and O1 storm flows. All of the pH values were near-neutral, with an overall minimum of 5.7 and an overall maximum pH of 8.6. The range of pH values observed may be seen in graphics of Appendix C.

4.3.8.3 Total Alkalinity

Alkalinity was only measured for the O2 and O3 baseflow samples. The O3 baseflow samples generally had a higher total alkalinity (but a lower pH) than did the O2 baseflow samples. The higher total alkalinity of the O3 samples was surprising because (referring to the nitrogen section) nitrification probably took place where the O3 flows exited the soil. Nitrification is known to consume alkalinity (Grady, Daigger, and Lim, 1999). This apparently contradictory observation may be due to higher alkalinity values in the groundwater flows, which would be consistent with the higher values of hardness as discussed in Section 4.3.6.1. Unfortunately, alkalinity was not measured in the lysimeter samples. Figure 4.18 shows total alkalinity and pH with time for the O2 and O3 baseflow samples.

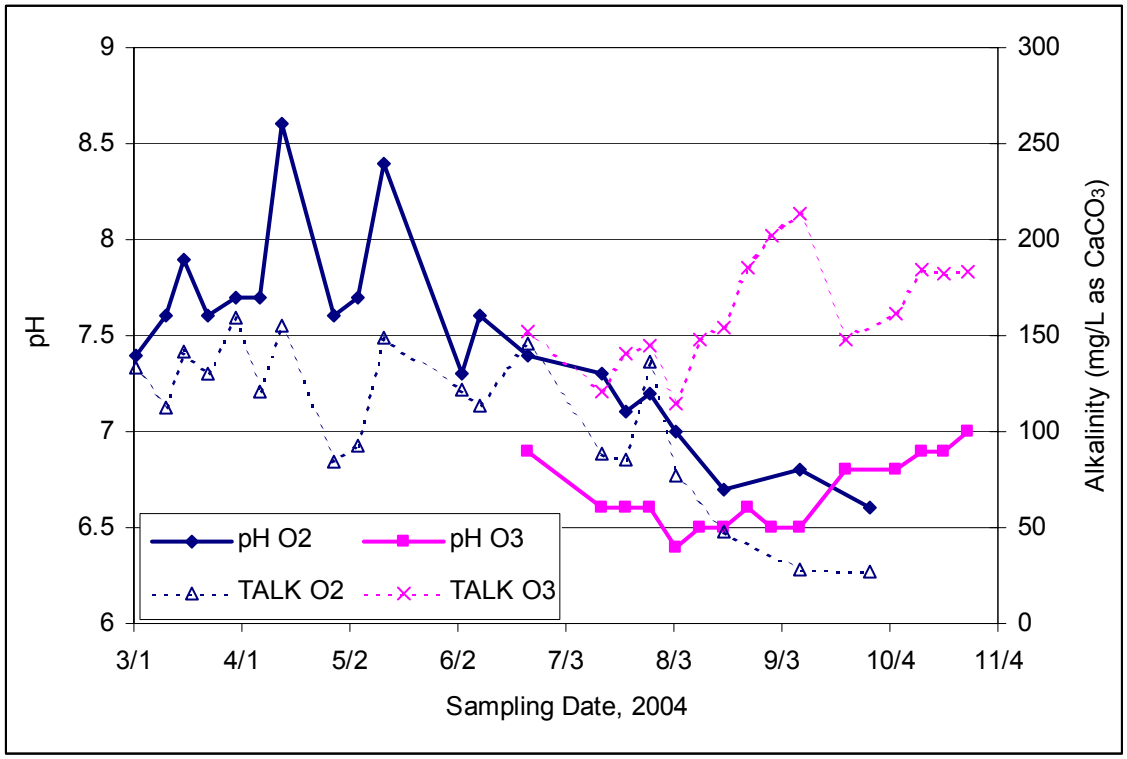

Figure 4.18. pH and total alkalinity with time for the baseflow samples O2 and O3.

4.3.8.4 Conductivity

Conductivity was measured for both the storm flows I1 and O2 and for the baseflows O2 and O3, but not for any of the lysimeter samples. Reported values were standardized to a temperature of 25° Celsius. Conductivity is an indirect measure of the total ionic species present in a water sample (Metcalf & Eddy, 2003). For the water samples taken at Kingsbrooke, the hardness ions calcium and magnesium seemed to be two of the principal ions present, and the conductivity generally followed their concentrations. As shown in the Figures 4.19 and 4.20, similar trends were observed for conductivity as for hardness. Figure 4.19 shows average conductivity and hardness values for all four sampling locations, normalized with respect to the I1 values, illustrating how conductivity and hardness are both low for storms I1 and O1, and high for outflow baseflows O2 and O3. Figure 4.20 shows conductivity and pH values with time for the baseflow samples. A similar plot could be made for the storm samples I1 and O1.

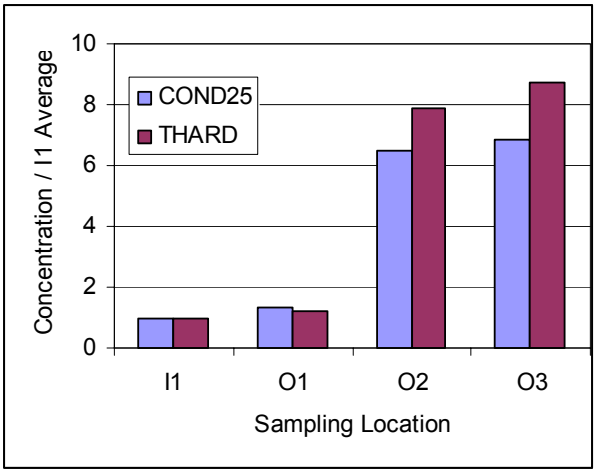

Figure 4.19. Comparison of conductivity and hardness sample averages, normalized with respect to the I1 values.

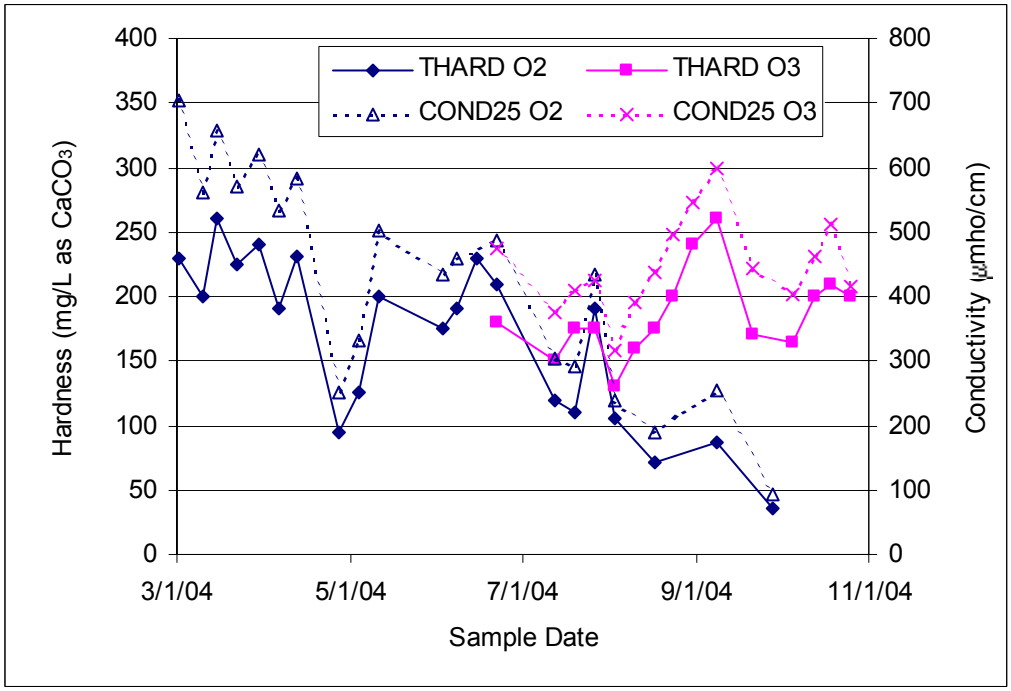

Figure 4.20. An illustration of how conductivity and hardness follow each other with time for the baseflow samples.

The storm flows from I1 and O1 exhibited low conductivities and were lognormally distributed. The conductivities for the O2 and O3 baseflow samples had a similar median value for conductivity, but the O2 baseflow conductivities had a much larger standard deviation, just like the hardness samples did.

4.3.9 Summary Results for All Pollutants

Some useful observations may be made from the concentration differences exhibited between the sampling locations:

- When comparing the baseflow samples for O2 and O3, it may seem that the concentrations for O2 were usually more similar to the storm concentrations than were the O3 concentrations. This may be explained by considering the flow data. Flows from the O2 location could only be sampled while there was flow passing through the outflow gage. Water was often still flowing at the O3 sampling location even the outflow gage was dry. As a result, it may be postulated that the O2 samples as a group represented higher flow conditions and more influence from overland storm flows than did the O3 samples, which came almost entirely from groundwater discharge.

- Among the lysimeters, samples from the L3clay lysimeter (inserted into the clay layer of the lower terrace) had significantly different analytical results from the other three lysimeters. The L3clay ammonia and TKN concentrations were much higher than samples from the other lysimeters, as were the COD and TOC concentrations. These differences may have been due to the naturally higher organic matter content of the topsoil, or the tendency of clay particles to sorb ammonium ions and other organic matter. The L3clay lysimeter samples also exhibited higher lead and zinc concentrations than samples from the other lysimeters. Clay particles have been reported to often account for more metal sorption than other soil particles (Watts, 1998).

- The inflow and outflow storm concentrations from I1 and O1, were generally more similar to each other for all constituents than to either the baseflow or the lysimeter sample concentrations. The only consistent difference between the I1 and O1 concentrations is visible in the probability distributions and tables in Appendix C. The outflow storm concentrations generally had a smaller standard deviation than the inflow storm concentrations. This suggested that some water storage occurred in the bioretention area, and as a result, some of the inflows from one storm mixed with those of the next storm before that water exited the facility. Several of the pollutants studied also showed a lower average outflow concentration than inflow concentration, accounting for the positive pollutant removal efficiencies calculated. Tables 4.12 and 4.13 list the calculated loads and pollutant removal efficiencies for all of the compounds studied. The tabular values represent the mean of the calculated values, ± the standard deviation of those values.

Table 4.12. Average loads and pollutant removal efficiencies for nutrients and for water.

	Flow Vol ** (10^6 gal)		OP (kg)		TP (kg)		NH3_N (kg)		Org_N (kg)		TKN (kg)		OX_N (kg)		TN (kg)	
Overland Inflow	5.01	±0.10	4.21	±0.19	6.51	±0.23	3.52	±0.13	17.32	±0.60	20.84	±0.64	10.46	+0.30	31.30	±0.82
Groundwater Inflow	0.81	±0.11	0.02	±0.01	0.11	±0.03	0.50	±0.07	1.42	±0.22	1.91	±0.27	0.02	+0.01	1.94	±0.30
Outflow Storms	5.25		2.79	±0.09	4.42	±0.11	1.56	±0.06	17.32	±0.26	18.87	±0.27	8.43	+0.16	27.31	±0.30
Outflow Baseflow	0.32		0.04	±0.01	0.09	±0.01	0.03	±0.00	0.80	±0.03	0.84	±0.03	0.16	+0.21	1.00	±0.21
Groundwater Outflow	0.03	±0.03	0.00	±0.00	0.00	±0.01	0.02	±0.02	0.06	±0.06	0.07	±0.08	0.00	+0.00	0.08	±0.08
Total Inflow Loads	6.06*	±0.08	4.23	±0.19	6.62	±0.23	4.02	±0.13	18.74	±0.57	22.75	±0.57	10.49	-+0.30	33.24	±0.73
Total Outflow Loads	6.07*	±0.07	2.83	±0.09	4.52	±0.10	1.61	±0.06	18.18	±0.27	19.78	±0.27	8.60	+0.26	28.38	±0.37
Pollutant Removal Efficiency	-11.2%	±13.5%	33.0%	±3.6%	31.7%	±2.8%	59.9%	±2.0%	2.9%	±3.2%	13.0%	±2.4%	17.9%	±3.4%	14.6%	±2.1%

* These total flow volumes include direct precipitation and evapotranspiration.

** The flow volume reductions listed in this table are only for overland flows: during this time period there was a net increase in overland runoff volume, probably due to groundwater influx. The large uncertainty in this calculations came from uncertainties in the volume of ungaged overland inflow.

Table 4.13. Average loads and pollutant removal efficiencies for organic matter, sediments, and metals.

	COD (kg)		TOC (kg)		TSS (kg)		SCA (kg)		SMG (kg)		EPB (g)		EZN (g)	
Overland Inflow	447	±12	126	±3	585	±31	128	±5	39	±12	48.2	±10.4	268	±54
Groundwater Inflow	56	±8	17	±3	0		316	±44	115	±16	5.0	±2.1	23	±10
Outflow Storms	446	±5	150	±2	412	±18	143	±4	52	±7	40.6	±13.8	241	±55
Outflow Baseflow	28	±1	11	±0	6	±1	47	±1	21	±1	1.9	±1.0	19	±3
Groundwater Outflow	2	±2	1	±1	0		12	±13	4	±5	0.2	±0.2	1	±1
Total Inflow Loads	503	-±10	143	±3	585	±31	444	±43	154	±20	53.3	±10.6	291	±55
Total Outflow Loads	476	±5	162	±2	418	±17	201	±13	78	±8	42.7	±13.8	261	±55
Pollutant Removal Efficiency	5.3%	±2.1%	-13.4%	±2.8%	28.4%	±4.7%	54.2%	±5.8%	48.7%	±8.9%	16.4%	±32.7%	6.8%	±27.1%

Figure 4.21 compares the relative magnitudes of the different loads (groundwater inflow, overland inflow, outflow storms, outflow baseflow, and groundwater outflow) as a percentage of the total inflow load for each constituent. Figure 4.21 clearly shows that most of the loads for calcium and magnesium came from groundwater, while for all the other constituents, the inflow and outflow storms contributed the greater loads. In contrast, the baseflow generally did not have a strong influence on the pollutant removal calculations.

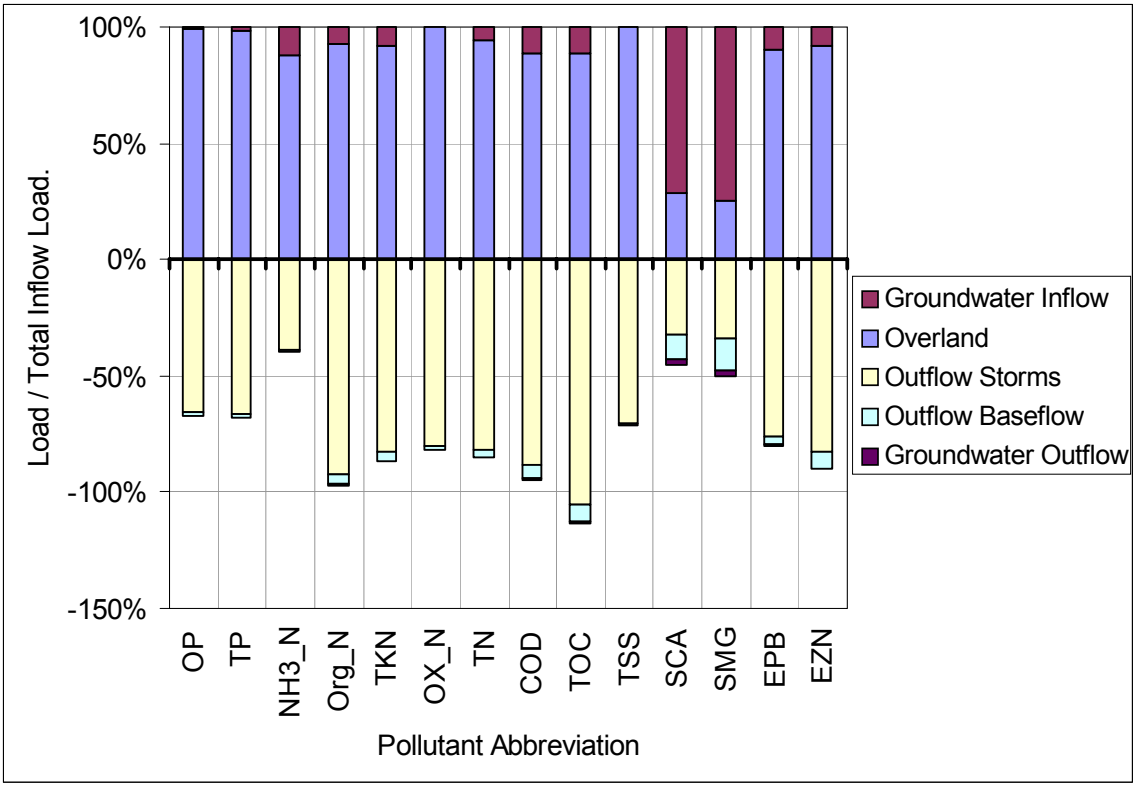

Figure 4.21. Inflow and outflow loads, normalized as a percentage of the total inflow load.

Figure 4.22 summarizes the pollutant removal efficiencies and uncertainties that were calculated using the methods developed in this study. The figure clearly illustrates the large uncertainties involved in calculating removal efficiencies for lead and zinc. As was noted earlier, a majority of the concentrations for both lead and zinc were less than the detection limits, which greatly influenced the uncertainty calculation.

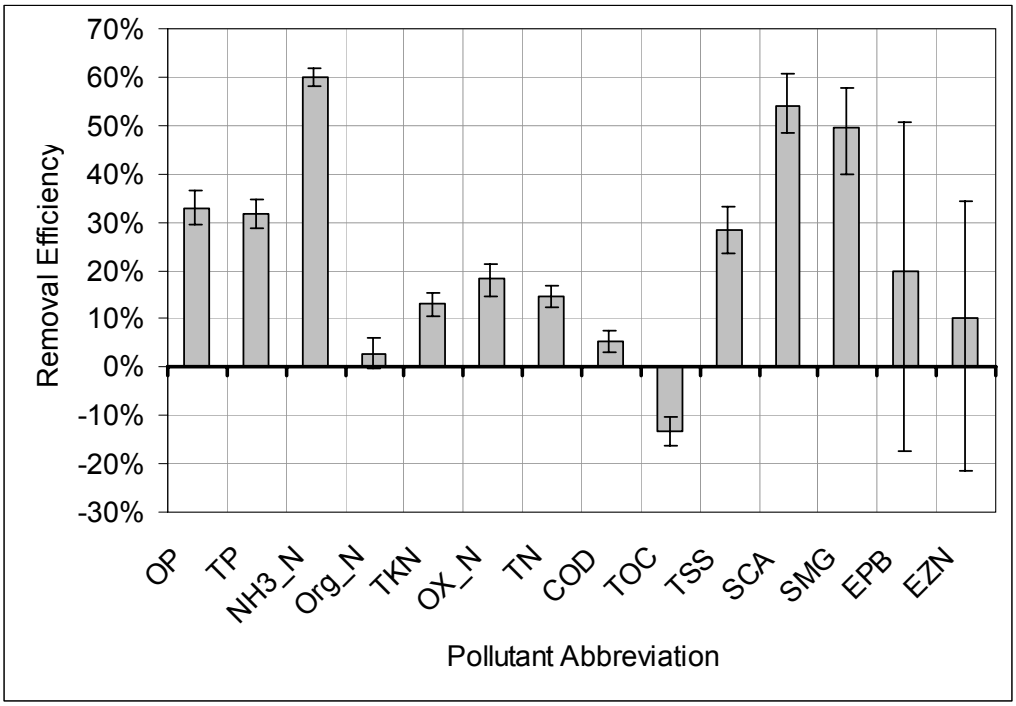

Figure 4.22. Pollutant removal efficiency and uncertainty intervals for each pollutant studied.

Table 4.14 compares the sensitivity of the pollutant removal efficiencies to variations in each of the parameters developed in Section 4.3.2. The values shown in Table 4.14 were calculated using the same procedures as shown previously in Table 4.5 as part of the example for total phosphorus. Overall, Table 4.14 reinforces what was observed previously, that most of the flows and most of the pollutant loads were associated with the overland inflow and with the outflow storms. Varying the concentrations used for non-sampled inflow and outflow storms (C) had the most significant effect on the pollutant removal efficiencies for most pollutants. In contrast, changes in parameters B, E, and F only affected the groundwater loads, so they had a major impact only on the pollutant removal efficiency for calcium and magnesium because only those constituents had sufficiently high groundwater concentrations.

Table 4.14. A comparison of the sensitivity of the pollutant removal efficiencies to variations in each of the parameters*.

		OP	TP	NH3_N	TKN	OX_N	COD	TOC	TSS	SCA	SMG	EPB	EZN
A		**1.33%**	**1.23%**	0.04%	0.72%	**1.68%**	0.37%	0.44%	**1.49%**	**4.74%**	**5.36%**	0.50%	0.82%
B		0.01%	0.02%	0.19%	0.17%	0.01%	0.22%	0.40%		**1.06%**	**1.07%**	0.19%	0.18%
C	Overland Inflow	**2.86%**	**2.08%**	**1.19%**	**1.94%**	**1.81%**	**1.55%**	**2.01%**	**3.62%**	0.50%	**1.96%**	**1.28%**	**3.59%**
	Groundwater Inflow	0.05%	0.24%	0.20%	0.18%	0.04%	0.21%	0.96%		0.23%	0.21%	**1.03%**	**2.40%**
	Outflow Storms	**2.15%**	**1.63%**	**1.59%**	**1.17%**	**1.56%**	**1.00%**	**1.30%**	**3.00%**	0.80%	**1.27%**	**1.82%**	**1.22%**
	Outflow Baseflow	0.13%	0.11%	0.04%	0.15%	**2.22%**	0.21%	0.25%	0.14%	0.34%	0.51%	0.16%	0.28%
	Groundwater Outflow	0.01%	0.02%	0.04%	0.02%	0.01%	0.03%	0.05%		0.07%	0.05%	0.09%	0.20%
D	Overland Inflow									0.02%	**3.53%**	**17.88%**	**18.35%**
	Groundwater Inflow	0.08%	0.02%			0.05%						**3.18%**	**2.08%**
	Outflow Storms										**4.29%**	**27.14%**	**19.94%**
	Outflow Baseflow	0.01%		0.01%		0.06%			0.01%			**2.14%**	0.95%
	Groundwater Outflow	0.00%	0.00%			0.00%						0.13%	0.00%
E		0.04%	0.11%	0.43%	0.66%	0.01%	1.00%	**1.20%**	0.00%	**2.89%**	**3.38%**	0.68%	0.63%
F		0.02%	0.06%	0.35%	0.39%	0.01%	0.54%	0.70%	0.00%	**2.22%**	**2.50%**	0.44%	0.39%
Overall Standard Deviation		3.63%	2.78%	1.97%	2.38%	3.41%	2.09%	2.81%	4.69%	5.83%	8.93%	32.66%	27.09%

*A summary of parameter definitions, as discussed in Section 4.3.2:

A. Drainage **A**rea ratio for the ungaged:gaged overland inflows.

B. Day for **B**eginning/ending the groundwater averaging calculations.

C. **C**oncentration used for unsampled storms or for periods when the baseflow or lysimeters were not sampled.

D. Assumed value for any concentrations that were less than the method **D**etection limit (MDL).

E. Multiplier for **E**vapotranspiration.

F. Lake Manassas Rain**F**all multiplier.

5 Summary and Conclusions

Hydrologic factors were found to have a large impact on the pollutant removal characteristics of the Kingsbrooke bioretention area. Generally, stormwater entering the area flowed directly out again after only a small period of detention. Peak runoff rates were observed to be reduced during smaller storms that followed dry spells, but for other storms the peak flowrate at the outflow gage often equaled the peak flowrate of the combined gaged and ungaged storm inflows. Like the peak flowrates, the total storm volumes were also not significantly reduced between the principal inflow and the outflow points. The low infiltrative capacity of the silt clay topsoil used in the site was probably the principal factor in the lack of significant stormwater retention. Some pollutant removal was observed to occur, but generally not at the levels of performance cited for other bioretention areas.

In general, the bioretention areas cited in the literature had high pollutant removal efficiencies for total suspended solids, total phosphorus, lead, and zinc. Pollutant removal efficiencies for all four constituents are illustrated in Figure 5.1 for this study, and also for other studies reported in the literature. The literature sources for those removal efficiencies are summarized below the figure. Several of the literature sources, especially Hunt and Jarrett (2004) for their Greensboro site, noted that the sediment that exited those bioretention areas originated from within the bioretention area soils rather than from the inflowing sediment. Frequently, pollutants were associated with the inflowing sediment but not with the outflowing sediment, such as copper, lead, and zinc. At Kingsbrooke, on the other hand, the removal efficiencies of total suspended solids, phosphorus, lead, and zinc (as shown in Figure 5.1), were all within the same order of magnitude. When examining the removal efficiencies of these sediment-related pollutants, the downstream sediment seemed to have the same characteristics as the upstream sediment. This supports the observation made previously, that stormwater passes through the Kingsbrooke bioretention area with limited infiltration. On the positive side, the Kingsbrooke site does not appear to lose sediment particles from its own soils.

Suspended sediment and phosphorus removals were found to be near 30%, but lead and zinc removals were computed to be only 16% and 7%, respectively. The lower metals removal may be explained by considering a series of factors. Metals sorb to the surface of suspended clay particles, and smaller particles have a greater surface area relative to their mass, so they may sorb more metal ions than would an identical mass of larger particles. However, larger particles have higher settling velocities than smaller particles. This may be seen in the removal performance shown in Figure 5.1, where the overall sediment removal was nearly 30%, and probably was due to removal of large particles. The low lead and zinc removal performance may be accounted for by the likely association of the metals with the smaller (and lower settling velocity) sediment particles that passed through the facility.

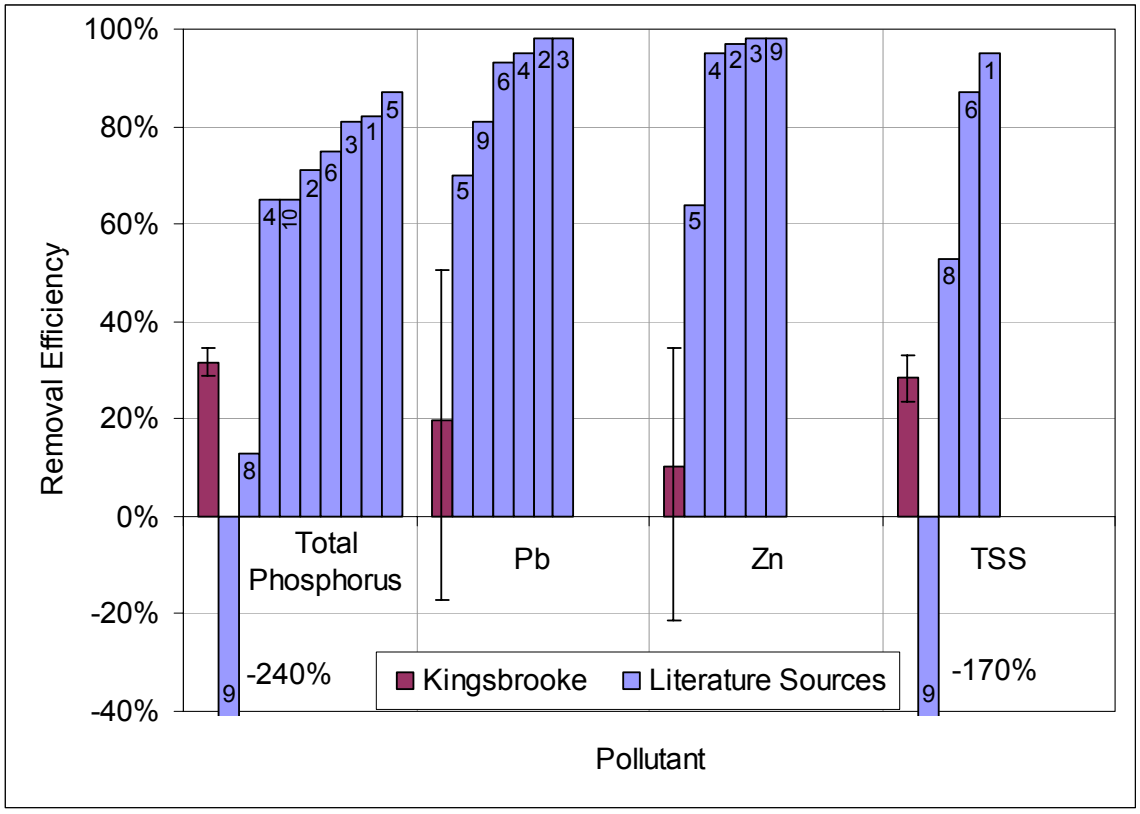

Figure 5.1. A comparison of pollutant removal efficiencies for phosphorus, lead, zinc, and suspended solids from the current study and selected values from the literature, referenced below.

Reference Key to Figures 5.1 and 5.2	*Researchers / Study Location*
1	*Coffman and Siviter (2004), Filterra ® Laboratory Experiments*
2	*Davis et al. (2001), Small Box Laboratory Experiments*
3	*Davis et al. (2001), Large Box Laboratory Experiments*
4	*Davis (2003), Greenbelt, Maryland, Field Study*
5	*Davis (2003), Inglewood Plaza Field Study in Landover, Maryland*
6	*Hsieh and Davis (2003), Other Maryland Field Studies*
7	*Kim (2001), Nitrate Removal Laboratory Bioretention Box*
8	*Yu (2001), Charlottesville, Virginia*
9	*Hunt and Jarrett (2004), Greensboro, North Carolina*
10	*Hunt and Jarrett (2004), Chapel Hill, North Carolina*

In Figure 5.2, nitrogen removal efficiencies are compared for Kingsbrooke and for several literature sources. The same reference numbers from Figure 5.1 are also used in Figure 5.2. In addition, three of the total nitrogen bars are marked with asterisks to indicate that those removal efficiencies were calculated independently based on nitrogen concentrations given in those literature sources. Ammonia removal (60%) at Kingsbrooke compared favorably with other bioretention areas, as did nitrate removal (20%). However, the pollutant removal efficiency for TKN at Kingsbrooke was significantly lower than the removals cited for all other bioretention areas except for the Greensboro, NC bioretention area (Hunt and Jarrett, 2004), which was known to leak soil particles through its underdrain system. This difference, like the difference between the Kingsbrooke and the literature TSS removals, may again be related to the different hydrologic characteristics and lower infiltration rate at the Kingsbrooke site. Organic matter (including organic nitrogen, which made up a majority of the TKN load) is often found in a particulate form, or in association

with suspended soil particles in urban stormwater. The two other measures of organic matter also exhibited low removal efficiencies, with only 5% removal for chemical oxygen demand (COD) and -13% removal for total organic carbon (TOC). Again, it would appear that the atypical soil characteristics at Kingsbrooke served to reduce the pollutant removal efficiencies of total suspended solids, total phosphorus, lead, zinc, organic matter, and total nitrogen.

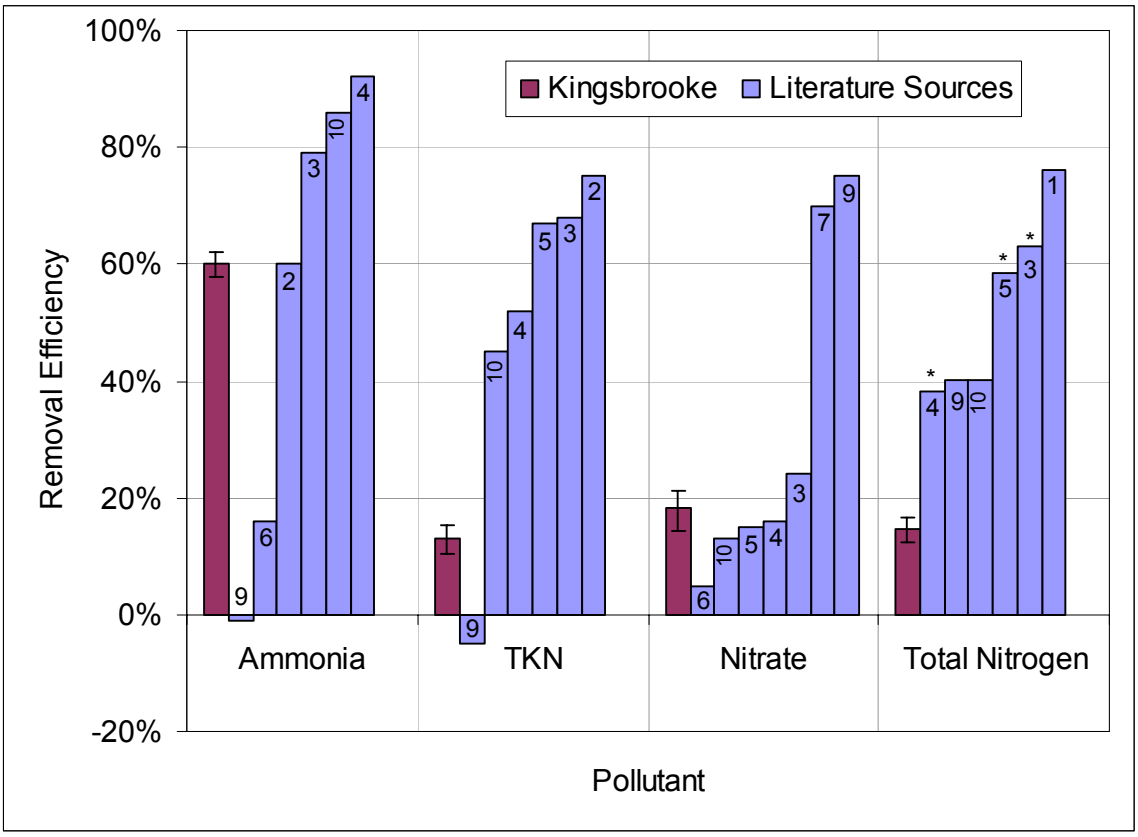

Figure 5.2. A comparison of the pollutant removal efficiencies for nitrogen species from Kingsbrooke with various literature sources cited in Table 2.9.

Overall, the observed performance of the Kingsbrooke bioretention area did not match the performance of other, more typical, bioretention areas in terms of either stormwater quality and quantity control. Of the various atypical aspects of this bioretention area, the high clay content of the soils probably had the most significant impact on the performance by lowering the capacity of the site to infiltrate stormwater. Secondary characteristics that contributed to these results included the large drainage to bioretention area ratio, a relatively shallow available ponding depth, and lower evapotranspiration potential caused by fewer large healthy trees. The influx of groundwater may have also reduced treatment capacity slightly by increasing soil moisture and inhibiting water infiltration. The unusual substitution of grass for mulch with ivy groundcover was not likely to have a significant impact on the results. In fact, turf grass may be preferable at a large site such as this one due to its ability to withstand higher stormwater flows.

The observations and data analysis performed in this study have better defined the performance characteristics of the Kingsbrooke bioretention area. Because the deviations from standard design practice appear to have impacted facility performance, some consideration should be given to assessing the relative impact of those deviations and, perhaps, the desirability of conducting a site rehabilitation. Several alternatives exist, including:

1. Maintain the bioretention area as it currently exists.

   Moderate density residential subdivisions such as the one draining to the Kingsbrooke bioretention area are typically not known for generating urban stormwater of high pollutant concentrations. In fact, the lead and zinc concentrations here were often too low to be measured. Concentrations for

nutrients and suspended sediments were also not found to be very high. As a result, in considering how funds should be allocated to improve regional water quality, the Kingsbrooke site may have a lower priority than other, more highly polluting, urban drainages. The first alternative, therefore, is simply to maintain the site in its current condition, possibly with some aesthetic improvements, such as regular removal of litter and pruning of dead tree branches.

2. Supplement with upstream BMPs such as community education programs or street sweeping.

   The water pollutant concentrations leaving the Kingsbrooke subdivision may be lowered using non-structural BMPs upstream of the bioretention area. Community education programs could be used to encourage residents to reduce the amount of fertilizers used in the drainage basin, while a street sweeping program may be able to reduce the amount of suspended solids that wash into the bioretention area. Neither of these activities would be likely to affect the bioretention area pollutant removal efficiency, but they would ultimately benefit downstream water quality.

3. Modify the bioretention area by tilling in compost or increasing the ponding depth.

   As suggested by Pitt (2002), the infiltration capacity of a soil may be improved by adding compost. Well-rotted compost would release fewer nutrients than fresh compost, while still providing the same benefit to soil texture. Using a rototiller to mix in the soil amendment may also reduce the observed compaction of the upper soil layer. Two principle difficulties exist with this approach. Tree roots may be damaged by the tilling operations and would pose an obstacle to the rototiller. Secondly, an erosion and sediment control plan would need to be implemented until turf grass becomes reestablished, to prevent soil erosion that would pose a hazard to water quality.

   Another possible modification could be an increase in the water ponding depth by raising the gabion walls. This modification should be fairly simple to implement, but over time, may result in damage to the vegetation by increasing the soil moisture and drowning the tree roots. A greater available ponding depth would allow for stormwater to be detained longer in the bioretention area, encouraging more infiltration.

4. Completely redesign the bioretention area.

   A complete rehabilitation of the Kingsbrooke bioretention area would be an expensive undertaking, but may be justified if it is determined to be necessary to attain the pollutant removal performance originally anticipated in the design. Significant improvements to the bioretention area infrastructure would be expected to result in significant improvements in pollutant removal efficiency. If, for example, the renovations could double pollutant removal efficiency, then the release of suspended solids could be lessened by about 250 kg per year.

   If this alternative is implemented, there are a number of design features that should be considered, both for the sake of improving water treatment efficiency and to simplify any follow-on analysis. A sandy soil with a high infiltration capacity mixed with well-aged compost should be used to replace the current topsoil, as specified in the *Prince George's County Bioretention Design Manual* (Winogradoff and Coffman, 2002). Installation of higher gabion walls would improve water ponding to the typical recommended depth of six inches. Adding an underdrain system would speed the passage of water through the soil, allowing for more infiltration during later storms. Also, as with the previous alternative, an erosion and sediment control plan would be necessary to protect water quality while the soil is being disturbed.

   To ease follow-on analysis of performance, the rehabilitated facility might be isolated from groundwater influence using an impermeable geotextile membrane. Diverting the ungaged overland inflow away from the bioretention area would also be helpful, but may be more difficult to accomplish. Lowering the elevation of the upper terrace would give more vertical space for free water flow through a gaging structure at the inflow point, and thereby avoid loss of data from submergence. If the underdrains of all three terraces were interconnected to a single exit point, the outflow could be analyzed separately from the overland outflow. Though not essential, the installation of lysimeters capable of measuring soil moisture content and/or devices for measuring the depth of water ponding may be helpful.

If the last alternative is implemented, it is recommended that a follow-on research project be designed to study the impacts of the improvements on pollutant removal efficiency. If post-rehabilitation pollutant removals are found to be significantly higher than the current removals, it would serve as an important lesson for adhering to accepted design and construction practice in the future with such facilities.

Each of the alternatives discussed above has costs and benefits, so care should be used in deciding which one to implement for the future. In its current configuration, the Kingsbrooke bioretention area does provide some benefits to downstream water quality, but improvements are possible. The question remains whether the possible benefits of those improvements justify their expense.

6 References

Accura-Flo, 2005. Frequently Asked Questions. *Available at* http://www.accuraflo.com/faq.htm. *Accessed in* December, 2005.

Allen, R.G., L.S. Pereira, D. Raes, and M. Smith, 1998. Crop Evapotranspiration – Guidelines for computing crop water requirements. FAO Irrigation and Drainage Paper 56. Food and Agriculture Organization of the United Nations, Rome, Italy. *Available at* http://www.fao.org/docrep/X0490E/x0490e00.htm#Contents. *Accessed in* June, 2004.

Americast, 2004. Filterra® Stormwater Bioretention Filtration System. *Available at* http://www.americastusa.com/filterra.html. *Accessed in* January, 2005.

Berthouex, P.M., and L.C. Brown, 1994. Statistics for Environmental Engineers. Lewis Publishers, New York.

Bourget Flagstone Company, 2005. Bluestone Natural Building Stone. *Available at* http://www.bourgetbros.com/flagstone/bluestone_index.htm. *Accessed in* March, 2005.

Charbeneau, Randall J., 2000. Groundwater Hydraulics and Pollutant Transport. Prentice Hall, Upper Saddle River, New Jersey.

Cheng, M.S., L.S. Coffman, Y. Zhang, and Z.J. Licsko, 2004. Comparison of Hydrological Responses from Low Impact Development with Conventional Development. *In:* Protection and Restoration of Urban and Rural Streams. American Society of Civil Engineers, Reston, Virginia. pp. 419-430.

Christianson, R.D., B.J. Barfield, J.C. Hayes, K. Gasem, and G.O. Brown 2004. Modeling Effectiveness of Bioretention Cells for Control of Stormwater Quantity and Quality Critical Transitions in Water and Environmental Resources Management. *In:* Proceedings of the 2004 World Water and Environmental Resources Congress. American Society of Civil Engineers, Reston, Virginia. pp. 1-7.

Coffman, L.S. and T. Siviter, 2004. Filterra® by Americast: Advanced Bioretention System Discussion of the Pollutant Removal Mechanisms and Design Strategies Critical Transitions in Water and Environmental Resources Management. *In:* Proceedings of the 2004 World Water and Environmental Resources Congress. American Society of Civil Engineers, Reston, Virginia. pp. 1-9.

Davis, A.P., 2005. Bioretention: Studies Results completed by the University of Maryland. *Available at* http://www.ence.umd.edu/~apdavis/Biodata.htm. *Accessed in* July, 2005.

Davis, A.P., M. Shokouhian, H. Sharma, and C. Minami, 2001. Laboratory Study of Biological Retention for Urban Stormwater Management. Water Environmental Research 73(1): 5-14.

Davis, A.P., M. Shokouhian, H. Sharma, C. Minami, and D. Winogradoff, 2003. Water Quality Improvement through Bioretention: Lead, Copper, and Zinc Removal. Water Environmental Research 75(1):73-82.

Dewberry & Davis, 1994. Kingsbrooke Phase II: BMP Bioretention Area Details & Specifications. Dewberry & Davis, Manassas, Virginia.

Doorenbos, J. and W.O Pruit, 1977. Guidelines for Predicting Crop Water Requirements. FAO Irrigation and Drainage Paper 24. Food and Agriculture Organization of the United Nations, Rome, Italy.

Emerson, C. and R.G. Traver, 2004. The Villanova Bio-Infiltration Traffic Island: Project Overview Critical Transitions in Water and Environmental Resources Management. *In:* Proceedings of the 2004 World Water and Environmental Resources Congress. American Society of Civil Engineers, Reston, Virginia. pp. 1-5.

Grady, C. P. L. Jr., Daigger, G. T. and Lim, H. C., 1999. Biological Wastewater Treatment, Second Edition. Marcel Dekker, Inc., New York, New York.

Hsieh, Chi-hsu and Allen P. Davis, 2003. Evaluation of Bioretention for Treatment of Urban Storm Water Runoff. *In:* World Water & Environmental Resources Congress 2003 and related symposia related to the congress. American Society of Civil Engineers, Reston, Virginia. pp. 1-8.

Hunt, W.F. and A.R. Jarrett, 2004. Evaluating Bioretention Areas from Two Field Sites in North Carolina Critical Transitions in Water and Environmental Resources Management. *In:* Proceedings of the 2004 World Water and Environmental Resources Congress. American Society of Civil Engineers, Reston, Virginia. pp. 1-10.

Kim, H., Seagren, E.A., and Davis, A.P., 2003. Engineered Bioretention for Removal of Nitrate from Stormwater Runoff. Water Environmental Research, 75(4), 355-367.

Lyon, B.E. and C.F. Land, 2004. Confidence Limits for Linear Functions of the Normal Mean and Variance. *Available at* http://conflimit.nci.nih.gov. *Accessed in* February, 2005.

Metcalf & Eddy, 2003. Wastewater Engineering: Treatment and Reuse, 4th Edition. McGraw-Hill, Boston, Massachusetts.

NOAA Baltimore/Washington Weather Forecast Office, 2004. Preliminary Climatology Data. *Available at* http://www.weather.gov/climate/index.php?wfo=lwx. *Accessed in* November, 2004.

Nordberg, T.M. and S.T. Thorolfsson, 2004. Low Impact Development and Bioretention Areas in Cold Climates Critical Transitions in Water and Environmental Resources Management. *In:* Proceedings of the 2004 World Water and Environmental Resources Congress. American Society of Civil Engineers, Reston, Virginia. pp. 1-9.

Occoquan Watershed Monitoring Laboratory, 2001. Quality Assurance Plan for the Occoquan Watershed Monitoring Laboratory. Virginia Tech, Manassas, Virginia.

Pitt, Robert, Shen-En Chen, and Shirley Clark, 2002. Compacted Urban Soils Effects on Infiltration and Bioretention Stormwater Control Designs Global Solutions for Urban Drainage. *In:* Proceedings of the Ninth International Conference on Urban Drainage. American Society of Civil Engineers, Reston, Virginia. pp. 1-21.

Prince William County, Virginia, Geographic Informations Systems Division. County Mapper, online interactive GIS application. *Available at* http://www.co.prince-william.va.us/default.aspx?topic=010107000120001312. *Accessed in* March, 2004.

Rushton, B., 2001. Florida Aquarium Parking Lot, a Treatment Train Approach for Stormwater Management. Southwest Florida Watershed Management District, Brooksville, Florida.

Seattle Public Utilities, 2003. Natural Drainage Overview. *Available at* http://www.seattle.gov/util/About_SPU/Drainage_&_Sewer_System/Natural_Drainage_Systems/Natural_Drainage_Overview/index.asp. *Accessed in* December, 2003.

U.S. Department of Agriculture, 1979. Field Manual for Research in Agricultural Hydrology, Agriculture Handbook Number 224. United States Department of Agriculture, Washington, D.C.

U.S. Environmental Protection Agency, 2000. Bioretention Applications: Inglewood Demonstration Project, Largo, Maryland and Florida Aquarium, Tampa, Florida. EPA-841-B-00-005A. Environmental Protection Agency, Washington, D.C.

U.S. Environmental Protection Agency, 1994. Land Application of Sewage Sludge: A Guide for Land Appliers on the Requirements of the Federal Standards for the Use or Disposal of Sewage Sludge, 40 CFR Part 503. *Available at* http://www.epa.gov/owm/mtb/biosolids/sludge.pdf. *Accessed in* May, 2004.

Watts, R.J., 1998. Hazardous Wastes: Sources, Pathways, Receptors. John Wiley & Sons, Inc., New York.

Winogradoff, D.A. and L.S. Coffman, 2002. Prince George's County Bioretention Manual. Programs and Planning Division of the Department of Environmental Resources, Prince George's County, Maryland. *Available at* http://www.goprincegeorgescounty.com/Government/AgencyIndex/DER/PPD/LID/bioretention.asp?h=20&s=&n=50&n1=160. *Accessed in* February, 2004.

Yu, S.L., M.D. Stopinski, and J.X. Zhen, 2001. Field Monitoring and Evaluation of Stormwater Ultra-Urban BMPs. *Available at* http://www.people.virginia.edu/~enqstorm/pdf/ultraBMP.pdf. *Accessed in* March, 2004.

Yu, S.L. and T.E. Langan, 1999. Controlling Highway Runoff Pollution in Drinking Water Supply Reservoir Watersheds. Virginia Transportation Research Council, Charlottesville, Virginia. *Available at* http://virginiadot.org/vtrc/main/online_reports/pdf/00-r7.pdf. *Accessed in* February, 2004.